INFORMATION TO USERS

This manuscript has been reproduced from the microfilm master. UMI films the text directly from the original or copy submitted. Thus, some thesis and dissertation copies are in typewriter face, while others may be from any type of computer printer.

The quality of this reproduction is dependent upon the quality of the copy submitted. Broken or indistinct print, colored or poor quality illustrations and photographs, print bleedthrough, substandard margins, and improper alignment can adversely affect reproduction.

In the unlikely event that the author did not send UMI a complete manuscript and there are missing pages, these will be noted. Also, if unauthorized copyright material had to be removed, a note will indicate the deletion.

Oversize materials (e.g., maps, drawings, charts) are reproduced by sectioning the original, beginning at the upper left-hand corner and continuing from left to right in equal sections with small overlaps.

Photographs included in the original manuscript have been reproduced xerographically in this copy. Higher quality 6" x 9" black and white photographic prints are available for any photographs or illustrations appearing in this copy for an additional charge. Contact UMI directly to order.

ProQuest Information and Learning
300 North Zeeb Road, Ann Arbor, MI 48106-1346 USA
800-521-0600

University of Alberta

Investigation of Rapamycin and Rapamycin Metabolites

by

Heather Lee Gallant-Haidner

A thesis submitted to the Faculty of Graduate Studies and Research in partial fulfillment of the requirements for the degree of Doctor of Philosophy

in

Medical Sciences -
Laboratory Medicine and Pathology

Edmonton, Alberta
Fall 2001

True end is not in the reaching of the limit,
but in a completion, which is limitless.

Rabindranath Tagore

ABSTRACT

INVESTIGATION OF RAPAMYCIN AND RAPAMYCIN METABOLITES

Rapamycin is an immunosuppressive drug used in organ transplantation. It is metabolised to a number of products. It is not known what the relevance of these metabolites is – if they posses immunosuppressive, or toxic activity; what their concentrations are in blood; if they should be monitored clinically in transplant patients. To answer these questions, rapamycin metabolites were tested extensively. First, metabolites were generated using a microbial system expressing cytochrome P450 3A enzyme. The metabolites were purified and five metabolites were structurally identified by high performance liquid chromatography with mass spectrometry detection (HPLC-MS). They have been named according to the structural change(s) they posses: 27-, 39-O-di-demethylrapamycin, C(1-14)-hydroxyrapamycin, C(15-27)-hydroxyrapamycin, 16-O-demethylrapamycin and 39-O-demethylrapamycin. The immunosuppressive activity of these metabolites was evaluated using the mixed lymphocyte reaction. The immunosuppressive activity of the metabolites ranged from 0.1% to 17.3% of rapamycin. The toxic activity of these metabolites was investigated in an *in vitro* vascular endothelial vasoactive substance release assay; results confirm that it is not an important mode of toxicity for rapamycin or its metabolites. A method was developed for measurement of five metabolites in clinical and research specimens by HPLC-MS. A study investigating differences in canine portal and systemic pharmacokinetics of rapamycin revealed rapamycin oral dosing produces an appropriate pharmacokinetic profile for liver and portal vein embolised pancreatic islet transplantation, as differences between portal and systemic peak levels were negligible. Rapamycin and rapamycin metabolite levels were also measured in liver transplant patients on a compassionate release program. None of the five metabolites evaluated were present in concentrations that exceeded 30% of rapamycin in these liver transplant patients. Overall, given the new information on the concentrations and immunosuppressive activities, the five metabolites tested do not contribute significantly to immunosuppression. While further study of the metabolites of rapamycin should be pursued, at this time rapamycin alone should be measured for therapeutic drug monitoring and dosage adjustment in transplant patients.

ACKNOWLEDGEMENTS

I extend my appreciation to many individuals who contributed to my experiences and research during the course of my studies.

In particular, I thank Dr Randall Yatscoff for his support; for encouraging me to become an independent thinker and for providing an environment in which to explore science.

I thank my graduate supervisory committee members, Dr. P.F. Halloran, Dr. K.M. Kane, and Dr. D.F. LeGatt for their expertise and guidance throughout my studies. I also extend my appreciation to the examining committee for providing an insightful examination environment and for their review of my thesis and discussion of my work. Special thanks go to Dr. U. Christians for his work as external examiner and for a very stimulating meeting, and to Dr. G. Baker for his work as an additional examiner and his thoughtful questioning. I also thank Dr. N.M. Kneteman and Dr.A.J. Malcolm for collaboration and advice during my studies.

I also appreciate the technical assistance and friendship offered by the staff Isotechnika, especially that of Leslie Schmidt.

I am also grateful for financial support provided in the form of scholarships and awards from the University of Alberta Faculty of Medicine, the Faculty of Graduate Studies and Research and the Capitol Health Authority.

TABLE OF CONTENTS

			Page
I.	INTRODUCTION		1
	1.	THE ROOTS OF TRANSPLANTATION	1
	2.	UNDESIRABLE EFFECTS OF IMMUNOSUPPRESSION	5
	3.	IMMUNOBIOLOGY OF ORGAN ALLOGRAFT REJECTION	8
		a. Mechanism of T-cell Activation	9
		b. Requirement for Co-stimulation	11
		c. Cell Proliferation: the Cell Cycle	12
	4.	THE CYCLOSPORINE ERA	13
	5.	THE SEARCH FOR NEW IMMUNOSUPPRESSIVE DRUGS	15
		a. Tacrolimus	16
		b. Mycophenolate Mofetil	17
		c. Rapamycin	18
	6.	MECHANISM OF ACTION OF RAPAMYCIN	21
	7.	PHARMACOKINETICS AND METABOLISM OF RAPAMYCIN	23
	8.	REFERENCES	25
II.	OBJECTIVES		37
	1.	RATIONALE	37
	2.	HYPOTHESIS	38
	3.	SPECIFIC AIMS	38
	4.	REFERENCES	39
III.	ISOLATION AND CHARACTERIZATION OF RAPAMYCIN METABOLITES		40
	1.	RATIONALE	40
	2.	MATERIALS AND METHODS	40
		a. Source of drugs and specimens	40
		b. Measurement of rapamycin in whole blood by HPLC	41
		c. Investigation of urine as a source of rapamycin metabolites	42
		d. Investigation of rapamycin metabolites in renal transplant patient blood	43
		e. investigation of rapamycin metabolite production by rabbit liver microsomal preparations	44
		f. investigation of a microbial metabolite generation system	45
		g. Investigation of the polar Phase II metabolites of rapamycin	46
		h. structural identification and confirmation of purity of isolated rapamycin metabolites by HPLC-MS	47
		i. quantification of rapamycin metabolites by HPLC-UV	48

3. RESULTS 49
a. urine as a source of rapamycin metabolites 49
b. identification of rapamycin metabolites in renal transplant patient blood 49
c. rapamycin metabolites from liver microsomes 55
d. microbial generation of rapamycin metabolites 57
e. Investigation of the polar Phase II metabolites of rapamycin 60
f. structural identification and confirmation of purity of isolated rapamycin metabolites by HPLC-MS 62
g. metabolite purity assessment 78
h. quantification of rapamycin metabolites by HPLC-UV 80
4. DISCUSSION 82
5. REFERENCES 91
IV. ACTIVITY OF RAPAMYCIN METABOLITES 92
1. RATIONALE 92
2. MATERIALS AND METHODS 92
a. source of drugs and specimens 92
b. Mixed Lymphocyte Reaction 92
c. Endothelin/Prostacyclin release assays 95
d. rapamycin Immunoassay 98
e. cross reactivity determination 99
f. minor immunophilin binding study 100
3. RESULTS 101
a. Mixed Lymphocyte Reaction 101
b. Endothelin/Prostacyclin release assays 105
c. rapamycin Immunoassay 107
d. minor immunophilin binding study 110
4. DISCUSSION 112
5. REFERENCES 120
V. RAPAMYCIN METABOLITE QUANTIFICATION BY LCMS 122
1. RATIONALE 122
2. MATERIALS AND METHODS 122
a. LC-MS quantitative assay for rapamycin and five metabolites 122
b. standardisation and quality control preparation 123
c. assay validation 124
d. rapamycin metabolite standardisation 125
e. data manipulation 125

3. RESULTS 125
a. recovery determination 125
b. rapamycin standard curve and quality control 127
c. method comparison, LC-UV and LC-MS 133
d. extrapolated rapamycin metabolite response curves 137
4. DISCUSSION 140
5. REFERENCES 148

VI. CANINE PORTAL AND SYSTEMIC PHARMACOKINETICS OF RAPAMYCIN 150
1. RATIONALE 150
2. MATERIALS AND METHODS 150
a. surgical procedure 150
b. pharmacokinetic study 152
c. drug and metabolite analysis 153
d. pharmacokinetic and statistical analysis 153
3. RESULTS 153
a. rapamycin pharmacokinetics 153
b. normalised rapamycin pharmacokinetics 155
c. rapamycin metabolite profiles in the dog 163
4. DISCUSSION 167
5. REFERENCES 177

VII. RAPAMYCIN PHARMACOKINETICS AND STEADY STATE METABOLITE LEVELS IN LIVER TRANSPLANT PATIENTS 179
1. RATIONALE 179
2. MATERIALS AND METHODS 179
a. source of drugs and metabolites 179
b. patient samples 179
c. rapamycin and metabolite concentration determination 180
d. pharmacokinetic and statistical calculations 180
3. RESULTS 180
a. rapamycin pharmacokinetics in liver transplant patients 180
b. rapamycin metabolite levels in liver transplant patients 182
4. DISCUSSION 191
5. REFERENCES 194

VIII. CONCLUSIONS 195

LIST OF FIGURES

Figure		Page
I – 1	Structure of Rapamycin	19
III – 1	UV Spectral Profile of rapamycin-treated patient urine	50
III – 2	ESI-MS fragmentation profile of rapamycin	52
III – 3	LC-MS Profile of rapamycin metabolites in human whole blood	54
III – 4	LC-MS Profile of rapamycin metabolites generated in a rabbit microsomal system	56
III – 5	LC-MS Profile of rapamycin metabolites generated in a microbial culture	58
III – 6	LC-MS Profile of rapamycin metabolites generated in a microbial culture, with extended incubation time	59
III – 7	ESI-MS fragmentation profile of RC5	65
III – 8	Structure of 27-, 39-O-didemethylrapamycin	67
III – 9	ESI-MS fragmentation profile of RD1	68
III – 10	Structure of (C1-C14)-hydroxyrapamycin	70
III – 11	ESI-MS fragmentation profile of RD3	71
III – 12	Structure of (C15-C27)-hydroxyrapamycin	73
III – 13	ESI-MS fragmentation profile of RD4	74
III – 14	Structure of 16-O-demethylrapamycin	76
III – 15	ESI-MS fragmentation profile of RF1	77
III – 16	Structure of 39-O-demethylrapamycin	79
IV-1	Mixed Lymphocyte Reaction profile: rapamycin and 5 metabolites	102
IV-2	MLR of Rapamycin and 5 metabolites; ED50	104
IV-3	ET-1 Production in NHMC	106
V-1	Rapamycin analysis by LC-MS: Standard Curve	128
V-2	Correlation of HPLC-UV versus HPLC-MS	135
V-3	Bland-Altman plot of rapamycin analysis by LC-UV vs. LC-MS	136
V-4	Bias in rapamycin determination by LC-UV vs. LC-MS	138
V-5	Rapamycin metabolites slope response by LC-MS	139
VI-1	Pharmacokinetic profiles of rapamycin in the dog	154
VI-2	Pharmacokinetic profiles of rapamycin in the dog normalised to maximum systemic level	157
VI-3	Pharmacokinetic profiles of rapamycin in the dog normalised to maximum portal level	159
VI-4	Rapamycin metabolites over the dosing interval in dog 1	164
VI-5	Rapamycin metabolites over the dosing interval in Dog 2	165
VI-6	Canine rapamycin and metabolite levels at 2h and 8h post dose	166

VI-7	Measured rapamycin metabolite ratios in the acute and chronic dosing intervals in the dog	168
VII-1	Rapamycin pharmacokinetic profile in liver transplant patients	181
VII-2	Dose-corrected rapamycin pharmacokinetic profile in liver transplant patients	184
VII-3	Rapamycin metabolite levels in liver transplant patients	185
VII-4	Rapamycin metabolite ratios in liver transplant patients	186
VII-5	Total measured metabolite ratios in liver transplant patients over the dosing interval	188
VII-6	Steady state rapamycin metabolite concentrations in liver transplant patients	189
VII-7	Total measured metabolite ratios at steady state	190

LIST OF TABLES

Table		Page
III – 1	Immunosuppressive and immunophilin binding of four peaks isolated from the urine of rapamycin treated patients	51
III-2	Rapamycin metabolites sources	61
III-3	Proposed structures of five rapamycin metabolites	63
III-4	Purified, isolated rapamycin metabolite yield from microbial culture	88
IV-1	Immunosuppressive activity of rapamycin and 5 metabolites by MLR	103
IV-2	Urine substance cross reactivity by MEIA	108
IV-3	Rapamycin metabolte cross reactivity in rapamycin immunoassay MEIA	109
IV-4	Immunophilin binding of rapamycin metabolites	111
V-1	Percent recovery of rapamycin and DMR by LC-MS	126
V-2	Compiled calculated standard curve parameters for LC-MS rapamycin assay	129
V-3	LC-MS assay for rapamycin: 40 hour on instrument QC stability	131
V-4	Rapamycin by LC-MS: quality control results	132
V-5	Rapamycin by LC-UV cumulative QC data	134
V-6	Rapamycin methodology comparison	142
V-7	Rapamycin metabolites; methodology comparison	146
VI-1	Canine rapamycin PK parameters	156
VI-2	SYSmax normalised canine rapamycin PK parameters	158
VI-3	PORTmax normalised canine rapamycin PK parameters	160
VI-4	Canine rapamycin AUC and Cmax	162
VII-1	Human PK parameter summary, rapamycin oral dose in liver transplant patients	183
VIII-1	Rapamycin metabolite immunosuppressive index	198

ABBREVIATIONS AND SYMBOLS

%	percent
"	inch
°C	degrees celcius
5' TOP	5' terminal oligopyrimidine
6-MP	6-mercaptopurine
Å	angstrom
ALG	anti-lymphocyte globulin
APC	antigen presenting cell
ATCC	American Type Culture Collection
AUC	area under the time-concentration curve
AZA	azathioprine
B	binding
CD	cluster designation
Ci	Curie
Cl	Clearance
Cmax	maximal concentration
CsA	cyclosporine A
CV	coefficient of variation
CYP	cytochrome protein
d	day
D	drug concentration
Da	daltons
DAG	diacylglycerol
Dm	drug concentration required for ED_{50}
DMR	demethoxyrapamycin
DNA	deoxyribonucleic acid
ED_{50}	point where 50% inhibition is achieved
eIF	elongation initiation factor
ESI	electrospray interface
ET	endothelin
F	bioavailability
Fa	fraction affected
FAB	fast atom bombardment
FKBP	FK506 binding protein
FRAP	FKBP and rapamycin associated protein

Fu	fraction unaffected
g	gram
g	gravity
GFR	glomerular filtration rate
GMP	guanosine monophosphate
GTP	guanosine trisphosphate
h	hour
HPLC	high performance liquid chromatography
IBA	immunophilin binding assay
ICAM	intracellular adhesion molecule
IGF	insulin-like growth factor
IL	interleukin
IL-2R	interleukin 2 receptor
IMPDH	inosine monophosphate dehydrogenase
IP_3	inositol trisphosphate
iU	international enzyme activity unit
IV	intraveneous
L	liter
LFA	leukocyte factor antigen
LOD	limit of detection
LOQ	limit of quantification
m	meter
M	molar
m/z	mass to charge ratio
MEIA	microparticle enzyme immuno assay
MHC	major histocompatibility complex
min	minute
MLR	mixed lymphocyte reaction
MMF	mycopheolate mofetil
MPA	mycophenolic acid
MPAG	mycophenolic acid glucuronide conjugate
mRNA	messenger ribonucleic acid
MS	mass spectrometer
MSD	mass selective detector
mTOR	mammalian target of rapamycin
N	normality
n	number

NADPH	nicotine adenine dinucleotide phosphate
NF-AT	nuclear factor of activated T-cells
NHMC	normal human mesangial cell
NMR	nuclear magnetic resonance
NR	not reported, no result
PG	prostaglandin
p-gp	p-glycoprotein
pH	negative log of hydrogen ion concentration
PHA	phytohemagglutinin
PIP2	phosphatidyl inositol bisphosphate
PK	pharmacokinetic
PKC	protein kinase C
PORT	portal
PTK	protein tyrosine kinase
QC	quality control
RBC	red blood cell
RIA	radioactive immuno assay
S	Svedberg unit
SD	standard deviation
SPE	solid phase extraction
SYS	systemic
$t_{1/2}$	half life
TCR	T-cell receptor
TDM	therapeutic drug monitoring
UMP	uridine monophosphate
UTR	untranslated region
UV	ultra violet
v	volume
VLA	very late antigen
Vz	apparent volume of distribution
w	weight
WBC	white blood cell
XR	cross reactivity

I. INTRODUCTION

1. THE ROOTS OF TRANSPLANTATION

The concept of replacing a diseased organ with a healthy one, the replacement of amputated limbs and the exchange of organs between species has existed in the mythic aspects of society for thousands of years. Although we are not able to test the validity, rationale or authenticity and truths that lie behind myth, as we would test a scientific hypothesis, myths represent a combination of popularised belief and accepted diversion. They are used to immortalise concepts, values and events, for teaching, entertainment and to communicate hopes, unproven ideas and desires. Myth is essentially a new inflection or redaction of a meaningful human act, historic or otherwise. This is quite true of the myth of transplantation.

There are ancient tales of transplantation. In the Pur'a'nas, Hindu scriptures, it is depicted that the 'destroyer/rebuilder God', Siva, performs cross-species transplantation (xenotransplantation) on two separate occasions. Dashka, a sage, and another God, Ganesha, became surgical subjects after Siva beheaded them[1,2]. The Gods requested that Siva replace their heads in penance for his sudden outbursts, and he did so accordingly. However, because the heads were misplaced, Dashka received the head of a ram, and Ganesha, the head of an elephant. These accounts are reputedly five thousand years old. There was no need for immunosuppression in this myth, and surgical expertise seemed irrelevant. The patients were ritually washed and prepared, but received no medication to facilitate graft function or dampen immune response.

In the modern age, transplantation was re-visited in less mythic proportions. Initially, simple experiments were conducted. In 1902, Ullman showed that a kidney could be removed from a dog and re-implanted into the same animal without loss of function. Next came experimental renal transplantation between dogs and from dog to goat, also performed by Ullman, Unger and Carrel[3]They claimed technical (surgical) success, but noted loss of function within one to two

weeks if the donor and recipient were both canine, and loss of function in several hours if the organ was from another species (a xenograft). A mysterious process was responsible. Only a few short years later, the first well documented kidney transplants in humans were conducted, with two xenografts performed, unsuccessfully, by Jaboulay and Unger[3]. Again, the reason for failure was obscure.

In 1933, Vorony performed six human transplants using cadavers as donors. None achieved substantial graft function[3]. The grafts failed rapidly, and the subjects died soon after receiving these xenografts. However, as the "artificial kidney" or dialysis machine had not yet been invented and there was no alternative treatment for renal failure, transplantation research continued. Surgical advances meant that by the early 1950s, cadaveric kidneys could be transplanted and function reasonably for several weeks[4], but without any immunosuppression, the grafts all eventually failed, due to a mysterious bodily process where the organ graft was "rejected".

It was not until the reason for transplant failure was elucidated in the 1940s that transplantation research could proceed in a rational manner. Medawar described how the rejection process is mediated by active, acquired immunity and ultimately leads to the destruction of transplanted tissues and organs[5]. An active search for treatments to suppress this immune response followed.

In 1954, Murray and associates performed a successful kidney transplant between identical twins[6]. This event was extremely important, and timely as it demonstrated that in the absence of rejection, a transplanted kidney could function for an extended period of time, in a physiologically relevant manner. It also demonstrated that an identical twin donor lacked the intrinsic difference that would normally have caused rejection of the organ. It was not allo-antigenic.

The search for chemical and physical immunologic intervention (immunosuppression) was thusly kindled. Previously described immunological treatments were revisited in an effort to suppress the recipient's immune system and facilitate the acceptance of the graft. Radiotherapy that had been used first in 1908 to inhibit antibody responses, then in 1914 to inhibit cell-mediated responses was reintroduced in the late 1950s for transplant immunosuppression[7]. Patients were given a better chance of attaining good graft function, but had to endure radiation-induced side effects. Morbidity was still unacceptable, as radiation–induced bone marrow aplasia and subsequent infections killed most patients.

The development of purine analogues in 1954 for use in the treatment of leukemia[8] led to a turning point in transplantation research. In 1959, Schwartz and Dameshek demonstrated the immunosuppressive properties of the purine analog 6-mercaptopurine (6-MP) to suppress antibody responses and delay the rejection of skin allografts in the rabbit[9]. More successful transplant studies in the canine model followed[10], and after 1961, azathioprine (AZA), a more reliably bio-available derivative of 6-MP, was in clinical use[11].

It was readily apparent that AZA alone was not sufficient for prevention of allograft rejection, and corticosteroids were soon added to the immunosuppressive regimen. Steroids were used in high doses for treating rejection, and for use in the immediate post-transplant period for induction therapy[12,13]. The standard immunosuppressive treatment for renal transplantation from 1966 until approximately 1978 was AZA coupled with steroids. Patient survival at one year post-transplant was 50% to 60%, with considerable morbidity partially attributable to high doses of steroids. It wasn't until the mid to late 1970s that studies were done to evaluate the efficacy of low doses of maintenance steroids. It was quickly apparent that low steroid dosing did not result in more graft rejection, and reduced the incidence of steroid-associated toxicity by half[14].

Purified anti-lymphocyte globulin (ALG) was introduced in the 1970s, both to treat steroid-resistant rejection and for induction therapy in the early post-transplant period[15]. This agent

was a slight improvement upon the crude anti-sera prepared in the 1960s by Woodruff[16] and Waksman[16]. Initially, antisera was prepared by injecting the fraction of human white blood cells (WBC) into animals, such as the horse, and harvesting the antibodies for injection into the patient[18]. Early preparations were effective at depleting the lymphocyte population and promoted graft survival. However, they were non-specific and depleted all WBC types due to cross reactivity with granulocytes and monocytes. The more advanced preparations of the 1970s were less polyreactive, but were still associated with significant morbidity due to serious immunodepression and susceptibility to viral infections and late oncologic complications[19,20]. Also, these antisera produced an immune response themselves, as recipients developed species-dependent, neutralising anti-ALG antibodies, which precluded long-term or repeated use[21].

Serendipitous discovery of cyclosporine A (CsA) in the early 1970s proved to dramatically advance the field of transplantation through improved immunosuppression. CsA is a unique cyclic undecapeptide produced by the fungus *Tolypocladium inflatum Gams*. With antifungal and immunosuppressive properties, *in vitro* and experimental transplantation studies using CsA in the rat showed strong potency[22]. By 1978, several small clinical studies (primarily with renal transplantation) had been done, with favourable results[23,24]. Large multicentre clinical trials with high-dose CsA mono-therapy with renal transplantation followed in the early 1980s, with a significant (15%) improvement to graft survival at one year, as compared to the control group on AZA[25]. Renal transplantation was now the treatment of choice for end-stage renal failure.

Unfortunately, the side effects of CsA were too significant to overlook. As most of the side effects were dose-dependent, several protocols were developed and tested to reduce CsA exposure. These involved the use of more than one immunosuppressive agent at a time, with or without induction therapy, or switching from one agent to another as toxic symptoms became problematic or adding agents as rejection episodes occurred. The most common therapy

became "triple therapy" of CsA, AZA and steroids, which is not necessarily the best combination in terms of efficacy, but is easy to manage and has only moderate side effects[26].

2. UNDESIRABLE EFFECTS OF IMMUNOSUPPRESSION

Transplantation is now a viable and preferred treatment modality for end-stage renal, cardiac, liver and lung disease. For renal failure, it provides a number of advantages over dialysis by avoiding certain hematologic, biochemical and other physical complications associated with these therapeutic treatments[27]. There is also economic advantage, as the cost of maintenance immunosuppression and medical follow-up is significantly lower for a renal transplant patient than the cost of a dialysis programme for a patient with renal failure in the course of a year[28]. Overall, quality of life is significantly better in many aspects for transplant recipients than for their cohorts for at least five years after transplantation[29,30].

However, transplantation is not without disadvantage. In addition to the threat of recurrent disease and loss of the grafted organ[31], come the many complications associated with transplantation surgery[32] and immunosuppressive therapy[33]. Immunosuppression is extremely important for a transplant recipient. It is, with very rare exceptions, a necessity to suppress the recipient's immune system in order to ensure that the graft is not rejected and destroyed. The suppression of these host responses to the graft requires both the cell-mediated and humoral aspects of the immune system to be affected. As many immune response pathways are conserved, this also results in a decreased ability to respond to foreign antigen and pathogens, and may facilitate opportunistic infection.

As viral immunity requires intact cell-mediated response, viral infections are common in transplant patients. Although viral infection may be mild in other situations, in the transplant patient, primary infection and reactivation of viral disease

can be extremely serious and even fatal. Etiologic agents include Cytomegalovirus, adenovirus (in the pediatric patient), Epstein-Barr virus, the hepatitis viruses, Human Papilloma virus, Herpes Simplex viruses and Vericella zoster[34]. In the instance of Epstein-Barr virus, virally induced B-cell proliferation and its subsequent role in lymphoma formation is another potentially fatal complication[35].

Because of generalised immunosuppression, bacterial infections are also common in the transplant patient, with a majority being caused by species of *Enterobacteriaceae.* Increased incidence of fungal infection also occurs, such as apergillosis and *Pneumocystis carinii* pneumonias, but also dissemination/septicemia and invasive disease[36].

Perhaps due to decreased immune surveillance, there is an increase in tumour formation in the immunosuppressed patient. This may result from a decreased ability of the host to detect and eliminate neoplastic cells that have undergone somatic mutation or are virally infected and multiply uncontrollably[35]. There is an increased incidence of rare tumours, such as Kaposi's sarcoma, squamous cell carcinoma of the skin, and non-Hodgkin's lymphomas[35]. There is also a disproportionately high incidence of cancers of the ureter, thyroid, vulva and vagina, and esophagus[37]. This is further complicated by the mutagenic potential of some of the immunosuppressive agents still in use. AZA can cause chromosomal breaks, which may precede mutagenisis and transformation[38]. These oncogenic complications are common to primary, acquired and other induced immunodeficiencies.

Immunosuppressive agents each have specific toxic effects. Standard immunosuppressive therapy still consists of administration of a combination of drugs to prevent rejection, and short courses of high doses of a given agent to treat

rejection episodes[39]. Combinations of two to three drugs directed at different targets in the activation pathway of the T-cell is desirable. Through synergistic interaction, this can increase the efficacy of treatment, and decrease toxicity by limiting drug exposure to individual agents[40,41]. The most common combination remains "Triple Therapy" of either CsA or tacrolimus, with either AZA or MMF,and prednisone or prednisolone (steroids). Although therapy is individualised and closely monitored in an effort to minimise toxicity, there appear to be some almost unavoidable effects of immunosuppressive drug therapy.

AZA is an antiproliferative agent, is myelotoxic, and can result in leukopenia, thrombocytopenia and anemia[42]. Episodic hematological toxicity, which is directly related to AZA dose, occurs in approximately 50% of renal transplant recipients[43]. Other side effects include megaloblastic erythrocyte changes, chronic veno-occlusive hepatic changes, acute pancreatitis and gastrointestinal effects, alopecia, skin thinning and fragility and increased risk of malignant tumours[42]. Withdrawal of AZA results in bone marrow recovery, but it is needed at high doses to achieve effective prophylactic immunosuppression. As it is a competitive inhibitor of inosine monophosphate dehydrogenase (IMPDH), it is needed at high concentrations to exert anti-metabolic effects[38].

Corticosteroid use is varied, but nearly ubiquitous in transplantation[44]. This is partly due to the numerous and frequent side effects of steroid use. In the early post-transplant period, steroids are used for prophylaxis at high dosage, and tapered in the weeks and months after grafting. Steroids are often administered in short courses of high dose for treatment of rejection episodes, as required. Where clinically warranted or to spare the patient steroid exposure, the dose may be administered on alternate days, or may be withdrawn completely[45]. Steroid withdrawal is a desirable goal for most patients.

Steroid use is strongly linked with hypercholesterolemia[46],obesity, hypertension, avascular necrosis, impaired wound healing, cataract formation, osteoporosis, diabetes mellitus, pancreatitis, psychiatric disorders, impaired growth and development[42], peptic ulceration, tendon and muscle disease and peripheral neuropathy[47]. Further complications can occur in patients who require prolonged high dose steroid therapy, such as pediatric patients, who can develop a cushingoid appearance, with abnormal hair growth, truncal obesity and excess facial fat deposits, along with decreased ability to attain normal height and stature[42].

3. IMMUNOBIOLOGY OF ORGAN ALLOGRAFT REJECTION

Ongoing success in transplantation today is primarily due to drug-mediated immunosuppression. Historically, chemical means were employed to dampen the immune response and prolong allograft survival without an understanding of how they worked. This was coupled with a lack of clear understanding of how the immune system recognised and mounted a response to the grafted tissue. Things are quite different today. In the age of rational drug design, an understanding of the mechanism of action of a given agent is one of the first problems solved scientifically. Likewise, an understanding of the mechanism of allorejection and parallel processes has enabled better use of drugs for immunosuppression, and fuelled development and research into new products and applications. Where the drug fits in is very important, and often is very interesting.

Allograft rejection occurs as a result of co-ordinated activation of alloreactive T-cells and antigen presenting cells (APC). Through the release of inflammatory mediators, cytokines and through cell-cell contact, helper T-cells (CD4+), cytotoxic T-cells(CD8+), antibody secreting B-cells and other pro-inflammatory cells are recruited. Cells that respond to alloantigen are activated to proliferate, respond and are concentrated in the graft and in the regional lymph nodes. A massive anti-allograft response is mounted[48].

a. Mechanism of T-cell Activation

T-cell activation is a highly complicated and regulated process. It begins when the T-cell recognises peptide fragments that were processed by an APC and presented in the binding groove of the major histocompatibility complex proteins (MHC) on the surface of that APC[49,50]. Some T-cells are able to recognise donor antigens in the context of donor APC, as in direct recognition, where other T-cells recognise the donor antigens that are processed and presented by self APC, as in indirect recognition[51]. The significance of each of these processes to allorejection or allotolerance remains undefined.

The T-cell receptor (TCR) is the starting point of this cellular reaction. It is the TCR that interacts specifically with MHC-peptide to initiate signal that travels from the cell membrane of the T-cell to the nucleus. The T-cell must have a TCR specific for the peptide antigen, and must recognise both the MHC molecule and the peptide within the binding site of MHC. Although the TCR-MHC interaction is of utmost importance, it is of low affinity, and the TCR does not have the cytoplasmic equipment to participate in signal transduction. The complex is first stabilised by the action of co-expressed proteins on the T-cell. CD4 and CD8 serve this purpose, bind to non-polymorphic domains on MHC class II and class I molecules, respectively, and are expressed on exclusive T-cell subsets[52]. Antigen-MHC binding induces a conformational change in the TCR-associated complex, CD3, which initiates intracellular signalling through the generation of second messengers[53,54].

Protein tyrosine kinase (PTK) activity mediates the next step. $p59^{fyn}$ and ZAP70, two PTKs of the src-homology family, are associated with the TCR/CD3 complex. Another src PTK, $p56^{lck}$, is associated with the cytoplasmic domain of CD4 and CD8[55]. Antigen binding is rapidly followed by phosphorylation of CD3 α,β and γ. chains. The protein tyrosine phosphatse, CD45 is recruited to the site and activates $p56^{lck}$ by dephosphorylating tyrosine 505 (Y505), the autoinhibitory site[55].

This is where the calcium-mediated processes begin. Tyrosine phosphorylation of phospholipase $C\gamma_1$ follows, and its activation results in the enzymatic hydrolysis of membrane lipids. Phosphoinositol 4,5-bisphosphate (PIP_2) is rapidly hydrolyzed to generate two intracellular second messengers: inositol 1,4,5-trisphosphate (IP_3) and diacylglycerol (DAG)[56]. IP_3 mobilises calcium ions (Ca^{2+}) from intracellular stores, which facilitates the binding of DAG to protein kinase C (PKC). This enables the localisation of PKC to the membrane, where the serine/threonine kinase is active and able to phosphorylate several substrates, including I-κB)[56].

The sustained increase in intracellular Ca^{2+} also results in the activation of the calcium-dependent protein, calmodulin, and the activation of calmodulin-dependent kinases and the calmodulin-dependent phosphatase, calcineurin[57]. Calcineurin cleaves the phosphate from several components, including the cytosolic component of the nuclear factor of activated T-cells (NF-ATc). This dephosphorylation enables NF-ATc to translocate to the nucleus and combine with the nuclear component of NF-ATn, to form a heterodimer that binds the IL-2 promoter and contributes to IL-2 transcription[58].

IL-2 is the autocrine growth factor for most normal T-cells. Transcription of IL-2 followed by its production and secretion are required for the proliferative aspect of T-cell activation, preceding cellular effector formation and enabling clonal expansion. The transcription of IL-2 begins approximately one hour after TCR/CD3 engagement by antigen-MHC[58], and occurs in a temporally organised manner with the production and activation of many cellular factors. The expression of more than 70 molecules is required for the synthesis of a single growth factor such as IL-2[35].

Autocrine-induced T-cell proliferation is a consequence of IL-2 production and subsequent signalling[59,60]. After the secretion of IL-2, the lymphocyte is able to upregulate the expression of the p55 subunit (β-chain) of the cell-surface receptor for IL-2 (IL-2R), which is present only at

very low levels on unstimulated T-cells, and produce the α-chain, which is only present on the surface of activated T-cells. α and β, together with the IL-2 specific γ-chain, come together to form the high-affinity heterotrimeric IL-2 receptor. β and γ-chains contain cytoplasmic domains required for intracellular signaling[61]. The receptor affinity and expression modulation occur as a result of binding of IL-2 to low affinity IL-2R in small amounts, and as a consequence of TCR engagement[62].

Signaling from IL-2R occurs in a protein tyrosinekinase (PTK)-dependent manner. Several src protein tyrosine kinases are associated with the IL-2 receptor[63], as is Raf-1, a protein serine/threonine kinase which later translocates to the cytosol in an IL-2-dependent fashion[64]. The events that follow are not well defined: IL-2 stimulation leads to the expression of DNA binding proteins including c-jun, c-fos, c-myc, which each contribute to cell cycle progression[65]. Thus IL-2 binding and subsequent signalling through the high affinity receptor is an initiator of mitosis.

b. Requirement for Costimulation

T-cell signaling by way of the TCR is insufficient for T-cell proliferation – complete activation is contingent upon the reception of a secondary signal in addition to the antigenic interaction of antigen-specific T-cell and APC. The T-cell has many cell surface proteins that can interact with ligands on the APC to constitute such a signal. Examples include: T-cell CD2 interaction with CD58 (leukocyte factor antigen, LFA-3) on the APC; T-cell CD11a/CD18 (LFA-1) interaction with CD54 (ICAM-1); T-cell CD5 interaction with APC CD72[66,67]. The net result of delivery of both the antigenic signal and the second, co-stimulatory signal is stable transcription of IL-2 and other genes contributing to T-cell activation and proliferation.

There is a variety of cytokines secreted by APC that can also provide the costimulatory signal via Ca^{2+}-dependent signaling pathways, like IL-11 and IL-6[68]. Further, only stimulated APCs express B7/BB1 cell-surface proteins, and activated T-cells often express the B7-ligand binding

proteins CD28 and CTLA-4. CD28 stimulates a Ca^{2+}-independent pathway that leads to stable IL-2, IL-2R alpha and other genes resulting in vigorous proliferation[69-71]. The Ca^{2+}-dependent pathway, mediated by cytokines, is sensitive to CsA, whereas the Ca^{2+}-independent pathway, mediated by CD28/CTLA-4, is relatively resistant to the cellular inhibition by CsA[72].

B-cell stimulation is also governed by the two-signal system. Both antigenic and co-stimulatory signals are required[73,74]. The antigen binds the B-cell surface immunoglobulin, providing signal one, and the co-stimulation requirement is fulfilled by T-cell derived cytokines (IL-2, IL-4) or by CD40-CD40 ligand interaction[74].

c. Cell Proliferation – the Cell Cycle

Mitosis is the process of cell division in somatic cells. The actual step of cell division is preceded by many cellular events that have been organised into the process called the cell cycle, which is divided into distinct phases. Cells begin the cell cycle containing a single copy (1n) of the chromosomal material. The cell spends a period of time in the first growth phase (G1), where cellular components are produced, proteins and other required structures and molecules are synthesised and nutrients are absorbed. This is followed by the synthesis phase (S) where DNA replication occurs. The cell now has two complete copies of the chromosomal material (2n). A second growth phase (G2) separates S phase from mitosis (M) phase. In M phase, the nuclear division occurs and is closely followed by cellular division[75].

M phase is further separated into several sub-phases. The chromosomes condense and separate from one another, the mitotic spindle is formed and the nuclear membrane dissolves during prophase. The individual chromosomes are aligned on the mitotic spindle briefly during metaphase. The cell divides the copies of nuclear material during anaphase, as one copy of the chromosomal material (1n) is pulled to each side of the cell. The chromosomes decondense and a nuclear membrane forms around each of the bundles of nuclear material

during telophase, and the cell cycle is complete when the cell divides itself into two during the process of cytokinesis[75].

Mitosis is a highly regulated process with many cellular conditions that must be met at each stage before the next phase of the cell-cycle can be entered. These are also called checkpoints.

Deoxyribonucleic acid (DNA) synthesis in S phase is a critical step in mitosis. In order for DNA synthesis to occur, there must be an adequate nucleotide pool accumulated. This requires a tremendous outlay of energy and material for chemical construction of the DNA. Nucleotide synthesis is accomplished by two groups of cellular pathways. The *de novo* pathways provides for synthesis of nucleotides from low molecular weight precursors, and the salvage pathways use pre-formed, semi-degraded purine or pyrimidine compounds for synthesis of new nucleotides.

4. THE CYCLOSPORINE ERA

CsA was introduced in 1983, and resulted in an increase of graft survival of 20% at one year[76]. It made liver, pancreas, lung and cardiac transplantation practical and successful in addition to renal transplantation[23]. Despite over fifteen years of clinical experience with CsA, it remains one of the more difficult drugs to use safely and effectively[77-80]. Narrow therapeutic range, variability in absorption[81] and metabolism[82], numerous drug interactions, and its own toxic effects are ongoing challenges.

Nephrotoxicity is the most serious toxic effect of CsA therapy[83]. It is almost uniformly present in CsA-treated patients, and has functional, structural, and chronic, irreversible components.

Functional changes in the kidney occur as a result of decreased renal blood flow. Altered vasoactive substance (endothelin/prostacyclin) balance leads to renal hypertension by vasoconstriction of the afferent arteriole[83,84]. This leads to decreased renal perfusion, causing functional changes such as decreased glomerular filtration rate (GFR) and altered tubular resorption. Biochemical effects of these functional changes are decreased serum magnesium, increased serum calcium and uric Acid[84,85], increased serum creatinine and urea, and excretion of enzymes and aminoacids in the urine[83,86].

CsA also induces structural changes in the renal tubules, with vacuolisation of the proximal tubule, the appearance of giant mitochondria, cellular necrosis and micro-calcification within the proximal and distal tubules[84,85]. This also may account for some of the biochemical changes associated with CsA toxicity.

Both the functional and structural changes described here are reversible if addressed early with CsA dose reduction[84,86]. If not addressed, irreversible chronic renal changes occur. Progressive interstitial fibrosis and arterial atrophy typify these chronic changes. Chronic CsA toxicity is not reversible by dose reduction and is thought to be due to chronic alterations in renal vascular tone. This leads to histological changes such as glomerular collapse and arteriolopathy, followed by fibrosis in a typically banded pattern.

Other prevalent and unpleasant effects of CsA therapy include: peripheral tremor and other neurologic toxicity, which occurs in approximately 20% of treated patients[77,87]; hepatotoxicity, occurring in about 50%[77,88]; vascular complications stemming from increased platelet aggregation and altered prostaglandin secretion,

leading to hypertension[89]; CsA associated hyperlipidemia[90]; gum hyperplasia hypertrichosis of the skin; and diabetogenesis[91].

The mechanism of action of CsA has been described in some detail. CsA enters the cell and binds to its intracellular receptor, cyclophilin. The CsA-cyclophilin complex binds to calcineurin, in a pentamer that includes calcium and calmodulin. This inhibits the phosphatase activity of calcineurin, preventing the dephosphorylation of nuclear factor of activated T-cells (NF-AT), preventing its translocation to the nucleus, where it would activate the expression of lymphokine genes[92]. One such gene encodes the T-cell activation factor: interleukin-2 (IL-2). It is also thought that several toxic side effects of CsA are calcium-mediated and are related to calcineurin inhibition in various tissues.

Measures have been taken to try to improve CsA therapy. There is a strong, well-supported movement to routinely monitor drug levels for dosage adjustment[93,94] and to optimise and individualise therapy through pharmacokinetic profile analysis[95]. Additionally, a new microemulsion oral formulation was developed, tested and introduced in an attempt to decrease variability in absorption and normalise pharmacokinetic parameters[96,97]

5. THE SEARCH FOR NEW IMMUNOSUPPRESSIVE DRUGS

Even with triple therapy, acute rejection occurs in approximately 50% of patients. This leads to requirement for additional immunosuppression in short courses. This is usually accomplished by an increase in frequency of administration and/or dose of steroids, or administration of ALG or MALB to deplete the offensive lymphocyte population. As this therapy is non-specific, it results in the suppression of the entire immune system. The net result is a dampening or reversal of the rejection episode, but also increased risk of infective and oncologic complication.

The increases in morbidity and mortality caused by acute rejection, toxic, infectious and neoplastic complication, coupled with increased costs of diagnosis and treatment is a significant burden. This has fuelled the search for new drugs for use in immunosuppression, and their development and refinement. The goal is to develop new compounds that are more selective and specific for immunosuppression of allotransplantation, and which exhibit fewer toxic effects. In the past ten years, several of these compounds have found their way to the clinic, and use is expanding. Specifically, tacrolimus, mycophenolate mofetil, mizoribine and rapamycin will be discussed.

a. Tacrolimus

Tacrolimus (FK506, Fujisawa) is produced by *Streptomyces tsukabaensis* and has an unusual chemical structure. It is a macrolide lactone with a hemiketal masked α,β-diketoamide incorporated into a 23-membered ring[98].

Tacrolimus has 10 to 100 times the immunosuppressive potency of CsA *in vitro*[99], and suppresses the secretion of IL-2 in lymphocytes by acting early in the T-cell activation pathway. It first binds to its intracellular binding protein, the 12 kDa FK506 binding protein (FKBP-12)[99]. Like CsA-cyclophilin, the tacrolimus-FKBP-12 complex binds to calcineurin, in a pentamer that includes calcium and calmodulin. This inhibits the phosphatase activity of calcineurin, preventing the dephosphorylation of NF-AT, preventing its translocation to the nucleus, where it would activate the expression of lymphokine genes[92].

Most clinical trials where tacrolimus replaced CsA in triple therapy showed that tacrolimus has slightly increased immunosuppressive activity as compared to that of CsA[100-107]. For liver and kidney allograft trials, patient and graft survival at one year were not improved with tacrolimus therapy[100-107]. However, the incidence of rejection at one year was decreased in the tacrolimus groups, as was the requirement for both total maintenance immunosuppression and adjuvant steroid usage. Where tacrolimus was used at low or concentration controlled dosages, the toxic

effects reported were similar or slightly worse when compared to the CsA groups, with the main area of concern being nephrotoxicity, neurotoxicity and diabetogenesis[100-107]. Further reports surfaced indicating that FK506 is suitable for rescue therapy for patients on CsA with steroid-resistant acute rejection[108-111]. Despite a lack of clear improvement in patient and graft survival, by decreasing acute rejection in the first year post-transplant, tacrolimus may provide advantage in long term graft survival, as predicted by actuarial studies[107].

Tacrolimus and CsA have similar effects on the lymphocyte and similar short-term outcomes and tacrolimus is now being used in some centres as replacement for CsA in double and triple therapy for prophylaxis for organ allotransplantation.

b. Mycophenolate Mofetil

The prodrug mycophenolate mofetil (MMF, Cellcept, Roche) is a semi-synthetic derivative of mycophenolic acid (MPA), which is a product of several *Penecillium* species[113]. The morpholinoethyl ester of MPA was constructed to decrease gastrointestinal effects and increase bioavailability of MPA in oral formulation[114,115].

MMF is rapidly reconverted, *in vivo* by ubiquitous cytosolic non-specific esterases, to the active compound, MPA[116]. MPA is a non-competitive inhibitor of the rate-limiting enzyme for *de novo* purine biosynthesis, namely inosine monophosphate dehydrogenase (IMPDH) type II[117], which is preferentially used by T and B lymphocytes during replication[38]. Thus, lymphoproliferation is inhibited, almost selectively, by MPA.

There are important *in vitro* effects of MPA as well. After alloantigen or mitogen stimulation, T and B lymphocyte proliferation is inhibited, as are antibody formation and cytotoxic T-cell generation[118,119]. The depletion of purine nucleotides also leads to the inhibition of glycosylation of leukocyte and endothelial cell glycoproteins, as guanine triphosphate (GTP) and uridine monophosphate (UMP) are required by GTP- and UMP-dependent fucosyl- and mannosyl-

transferases [120,121]. Glycosylation is a critical step in the expression of functional adhesion molecules including L-selectin, E-selectin and very late activation antigen (VLA)-4[122,123]. Theoretically, this could impair lymphocyte and other immune cell chemotaxis and migration in addition to lymphocyte activation and proliferation.

Encouraging results emerged in animal models of transplantation, including kidney, heart and small bowel[124]. A large clinical study followed, and in three composite trials, MMF, in two fixed doses, was compared to both placebo and AZA[125-128]. At one year, patients receiving MMF had a decreased incidence of biopsy-proven rejection and fewer requirements for steroids and anti-lymphocyte therapy for rejection episodes and steroid-resistant rejection, as compared to both the AZA and placebo groups. Patient survival was not significantly different, and graft survival was marginally better in the MMF groups. The safety profile of MMF was found to be similar to that of AZA, with only a slight increase in diarrhoea in the MMF group.

MMF was designed to replace AZA. It inhibits the same enzyme (IMPDH) by a mechanism that is more selective for lymphocytes, and may not adversely affect other organ systems and cell-types. Although the data from the clinical trials does not support the hypothesis that MMF is less toxic and more specific than AZA in the patient, this may not have been studied appropriately. It is difficult to assess the adequacy of treatment in a dose-controlled, rather than a concentration-controlled study. In the future, more experience, refined use and monitoring may improve the safety profile of this drug.

c. Rapamycin

Rapamycin (sirolimus, Wyeth-Ayerst) was discovered in 1975, and is produced by the filamentous bacterium *Streptomyces hygroscopicus*[129]. It has an interesting structure, depicted in Figure I-1. Rapamycin has considerable homology to tacrolimus, with a hemiketal masked α,β-diketoamide incorporated into its macrolide ring. Rapamycin was initially investigated for its antifungal[130] and anti-tumour activities[131]. It is also an inhibitor of the immune response[132-134]

Figure I-1 Structure of rapamycin

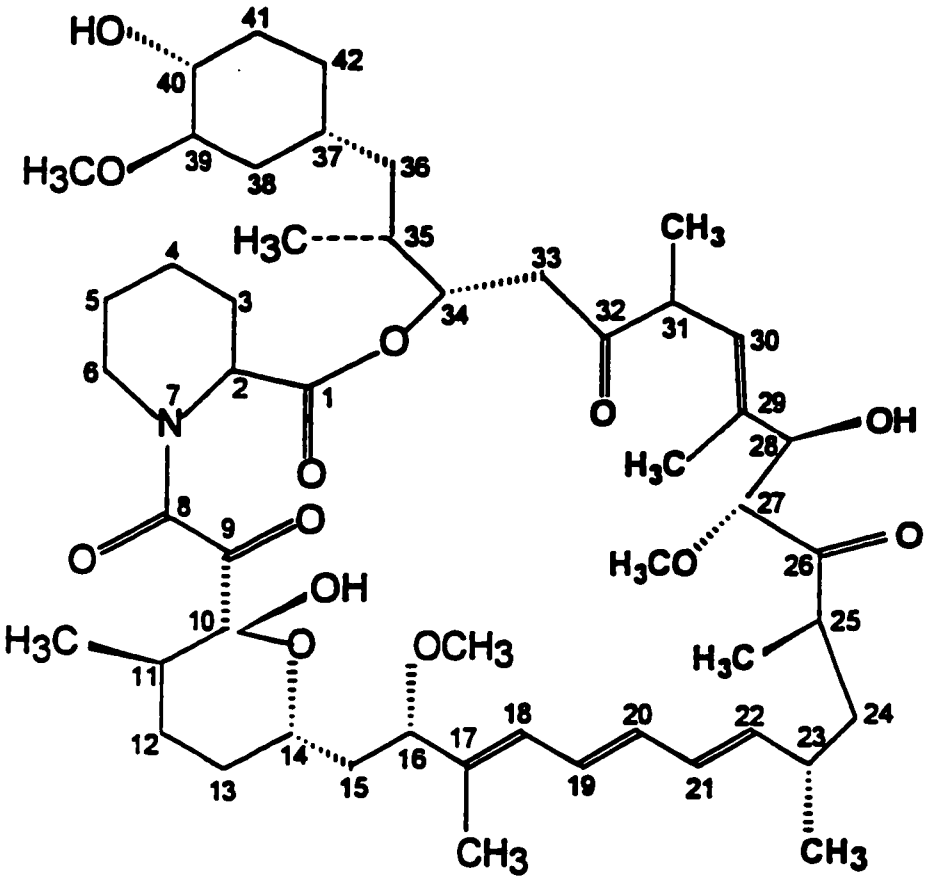

although initially its development was not pursued in this area. Only in the late 1980s, after tacrolimus was described and developed, and the search for structural analogues with similar activity was initiated, was rapamycin revisited and considered a candidate for immunosuppression.

In vitro studies demonstrate CsA and rapamycin act synergistically to inhibit T and B-cell proliferation[135,136]. Rapamycin and tacrolimus act in additive fashion in equimolar concentrations to inhibit concanavalin A stimulated T-cell proliferation[137,138], but are antagonistic when used in 50 to 1000 fold molar excess[136,138-149], suggesting that their common binding protein, FKBP-12, is the site of antagonism.

Like FK506, *in vitro*, rapamycin is 10 to 100 times more potent than CsA at inhibiting lymphoproliferation[150-152], but it acts on a T-cell pathway distinct from the calcium-dependent cytokine release pathway that FK506 and CsA inhibit. The mechanism of action of rapamycin is discussed later.

Animal models of allotransplantation indicate rapamycin is effective alone and is synergistic in combination with CsA at prolonging allograft survival[153-155]. In combination with mycophenolic acid, rapamycin provides for significant prolongation of xenograft survival[156].

Clinical trials with rapamycin are ongoing, and it has recently been approved for use in renal transplant recipients. The results from the phase IIA (efficacy) study in renal transplantation have been released. In this study, rapamycin was used at low and moderate dose in combination with concentration-controlled CsA and standard dose steroids. At one year post-transplant, there was a marked reduction in rejection episodes in the rapamycin groups (6.7% vs. 34%), and the withdrawal of steroids was facilitated as early as one-week post-transplant[157]. The multi-centre, randomized, placebo controlled phase IIB study in renal transplantation also showed that rapamycin decreased rejection rates at one year from 40% to <10% in patients

treated with full-dose CsA, and permitted the halving of CsA dosages in non-black recipients without compromising the allograft[152].

Quiescent renal transplant patients on CsA/steroids who were given rapamycin for two weeks were evaluated for alterations in biochemical, physical and hematologic parameters. Addition of rapamycin did not alter renal function (serum creatinine, GFR), liver function tests, triglycerides, or blood pressure or neurologic parameters. Cholesterol was significantly increased in the rapamycin-treated group, and both platelet and WBC counts were decreased as compared to controls[158]. It is notable that the side effect profiles of rapamycin and CsA do not overlap, and that rapamycin does not appear to potentiate CsA nephro- and neuro-toxicity in this patient population. However, the side effect profile of long-term rapamycin administration in clinical patients has been evaluated, and its efficacy and toxicity are frequently related to pharmacokinetic behaviour, including the trough concentration at steady state, the clearance, the magnitude of the area under the rapamycin concentration-time curve (AUC) or the CsA AUC in patients taking a rapamycin-CsA-prednisone regimen[159].

It is expected that rapamycin will be a drug used in conjunction with CsA. Because of their synergistic interactions, rapamycin will be used in conjunction with a reduced CsA and steroid dose.

6. MECHANISM OF ACTION OF RAPAMYCIN

Rapamycin has a mechanism of action distinct from all other known immunosuppressive drugs. Tacrolimus and CsA inhibit calcium-dependent cytokine release [160-164]. Instead, rapamycin interferes with a later step in the lymphocyte activation pathway – it inhibits the progression of the cytokine stimulated lymphocyte from G1 to S in the cell cycle by way of translational control. This results in anti-proliferative effects that are not restricted to cells of lymphoid origin.

Once inside the lymphocyte, rapamycin binds to its intracellular binding protein, FKBP-12[165]. The rapamycin-FKBP complex does not elicit cellular effects on its own. Instead, it binds to another protein. The intracellular target protein of rapamycin-FKBP12 is called the mammalian target of rapamycin (mTOR, also FKBP and rapamycin affector protein, FRAP)[166-169], a PI3K-related kinase (PIKK)[170-173]. Members of this recently described group of enzymes are each involved in one of two cellular functions: maintenance of cell-cycle checkpoints governing responses to DNA damage (ATM, ATR, DNA-PK)[174,175], or in the regulation of other kinases and binding proteins involved in the regulation of transcription.

p70 S6 kinase is a downstream enzyme regulated by mTOR, and it is responsible for the phosphorylation of the 40S ribosomal protein, S6[176]. This results in an increase in mRNA recruitment into polysomes and an increase in the rate of protein synthesis, with two to ten-fold preferential increase in translation of 5'-terminal oligopyrimidine (5'-TOP)-containing mRNA[177,178]. These 5'-TOP mRNAs encode the ribosomal proteins S3, S6, S14, S24 and translation elongation factors eEFIA and eEF2 – components and facilitators of protein synthesis and the secreted cytokine insulin-like growth factor 2 (IGF-2)[179]. As mTOR is regulated upstream by cytokine receptor-associated PI3K, the net result is the linkage of cytokine signaling from the receptor to selective increases in messenger ribonucleic acid (mRNA) translation in the cell.

p70 S6 kinase activity is regulated by numerous signaling pathways, not just by mTOR. It is phosphorylated on at least ten serine/threonine residues by various cytosolic kinases. Although only three of these serine/threonine phosphorylated residues are rapamycin sensitive, one (T389) appears to be crucial for p70 S6 kinase activity[180]. Treatment with rapamycin leads to inactivation of p70 S6 kinase and dephosphorylation of S6[176], but only results in a 15% decrease in protein synthesis[177,178,181].

p70 S6 kinase is not the end of the rapamycin story. Although rapamycin is a potent inhibitor of p70 S6 kinase in all cell types, not all cells go into cell-cycle arrest, nor are all inhibited from proliferating by exposure to rapamycin[182]. Further, p70 S6 kinase knockout mice remain fully sensitive to rapamycin inhibition of cell cycle progression[183]. This may be due to the role mTOR plays as an upstream regulator of PHAS-1 (4E-BP1), a binding protein that duly regulates the activity of eukaryotic initiation factor (eIF)-4E. Cellular exposure to rapamycin inhibits serum or mitogen-induced phosphorylation of PHAS-1[184], which prevents its dissociation from eIF-4E. In the absence of PHAS-1 binding, eIF-4E associates with eIF-4G, eIF-4A and eIF-4B, which assemble together on a strand of mRNA, forming an active holoenzyme (helicase) responsible for unravelling the 5'-untranslated region (5'-UTR) of the mRNA and facilitating ribosome binding[185]. Long complex 5'-UTR can form stable hairpins and participate in like structure formation, which needs to be deconvoluted before ribosome binding can occur. Translationally regulated mRNA with a particularly long, complex 5'-UTR include FGF-5, c-myc and ornithine decarboxylase[185].

eIF-4E is thus responsible for binding the 5'-methylguanosine cap of the mRNA and enabling the initiation of translation by the ribosome. Initiation of translation of mRNAs with long and highly structured 5'-UTR is permitted only after binding by eIF-4E and its accessory subunits. As initiation of translation is the rate limiting step in protein synthesis [186], and as mRNA for several critical G1-phase regulators contain this highly structured 5'-UTR[187-189], it is not hard to appreciate the importance of translational regulation in G1 to S phase progression, the role of mTOR in this process, and its inhibition by rapamycin.

7. PHARMACOKINETICS AND METABOLISM OF RAPAMYCIN

At the onset of this study, there was very little information available regarding the pharmacokinetics (PK) and metabolism of rapamycin. It was demonstrated that rapamycin is metabolised by rat small intestinal and human liver microsomes *in vitro*[190]. Rapamycin is a substrate for the cytochrome P-450 (CYP, EC 1.14.14.1) family of enzymes, and the CYP 3A

sub-family is primarily responsible for specific oxidative metabolism of rapamycin[191]. Several metabolites had been identified and generally described as being either demethylated, hydroxylated, dihydroxylated or demethylated and hydroxylated on portions of the parent molecule. The structural elucidation of only one metabolite is complete, with the positive identification of the 39-O-demethylrapamycin metabolite[190]. Two metabolites had been tested for immunosuppressive activity in the phytohemagglutinin (PHA)-stimulated lymphocyte assay. The 39-O-demethylated metabolite retained approximately 10% of the activity of rapamycin, and another hydroxylated metabolite tested retained approximately 15% activity[190].

The PK parameters for rapamycin have been determined in several animal models. Indications are that rapamycin in its oral, non-aqueous liquid formulation at relevant doses has a low and variable bioavaliability (F) in the order of 0.15, and a relatively long (~60h) half life ($T_{1/2}$)[191]. In the rabbit and canine transplantation models, doses producing whole blood trough levels of greater than 5-10 μg/L are associated with decreased incidence of allo-graft rejection, and levels of >60 μg/L are associated with increases in drug-related side-effects[192]. In the rat model, prolonged graft survival was reported with whole blood troughs >0.5 μg/L[193].

7. REFERENCES

1. Pustak P. Sacrifice for Dashka from Vayu Purana. Wilson HH. The Vishnu Purana. A system of Hindu mythology and tradition. Calcutta: Sankar Bhattacharya, 1961: 53.

2. Mackenzie DA. Indian Myths and Legends. Divinities of the Epic Period. Chapter 8. Long Wood Press, Inc., 1978: 138-84.

3. Hamilton D. Kidney Transplantation: a history. Morris PJ. Kidney Transplantation: Principles and Practice. 4th edition. Philadelphia, PA: Saunders, 1994: 1-7.

4. Hume DM, Merrill JP, Miller BF, Thorn GW. Experiences with renal homotransplantation in the human: report of nine cases. J Clin Invest 1955; 34:327-82.

5. Kuby J. Transplantation immunology. Kuby J. Immunology. 2 edition. New York: W.H. Freeman and Company, 1994: 559-70.

6. Murray JE, Merrill JP, Harrison JH. Kidney transplantation between seven pairs of identical twins. Ann Surg 1958; 148:343-59.

7. Kahan BD. Transplantation timeline. Transplantation 1991; 51:1-21.

8. Hitchings GH, Elion GB. The chemistry and biochemistry of purine analogs. Ann N Y Acad Sci 1954; 60:195-.

9. Schwartz R, Dameshek W. Drug-induced immunological tolerance. Nature 1959; 183:1682-3.

10. Calne RY. The rejection of renal homografts:inhibition in dogs by 6-mercaptopurine. Lancet 1960; 1:417-8.

11. Murray JW, Merrill JP, Harrison JH *et al.* Prolonged survival of human kidney homografts by immunosuppressive drug therapy. N Engl J Med 1963; 268:1315-23.

12. Goodwin WE, Mims MM, Kaufman JJ. Human renal transplant III: technical problems encountered in six cases of kidney homotransplantation. Trans Am Assoc Genitourin Surg 1962; 54:116.

13. Starzl TE, Marchioro TL, Waddell WR. The reversal of rejection in human renal homografts with subsequent development of homograft tolerance. Surg Gynecol Obstet 1963; 117:385-95.

14. Morris PJ, Chan L, French ME *et al.* Low dose oral prednisolone in renal transplantation. Lancet 1982; 1:525-7.

15. Powelson JA, Cosimi AB. Antilymphocyte globulin and monoclonal antibodies. Morris PJ, ed. Kidney Transplantation: Principles and Practice. 4 edition. Philadelphia, PA: Saunders, 1994: 215-32.

16. Howard RR, Asfis N, Woodruff MF. Comparative immunogenicity of anti-lymphocyte globulin in solution and adsorbed on lymphocytes. Nature 1968; 220:816-8.

17. Colley DG, Waksman BH. Cytotoxic effect of normal rabbit serum on lymphoid cells. Transplantation 1970; 9:395-404.

18. Woodruff MF. Antilymphocyte serum. Antibiot Chemother 1969; 15:234-49.

19. McLaughlin JS, Woodruff MF. Isolation of an active fraction of antilymphocyte serum. Surg Forum 1970; 21:279-81.

20. Sarles HE, Remmers AR, Fish JC *et al.* Depletion of lymphocytes for the protection of renal allografts. Arch Int Med 1970; 125:443-50.

21. Weksler ME, Bull G, Schwartz GH, Stenzel KH, Rubin AL. Immunologic response of graft recipients to antilymphocyte globulin: effect of prior treatment with aggregate-free gamma globulin. J Clin Invest 1970; 49:1589-95.

22. Borel JF, Feurer C, Magnee C *et al.* Effects of the new anti-lymphocyte peptide cyclosporin A in animals. Immunology 1977; 32:1017-25.

23. Calne RY, Rolles K, White DJK *et al.* Cyclosporine A initially as the only immunosuppressant in 34 recipients of cadaveric organs. Lancet 1979; 2:1033-6.

24. Powles RL, Barrett AJ, Clink H *et al.* Cyclosporin A for the treatment of graft versus host disease. Lancet 1980; 2:327-9.

25. European Multicentre Trial Study Group. European Multicentre Trial:cyclosporin A as the sole immunosuppressive agent in recipients of kidney allograft from cadaver donors. Lancet 1982; 2:57-60.

26. Morris PJ. Cyclosporine. Morris PJ, ed. Kidney Transplantation: Principles and Practice. 4 edition. Philadelphia, PA: Saunders, 179-201.

27. Keown PA. Emerging indications for the use of cyclosporine in organ transplantation and autoimmunity. Drugs 1990; 40:315-25.

28. Seifeldin RA. Cost and effectiveness analysis of immunosuppressive drug regimens in renal transplant UMI, Ann Arbor, MI: University of Minnesota, 1993.

29. Moltzahn AE, Burton JR, McCormick P *et al.* Edmonton, Canada: Hope Program, 1993.

30. Walden JA, Stevenson LW, Dracup K *et al.* Extended comparison of quality of life between stable heart failure patients and heart transplant recipients. J Heart Lung Transplant 1994; 13:1109-18.

31. Loughlin KR, Tilney NL, Ritchie JP. Urologic complications in 718 renal transplant patients. Surgery 1984; 297:297-302.

32. Allen RDM, Chapman JR. Renal transplantation. Chapter 9. London, UK: Edward Arnold Press, 1993.

33. Rossi SJ, Schroeder TJ, Hariharan S, First MR. Management of the adverse effects associated with immunosuppressive therapy. Drug Safery 1993; 9:104-31.

34. Koneru B, Jaffe R, Esquivel CO *et al.* Adenoviral infection in pediatric liver transplant recipients. JAMA 1987; 258:489-92.

35. Ryffel B. The carcinogenicity of ciclosporine. Toxicology 1994; 73:1-22.

36. Allen RDM, Chapman JR. Renal transplantation. Chapter 13. London, UK: Edward Arnold Press, 1993.

37. Sheil AGR. Complications of immunosuppression in renal allograft recipients: malignancy. Clin Transplant 1994; 5:573-9.

38. Natsumeda Y, Carr SF. Human type I and type II IMP dehydrogenase as drug targets. Ann N Y Acad Sci 1993; 696:88-93.

39. Perico N, Remuzzi G. Prevention of transplant rejection: current treatment, guidelines and future developments. Drugs 1997; 54:533-70.

40. Simmons R, Canafax D, Strand M. Management and prevention of cyclosporine A nephrotoxicity after renal transplant: use of low dose cyclosporine A, azathioprine and prednisone. Transplant Proc 1985; 17:266-75.

41. First M, Alexander J, Wodhwa N. The use of low doses of cyclosporine A, azathioprine and prednisone in renal transplantation. Transplant Proc 1986; 18:132-5.

42. Salaman FR. Immunosuppressive therapy. Lancaster, UK: MTP Press LTD, 1981.

43. Maddocks JL, Lennard L, Amess J, Amos R, Thomas RM. Azathioprine and severe bone marrow suppression. Lancet 1986; 1:156.

44. Bolman RM, Elick B, Olivari MT *et al.* Improved immunosuppression for heart transplantation. Heart Transplantation 1985; 4:315-8.

45. Katz MR, Barnhart GR, Szentpetery S *et al.* Are steroids essential for successful maintenance of immunosuppression for heart transplantation? J Heart Transplant 1987; 6:293-7.

46. Markell M, Friedmann E. Hyperlipidemial after organ transplantation . Am J Med 1989; 87:51-67N.

47. Carpenter CB. Immunosuppression in organ transplantation. New Engl J Med 1984; 297:297-302.

48. Suthanthiran M, Strom TB. Renal transplantation. N Engl J Med 1994; 331:365-76.

49. Unanue ER, Cerottoni J-C. Antigen presentation. FASEB J 1989; 3:2496-502.

50. Germain RN. MHC-dependent antigen processing and peptide presentation: providing ligands for T lymphocyte activation. Cell 1994; 76:287-99.

51. Shoskes DA, Wood KJ. Indirect presentation of MHC antigens in transplantation. Immunol Today 1994; 15:32-8.

52. Miceli MC, Parnes JR. The role of CD4 and CD8 in T-cell activation. Semin Immunol 1991; 3:133-41.

53. Weiss A, Littman D.R. Signal transduction by lymphocyte antigen receptors. Cell 1976; 263-264.

54. Clevers H, Alarcon B, Wildeman T, Terhorst C. The T-cell receptor/CD3 complex; a dynamic protein ensemble. Ann Rev Immunol 1988; 6:629-62.

55. Klausner RD, Samelson LE. T-cell antigen receptor activation pathways: the tyrosine kinase connection. Cell 1991; 64:875-8.

56. Nishizuka Y. Intracellular signaling by hydrolysis of phospholipids and activation of protien kinase C. Science 1992; 258:607-14.

57. Abbas AE, Lichtman AH, Pober JS. Cellular and Molecular immunology. Philadelphia, PA: Harcourt Brace, 1991.

58. Taniguchi T. Regulation of cytokine gene expression. Ann Rev Immunol 1988; 6:439-64.

59. Smith CA. Interleukin-2: inception, impact, and implications. Science 1988; 240:1169-76.

60. Waldmann TA. The interleukin-2 receptor. J Biol Chem 1991; 266:2681-4.

61. Takeshita T, Asao H, Ohtani K *et al.* Cloning of the gamma-chain of the IL-2 receptor. Science 1992; 257:379-82.

62. Schreiber SL, Crabtree GR. The mechanism of action of cyclosporine and FK-506. Immunol Today 1992; 13:136-42.

63. Hatakeyama M, Kono T, Kobayashi N *et al.* Interaction of the IL-2 receptor with the src-family kinase p56lck. Science 1991; 252 :523-8.

64. Maslinski W, Remillard B, Tsudo M, Strom TB. Interleukin-2 induces tyrosine kinase dependent translocation of active raf-1 from the IL-2 receptor into the cytosol. J Biol Chem 1991; 266:14167-70.

65. Shibuya H, Yoneyama M, Ninomiya-Tsuji J, Matsumoto K, Tanaguchi T. IL-2 and EGF receptors stimulate the hematopoietic cell cycle via different signaling pathways: demonstration of a novel role for c-myc. Cell 1992; 70:57-67.

66. Schwartz RH. T-cell anergy. Sci Am 1993; 269:62-71.

67. Suthanthrian M. Signaling features of T-cells: implications for the regulation of the anti-allograft response. Kidney Int 1993; 44:S3-S11.

68. Williams JM, DeLoria D, Hansen JA *et al.* The events of primary T-cell activation can be suppressed by use of sepharose-bound anti-T3 [64.1] monoclonal antibody and purified interleukin-1. J Immunol 1985; 135:2249-55.

69. June CH, Ledbetter JALPS, Thompson CB. Role of the CD28 receptor in T-cell activation. Immunol Today 1990; 11:211-6.

70. Linsley PS, Brady W, Urnes M, Grosmaire LS, Damle NK, Ledbetter JA. CTLA-4 is a second receptor for the B-cell activation antigen B7. J Exp Med 1991; 1974:561-9.

71. Thompson CB, Lindsten T, Ledbetter JA *et al.* CD28 activation pathway regulates the production of multiple T-cell derived lymphokines/cytokines. Proc Natl Acad Sci USA 1989; 86:1333-7.

72. Sigal NH, Lin CS, Siekierka JJ. Inhibition of human T-cell activation by FK506, rapamycin and cyclosporine A. Transplant Proc 1991; 23:1-5.

73. Bretcher P, Cohen MA. A theory of self-non-self discrimination: paralysis and induction involve the recognition of one and two determinants on an antigen, respectively. Science 1970; 169 :1042-9.

74. Clark EA, Ledbetter JA. How B and T-cells talk to each other. Nature 1994; 367:425-8.

75. Alberta B, Bray D, Lewis J, Raff M, Roberts K, Watson JD, eds. Molecular Biology of the Cell. New York, NY: Garland Publishing Inc, 1994: 864-5.

76. Thomson AW. Cyclosporine: mode of action and clinical applications. Doidrecht Kluwer Academic Publishers, 1989.

77. Bennett WM, Norman DJ. Action and toxicity of cyclosporine. Ann Rev Med 1986; 37:215-24.

78. Mihatsch MJ, Theil G, Ryffel B. Cyclosporin A: action and side effects. Toxicol Lett 1989; 46:125-39.

79. Mason J. Pharmacology of cyclosporine (Sandimmune): vii pathophysiology and toxicity of cyclosporine A in humans and animals. Pharmacol Rev 1989; 42:423-4.

80. Ryffel B, Foxwell BM, Gee A, Greiner B, Woerly G, Mihatsch M. Cyclosporine relationship of side effects to mode of action. Transplantation 1988; 41:90s-6s.

81. Kahan BD, Welsh M, Schoenberg L *et al.* Variable oral absorption of cyclosporine. Transplantation 1996; 62:599-606.

82. Awni WM, Kasiske BL, Heim-Duthoy K, Rao KV. Long term cyclosporine pharmacokinetic changes in renal transplant recipients: effects of binding and metabolism. Clin Pharmacol Ther 1989; 45:41-8.

83. Myers BD. Cyclosporine nephrotoxicity. Kidney Int 1986; 30:964-74.

84. Mason J. Renal side effects of cyclosporin A. Br J Dermatol 1990; 122(suppl 36):71-7.

85. Bergstrand A, Bohman SO, Farnsworth A *et al.* Renal histopathology in kidney transplant recipients immunosuppressed with cyclosporin A. Clin Nephrol 1985; 24:107-19.

86. Laskow DA, Curtis JJ, Luke RG *et al.* Cyclosporin induces changes in glomerular filtration rate and urea excretion. Am J Med 1990; 88:497-502.

87. de Groen PC, Aksamit AJ, Rakela J, Forbes GS, Krom RAF. Central nervous system toxicity after liver transplant: the role of cyclosporine and cholesterol. New Engl J Med 1987; 317:816-66.

88. Klintmalm GBG, Iwatsuki S, Starzl TE. Cyclosporin A hepatotoxicity in 66 renal allograft recipients. Transplantation 1981; 32:488-9.

89. Porter GA, Bennett WM, Sheps SG. Cyclosporine associated hypertension. Arch Intern Med 1990; 150:280-3.

90. Ballantyne CM, Podet EJ, Patsch WP *et al.* Effects of cyclosporine therapy on lipoprotein levels. JAMA 1989; 262:53-6.

91. Bennett WM, Serra J, Fisher S, Norman DJ, Barry JM. Cyclosporine in renal transplantation with hirsutism. Am J Kidney Disease 1985; 5:214.

92. Northrop JP, Ho SN, Chen L *et al.* NFAT components define a family of transcription factors targeted in T-cell activation. Nature 1994; 369:497-502.

93. Kahan BD. Cyclosporine. N Engl J Med 1989; 321:1725-38.

94. Oellerich M, Armstrong VW, Schutz E, Shaw LM. Therapeutic drug monitoring of cyclosporine. Clin Biochem 1998; 31:309-16.

95. Kahan BD. Individualisation of cyclosporine therapy using pharmacokinetic and pharmacodynamic parameters. Transplantation 1985; 40:457-76.

96. Kahan BD, Dunn J, Fitts C *et al.* Reduced inter-and intrasubject variability in cyclosporine pharmacokinetics in renal transplant recipients treated with micro-emulsion formulation in conjunction with fasting, low fat or high fat meals. Transplantation 1995; 59:505-11.

97. Barone G, Chang CT, Choc MG jr *et al.* The pharmacokinetics of a microemulsion formulation of cyclosporine in primary renal transplant recipients. Transplantation 1996; 61:875-80.

98. Tanaka H, Kuroda A, Marusawa H *et al.* Structure of FK506: a novel immunosuppressant isolated from streptomyces. J Am Chem Soc 1987; 109:5031-3.

99. Yoshimura N, Oka T. FK506, a new immunosuppressive agent: a review. J Immunol Immunopharmacol 1990; 10:32-6.

100. Todo S, Fung JJ, Tzakis AJ *et al.* One hundred ten consecutive primary orthotopic liver transplants under FK506 in adults. Transplant Proc 1991; 23:1397-402.

101. Fung J, Abu-Elmagd K, Jain A *et al.* A randomized trial of primary liver transplantation under immunosuppression with FK506 vs cyclosporine. Transplant Proc 1991; 23:2977-83.

102. US Multicenter FK506 Liver Study Group. A comparison of tacrolimus (FK506) and cyclosporine for immunosuppression in liver transplantation. N Engl J Med 1994; 1110-5.

103. European FK506 Multicentre Liver Study Group. Randomised trial comparing tacrolimus (FK506) and cyclosporine in prevention of liver allograft rejection. Lancet 1994; 344:423-8.

104. Starzl TE, Donner A, Eliasziw M *et al.* Randomised trialomania? The multicentre liver transplant trials of tacrolimus. Lancet 1995; 346:1346-50.

105. Steinmuller DR. FK506 and organ transplantation. Austin (TX): RG Landes Co., 1994.

106. van Hoof J. The European prospective randomised trial comparing tacrolimus and cyclosporin in the prevention of allograft rejection. XVI International Congress of the Transplantation Society.

107. FK506 US Kidney Transplant Multicenter Study Group. FK506 in kidney transplantation: results of the U.S. randomized, comparitive, phase III study. XVI International Congress of the Transplantation Society.

108. Mathew A, Talbot D, Minford E *et al.* Reversal of steroid resistant rejection in renal allograft recipients using FK506. Transplantation 1995; 60:1182-4.

109. Woodle ES, Thistlewaite J.R. jr, Gordon JH *et al.* A prospective, multicenter trial of FK 506 (tacrolimus) therapy for refractory acute renal allograft rejection . XVI International Congress of the Transplantation Society.

110. Jordan ML, Naraghi R, Shapiro R *et al.* Tacrolimus rescue therapy for renal allograft rejection five year experience. XVI International Congress of the Transplantation Society.

111. Jordan ML, Naraghi R, Shapiro R *et al.* Tacrolimus rescue therapy for renal allograft rejection: five years experience. Transplantation 1997; 63:223-8.

112. Gjertson DW, Cecka JM, Terasaki PI. The relative effects of FK506 and cyclosporine on short- and long-term kidney graft survival. Transplantation 1995; 60:1384-8.

113. Doerfler DL, Bartman CD, Campbell IM. Mycophenolic acid production by *Penicillium brevicompactum* in two media. Can J Microb 1979; 25:940-3.

114. Lee WA, Gu L, Miksztal ARICN, Nelson PH. Bioavailability of mycophenolic acid through amino acid derivitization. Pharma Res 1990; 7:161-6.

115. Nelson P, Eugui E, Wan C, Allison A. Synthesis and immunosuppressive activity of some side chain variants of mycophenolic acid. J Med Chem 1990; 33:833-8.

116. Wu LC. Mycophenolate mofetil: molecular mechanism of action. Perspect Drug Discov Design 1994; 4:185-204.

117. Franklin T, Cook J. The inhibition of nucleic acid synthesis by mycophenolc acid. Biochem J 1996; 113:515-24.

118. Allison AC, Eugui EM. Immunosuppressive and other effect of mycophenolic acid and an ester prodrug, mycopheolate mofetil. Immunol Rev 1993; 136:5-28.

119. Platz KP, Sollinger HW, Hullert DA, Eckhoff DE, Eugui EM, Allison AC. RS-61443: a new, potent immunosuppressive agent. Transplantation 1991; 51:27-31.

120. Allison AC, Eugui EM. Purine metabolism and immunosuppressive effects of mycophenolate mofetil. Clin Transplant 1996; 10:77-84.

121. Sokoloski JA, Sartorelli AC. Effects of the inhibitors of IMP dehydrogenase, tiazofurin and mycophenolic acid on glycoprotein metabolism. Molec Pharmacol 1996; 39:567-73.

122. Maly P, Thall A, Petryniak B *et al.* The alpha-1,3 fucosyl transferase FUC TVII controls leukocyte trafficking through an essential role in L-, E-, and P-selectin ligand biosynthesis. Cell 1996; 86:643-53.

123. Zheng M, Fang H, Hakomori S. Functional role of N-glycosylation in alpha-5, beta-1 integrin receptors: de-N-glycosylation induces dissociation or altered association of alpha-5, beta-1 subunits and concomitant loss of fibronectin binding activity. J Biol Chem 1994; 269:12325-31.

124. Allison A, Eugui EM. Mycophenolate mofetil, a rationally designed immunosuppressive drug. Clin Transplant 1993; 7:96-112.

125. Sollinger H. Mycophenolate mofetil for the prevention of acute rejection in primary cadaveric renal allograft recipients. Transplantation 1995; 60:225-32.

126. European Mycophenolate Mofetil Cooperative Study Group. Placebo-controlled study of mycophenolate mofetil combined with cyclosporine and corticosteroids for prevention of acute rejection. Lancet 1995; 345:1321-5.

127. Halloran PA. Pooled analysis of three randomized double blind clinical studies in prevention of rejection with mycophenolate mofetil in renal allograft recipients (the 1-year analysis) . American Society of Transplant Physicians 15th annual meeting.

128. Tricontinental Mycophenolate Mofetil Renal Transplantation Study Group. A blinded, randomized clinical trial for the prevention of acute rejection in cadaveric renal transplantation. Transplantation 1996; 61:1029-37.

129. Vezina C, Kudelis A, Seghal SN. Rapamycin (AY-22,989), a new antifungal antibiotic: I. Taxonomy of the producing streptomycete and isolation of the active principle. J Antibiot 1975; 28:721-6.

130. Seghal SN, Baker H, Vezina C. Rapamycin (AY-22,989), a new antifungal antibiotic: II. Fermentation, isolation and characterization. J Antibiot 1975; 28:727-32.

131. Houchens DP, Ovejera AA, Riblet SM, Slagel DE. Human brain tumor xenografts in nude mice as a chemotherapy model. Eur J Cancer Clin Oncol 1983; 19:799-805.

132. Martel RR, Klicius J, Galat S. Inhibition of the immune response by rapamycin, a new antifungal antibiotic. Can J Physiol Pharmacol 1977; 55:48-51.

133. Adams LM, Caccese R, Cummons T, Seghal SN, Chang JY. Effect of the immunosuppressant rapamycin and cyclosporine A on collagen induced arthritis in mice. FASEB J 1990; 4:A358 .

134. Chang JY, Sehgal SN. Pharmacology of Rapamycin: a new immunosuppressive agent. Br J Rheumatol 1991; 30:62-5.

135. Kahan BD, Gibbons S, Tejpal N, Stepkowski SM, Chou TC. Synergistic interactions of cyclosporine A and rapamycin to inhibit immune performances of normal human peripheral blood lymphocytes *in vitro*. Transplantation 1991; 51:232-9.

136. Dumont FJ, Melino MR, Staruch MJ, Koprak SL, Fisher PA, Sigal NH. The immunosuppressive macrolides FK-506 and roaomycin act as reciprocal antagonists in murine T-cells. J Immunol 1990; 144:1418-24.

137. Morris RE. Rapamycins: antifungal, antitumor, antiproliferatives and immunosuppressive macrolides. Transplant Rev 1992; 6:39-87.

138. Kay JE, Kromwel L, Doe SEA, Denyer M. Inhibition of T and B lymphocyte proliferation by rapamycin. J Immunol 1991; 72:544-9.

139. Hatfield SM, Mynderse JS, Roehm NW. Rapamycin and FK506 differentially inhibit mast cell cytokine production and cytokine-induced proliferation and act as reciprocal antagonists. J Pharmacol Exp Ther 1992; 261:970-6.

140. Bierer BE, Somers PK, Wandless TJ, Burakoff SJ, Schreiber SL. Probing immunosuppressant action with a non-natural immunophilin ligand. Science 1990; 250:556-9.

141. Bierer BE, Matila PS, Standaert RF *et al.* Two distinct signal transmission pathways in T-lymphs are inhibited by complexes formed between an immunophillin and either FK506 or rapamycin. Proc Natl Acad Sci USA 1990; 87:9231-5.

142. McCarthy SA, Cacchione RN, Mainwaring MS, Cairns JS. The effects of immunosuppressive drug on the regulation of activation induced apoptotic cell death in thymocytes. Transplantation 1992; 54:543-7.

143. DePaulis A, Cirillo R, Ciccarelli A, Condorelli M, Marone G. FK506, a potent novel inhibitor of the release of proinflammatory mediators from human fc epsilon RI+ cells. J Immunol 1991; 146:2374-81.

144. Hultsch T, Martin R, Hohman RJ. The effect of the immunophilin ligands rapamycin and FK506 on proliferation of mast cells and other hematopoietic cell lines. Mol Cell Biol 1992; 3:981-7.

145. Fruman DA, Mather PE, Burakoff SJ, Bierer BE. Correlation of calcineurin phosphatase activity and programmed cell death in murine T cell hybridomas. Eur J Immunol 1992; 22:2513-7.

146. Luo H, Chen H, Daloze P, Chang JY, St Louis G, Wu J. Inhibition of in vitro immunoglobulin production by rapamycin. Transplantation 1992; 53:1071-6.

147. Ferron GM, Jusko WJ. Species differences in sirolimus stability in humans, rabbits and rats. Drug Met Dispos 1998; 26:83-4.

148. Chung JIKJ, Crabtree GR, Blenis J. Rapamycin-FKBP specifically blocks growth-dependent activation of and signaling by the 70 kD S6 protein kinases. Cell 1992; 69:1227-36.

149. Kuo CJ, Chung J, Fiorentino DF, Flanagan WM, Blenis J, Crabtree GR. Rapamycin selectively inhibits interleukin-2 activation of p70 S6 kinase. Nature 1992; 358:70-3.

150. Wu J, Palladino MA, Figari IS, Morris RE. Comparative immuno-regulatory effects of rapamycin, FK506 and cyclosporine A on mitogen-induced cytokine production and lymphoproliferation. Transplant Proc 1991; 23:237-40.

151. Kahan BD, Chang JY, Sehgal SN. Preclinical evaluation of a potent immunosuppressive agent, rapamycin. Transplantation 1991; 52:185-91.

152. Kimball PM, Kerman RH, Kahan BD. Production of synergistic, non-identical mechanisms of immunosuppression by rapamycin and cyclosporine A. Transplantation 1991; 51:486-90.

153. Fryer J, Yatscoff RW, Pascoe EA, Thliveris J. The relationship of blood concentrations of rapamycin and cyclosporine to suppression of allograft rejection in a rabbit heterotopic heart transplant model. Transplantation 1993; 55:340-5.

154. Yakimets WJ, Lakey JR, Yatscoff RW *et al.* Combination low dose rapamycin and cyclosporine prolong canine pancreatic islet allograft survivall: rapamycin efficacy is blood level related. Transplantation 1993; 56:1293-8.

155. Granger DK, Cromwell JW, Chen SC *et al.* Prongation of renal allograft survival in a large animal model by rapamycin monotherapy. Transplantation 1995; 59:183-6.

156. Yatscoff RW, Wang S, Chackowsky P, Lowes N, Koshal A. Efficacy of rapamycin, RS-61443 and cyclophosphamide in the prolongation of survival of discordant pig-to-rabbit cardiac xenografts. Can J Cardiol 1994; 10:711-6.

157. Kahan BD. Sirolimus: a new agent for clinical renal transplantation. Transplant Proc 1997; 29:48-50.

158. Murgia MG, Jordan S, Kahan BD. The side effect profile of sirolimus: a phase I study in quiescent cyclosporine-prednisone-treated renal transplant patients. Kidney Int 1996; 49:209-16.

159. Kahan BD, Napoli KL, Kelly PA *et al.* Therapeutic drug monitoring of sirolimus: correlations with efficacy and toxicity. Transplant Rev 2000; 17:97-109.

160. Tocci MJ, Matkovich DA, Collier KA *et al.* The immunosuppressant FK105 selectively inhibits activation of early T-cell activation genes. J Immunol 1989; 143:718-26.

161. Lin CS, Bolta RC, Siekiera JJSNH. FK506 and cyclosporin A inhibit highly similar signal transduction pathways in human T-lymphocytes. Cell Immunol 1991; 133:269-84.

162. Emmel EA, Verweij CL, Durand *et al.* Cyclosporin A specifically inhibits function of nuclear proteins involved in T-cell activation. Cell 1989; 26:1617-20.

163. Granelli-Piperno A, Nolan P, Inzba K, Steinmann RM. The effect of immunosuppressive agents on the induction of nuclear factors that bind to sites on the interleukin-2 promoter. J Exp Med 1990; 1172:1869-72.

164. Liu J, Farmer JD, Lane WS, Friedman J, Weissman I, Schreiber SL. Calcineurin is a common target of cyclosporine A-cyclophilin and FK506-FKBP complexes. Cell 1991; 66:807-15.

165. Michnick SW, Rosen MK, Wandless TJ, Karplus M, Schreiber SL. Solution structure of FKBR, a rotamse enzyme and receptor for FK506 and rapamycin. Science 1992; 252:836-42.

166. Sabers CJ, Martin MM, Brunn GJ *et al.* Isolation of a protein target of the FKBP-12-rapamycin complex in mamalian cells. J Biol Chem 1995; 270:815-22.

167. Brown EJ, Albers MW, Shin TB *et al.* A mammalian protein targeted by G1-arresting rapamycin-receptor complex. Nature 1994; 369:756-8.

168. Sabatini DM, Erdjument-Bromage H, Liu M, Tempst P, Snyder SH. RAFT1: a mammalian protein that binds to FKBP12 in a rapamycin dependent fashion and is homologous to yeast TORs. Cell 1994; 89:35-43.

169. Chiu MI, Katz H, Berlin V. RAPT1, a mammailan homolog of yeast Tor, interacts with FKBP12/rapamycin complex. Proc Natl Acad Sci USA 1994; 91:12574-8.

170. Schmidt A, Kunz J, Hall MN. TOR2 is required for organization of the actin cytoskeleton in yeast. Proc Natl Acad Sci USA 1996; 93:13780-5.

171. Hunter T. When is a lipid kinase not a lipid kinase? When it is a protein kinase. Cell 1995; 83:1-4 .

172. Keith CT, Schreiber SL. PIK-related kinases: DNA repair, recombination, and cell-cycle checkpoints. Science 1995; 270:50-1.

173. Carpenter CL, Cantley LC. Phosphoinositide kinases. Curr Opin Cell Biol 1996; 8:153-8.

174. Westphal CH. Cell-cycle signaling: Atm displays its many talents. Curr Biol 1997; 7:R789-R792.

175. Westphal CH, Rowan S, Schmaltz C, Elson A, Fisher DE, Leder P. Atm and p53 cooperate in apoptosis and suppression of tumorogenesis, but not in resistance to acute radiation toxicity. Nature Genet 1997; 16:397-401.

176. Chou MM, Blenis J. The p70 S6 kinase: regulation of a kinase with multiple roles in mitogenic signaling. Curr Op Cell Biol 1995; 7:806-14.

177. Jeffries HB, Reinhard C, Kozma SC, Thomas G. Rapamycin selectively represses translation of "poly-pyrimidine tract" mRNA family. Proc Natl Acad Sci USA 1994; 91:4441-5.

178. Terada N, Patel HR, Takase K, Kohno K, Nairn AC, Gelfand EW. Rapamycin selectively inhibits translation of mRNAs encoding elongation factors and ribosomal proteins. PNAS USA 1994; 91:11477-81.

179. Brown EJ, Schreiber SL. A signaling pathway to translational control. Cell 1996; 86:517-20.

180. Dennis PB, Pullen N, Kozma SC, Thomas G. The principal rapamycin-sensitive $p70^{s6k}$ phosphorylation sites, T-229 and T-389, are differentially regulated by rapamycin-insensitive kinase kinases. Mol Cell Biol 1996; 16:6242-51.

181. Mendez R, Myers MGjr, White MF, Rhodes RL. Stimulation of protein synthesis, eukaryotic translation initiation factor 4E phosphorylation and PHAS-1 phosphorylation by insulin requires insulin receptor subtype 1 and phosphoinositol 3-kinase. Mol Cell Biol 1996; 16:2857-64.

182. Withers DJ, Seufferlein T, Mann D, Garcia B, Jones N, Rozengurt E. Rapamycin dissociates $p70^{s6k}$ activation from DNA synthesis stimulated by bombesin and insulin in Swiss 3T3 cells. J Biol Chem 1997; 272:2509-14.

183. Terada N (personal communication) cited in: Abram RT. Mammalian target of rapamycin: immunosuppressive drugs uncover a novel pathway to cytokine receptor signaling. Curr Op Immunol 1998; 10:330-6.

184. Beretta L, Gingras A-C, Svitkin YV, Hall M, Sonenberg N. Rapamycin blocks the phosphorylation of 4E-BP1 and inhibits cap-dependent initiation of translation. EMBO 1996; 15:658-64.

185. Sonenberg N. Mathews MB, Sonenberg N, eds. Translational Control. New York, NY: Cold Spring Harbor Press, 1996: 245-69.

186. Lawrence JCj, Abraham RT. PHAS/4E-BPs as regulators of mRNA translation and cell proliferation. Trends Biochem Sci 1997; 22:345-9.

187. Rosenwald IB, Kaspar R, Rousseau D *et al.* Eukaryotic translation initiation factor 4E regulates expression of cyclin D1 at transcriptional and post-translational levels. J Biol Chem 1995; 270:21176-80.

188. Rosenwald IB, Lazaris-Karatas A, Sonenberg N, Schmidt EV. Elevated levels of cyclin D1 protein in response to increased expression of eukaryotic initiation factor 4E. Mol Cell Biol 1993; 13:7358-63.

189. Rousseau D, Kaspar R, Rosenwald I, Gehrke L, Sonenberg N. Translational initiation of ornithine decarboxylase and nucleocytoplasmic transport of cyclin D1 mRNA are increased in cells over expressing eukaryotic initiation facor 4E. Proc Natl Acad Sci USA 1996; 93:1065-70.

190. Christians U, Sattler M, Schiebel H-M *et al.* Isolation of two immunosuppressive metabolites after *in vitro* metabolism of rapamycin. Drug Met Dispos 1992; 20:186-91.

191. Sattler M, Guengerich FP, Yun C-H, Christians U, Sewing K-F. Cytochrome P-450 enzymes are responsible for biotransformation of FK506 and rapamycin in man and rat. Drug Met Dispos 1992; 20:753-61.

192. Yatscoff RW, Wang P, Chan K, Hicks D, Zimmerman J. Rapamycin: distribution, pharmacokinetics and therapeutic range investigations. Ther Drug Monit 1995; 17:666-71.

193. Fuhler EN, DiJoseph JF, Armstrong A, Hicks DR, Beirle F, Sehgal SN. Pharmacokinetics and pharmacodynamics of oral rapamycin in rats receiving heterotopic heart-to-ear allografts. Pharm Res 1994; 11:S344.

II. OBJECTIVES

1. RATIONALE

The therapeutic monitoring of rapamycin has already been recommended[1]. The premise is to monitor drug exposure in order to decrease the risk of toxicity and unwanted side effects, to optimise immunosuppression and to evaluate patient compliance. For rapamycin, this recommendation was made based on experience with other immunosuppressive drugs.

It is presently not known if monitoring of rapamycin clinically will be necessary to minimise toxicity and/or optimise immunosuppression. During phase I and phase II clinical trials for rapamycin, no dosage adjustments were made, nor were any real-time drug levels provided to clinicians for interpretative use.

The model for the development of rapamycin monitoring protocol has been CsA. After CsA was introduced in the 1980s, information gradually became available regarding its metabolism and the clinical significance of its metabolites. Each of the metabolites of CsA have low immunosuppressive activity and negligible toxicity compared to that of parent drug. This is summarised as an aggregate clinical significance index, a representation of the immunosuppressive and toxic activities of each metabolite. This is a normalised ratio comparing metabolite activity and concentration to that of parent drug. For CsA metabolites, the clinical significance index is low, and it was deemed both unnecessary to measure metabolites of CsA clinically, and necessary to specifically determine levels of parent CsA for therapeutic drug monitoring.

At this time, the recommendation is for specific monitoring of parent rapamycin. At the onset of this study, there was very little information regarding the metabolism and the significance of rapamycin metabolites available. It was unknown if the recommendation for rapamycin

monitoring was appropriate, as it was unknown what contribution, if any, rapamycin metabolites make to immunosuppression and toxicity.

2. HYPOTHESIS

The metabolites of rapamycin have clinical significance.

3. SPECIFIC AIMS

The objective of this study is to determine the clinical significance of rapamycin metabolites. This will be accomplished through achievement of the following specific aims:

a. To elucidate metabolites of rapamycin, and define their structural distinctions.

b. To test metabolites of rapamycin for *in vitro* immunosuppressive and toxic activities.

c. To measure steady state levels of rapamycin metabolites in humans and animal subjects.

d. To calculate the pharmacokinetic parameters delineating rapamycin disposition, with attention to the relative contributions of pre-hepatic and hepatic factors in the canine model.

This information will be compiled into a clinical significance index for each rapamycin metabolite. It is hoped that the results of this study will determine the clinical significance of rapamycin metabolites as defined by their activity, toxicity and physiologic concentration. This information will be used to decide if concentrations of rapamycin metabolites should be measured to optimise immunosuppression and reduce toxicity in patients on rapamycin immunosuppressive therapy.

4. REFERENCES

1. Yatscoff RW, Boeckx R, Holt DW *et al*. Consensus guidelines for therapeutic drug monitoring of rapamycin: report of the consensus panel. Ther Drug Monit 1995; 17:676-80.

III. ISOLATION AND CHARACTERIZATION OF METABOLITES OF RAPAMYCIN

1. RATIONALE

The products of the biotransformation of rapamycin remain poorly defined. The aims of this study were to find a viable source for rapamycin metabolites and to isolate sufficient quantities of metabolites for identification, structural characterization and subsequent activity testing. Clinical specimens from patients on rapamycin were initially investigated as a metabolite source. Subsequently, rabbit liver microsomes and a microbial culture system were investigated as metabolite generation systems.

2. MATERIALS AND METHODS

a. Source of drugs and specimens

Rapamycin and 29-demethoxyrapamycin (DMR) were gifts from Wyeth-Ayerst Inc. (Princeton, NJ). Urine specimens were obtained as 24-hour continuous collections from stable renal transplant patients taking rapamycin as part of the clinical trials at the University of Texas Health Sciences Center in Houston, TX (K Napoli and BD Kahan). Type O EDTA-anticoagulated whole blood was obtained from the Canadian Red Cross Blood Service (Edmonton, AB) and was used for pooling. One unit of CPD-A1 anticoagulated whole blood was obtained from the University of Texas Health Sciences Center, from a renal transplant patient receiving rapamycin who was treated by therapeutic phlebotomy for polycythemia. Rapamycin metabolites were measured in EDTA anti-coagulated patient blood specimens from patients taking rapamycin on a compassionate release basis, treated at the University of Alberta Hospital (Edmonton, AB). These were drawn for the purpose of therapeutic drug monitoring of rapamycin, and no clinical sample collection was initiated solely for the purpose of research.

All animal work was done in compliance with the guidelines of the Canadian Council on Animal Care, and animals were cared for by personnel of the University of Alberta Health Sciences Laboratory Animal Services under the supervision of a veterinarian. Rabbits were given a

single daily oral dose of 5 mg/kg of rapamycin in a non-aqueous liquid oral formulation (Wyeth-Ayerst Inc., Princeton, NJ). Urine and fecal pellets were collected with the use of a metabolic cage over a period of 24 hours. Food and water were available throughout the collection period. Blood was obtained at 7 hours post-terminal dose by cardiac puncture with the rabbit anaesthetised with a standard ketamine-rompun-xylazine cocktail administered intramuscularly.

b. Measurement of rapamycin in whole blood by high performance liquid chromatography

The concentration of rapamycin in whole blood was measured by high performance liquid chromatography (HPLC) using a method modified from the procedure by Yatscoff and associates[1], which is briefly described here. To one mL of whole blood, 25 μL of 8 000 μg/L of ethanolic internal standard, demethoxyrapamycin (DMR) was added, followed by 1 mL of 1.33% (w/v) K_2CO_3 and 6 mL diethyl ether. The mixture was shaken on a reciprocating shaker for 10 min then centrifuged for 10 min at 800 *x g* to achieve partitioning. The ether layer was removed to a clean test tube and dried under a gentle stream of nitrogen. The residue was reconstituted with 300 μL of 70% (v/v) methanol in 0.1N sodium acetate buffer (pH=5.5), vortex mixed and centrifuged for 10 min at 800 *x g* to remove any sediment. The clear supernatant was collected for subsequent HPLC analysis.

Chromatographic separation was achieved using a C18 60Å 4 μM 3.9 x 150 mm Waters Novapak (Millipore, Bedford MA) reverse phase column, at a column temperature of 50°C, isocratically at 68% (v/v) methanol in deionized water, using a flow rate of 1.1 mL/min for 12 minutes followed by 0.8 mL/min for the remainder of the run. The injection volume was 100 μL and the run time was 40 minutes. Ultraviolet (UV) absorbance was monitored at 276 nm. The concentration of rapamycin was determined by the ratio of peak heights of rapamycin compared to DMR over a range defined by a standard curve, where the relationship was found to be linear.

The method described here was not suitable for the separation and analysis of rapamycin metabolites. Because of inappropriate and incomplete separation over a very long period of time, modifications were made to the basic procedure for a variety of applications. These are described in detail in the following sections.

c. Investigation of urine as a source of rapamycin metabolites

The rapamycin patient urine specimens were frozen at -40°C, transported on dry ice and stored at -70°C until extracted. Urine specimens (2L) were individually thawed, the pH adjusted to 10.0 with K_2CO_3 (Fisher Scientific, Ottawa ON) and extracted in portions of 200 mL with an equal amount of anhydrous ethyl ether (Fisher Scientific, Ottawa ON) with shaking. The aqueous layer was discarded and the extraction repeated one or two more times with an equivalent amount of fresh alkalinised urine. The ether layers were then washed with an equal volume of 0.1 N HCl, pooled together and evaporated to dryness. The residue was reconstituted in 1.5 mL of 100% HPLC grade methanol (Fisher Scientific, Ottawa ON) and stored frozen at -70°C until HPLC separation was performed.

Chromatographic separation was achieved on a C18 60Å 4 μM 3.9 x 150 mm Waters Novapak (Millipore, Bedford MA) reverse phase column, at a column temperature of 50°C, using a linear gradient mobile phase of 65% (v/v) methanol in distilled, deionized water acidified with HCl (pH 3.0) at time zero, to 85% (v/v) methanol in acidified water at 60 minutes, using a flow rate of 1.1 mL/min.

Peaks eluting from the column were classified as candidate metabolites based on their UV profile using a diode array detector (Varian 9050, Varian Canada Inc, Mississauga ON). Absorption maxima at 288, 276, 266 nm, based on the characteristic UV absorbance profile of rapamycin was used as the positive criterion for further investigation. Peaks were collected manually, pooled and dried under a gentle stream of air for 5 minutes per mL of mobile phase, but not to dryness, then applied *in toto* to Supelclean LC-18 6 mL (Supelco, Bellefonte, PA) solid phase extraction tubes for recovery. Each extraction tube was dried with vacuum not exceeding 5 mm Hg and the

metabolites eluted with 100% HPLC grade acetonitrile (Fisher Scientific, Ottawa ON), dried under air, reconstituted in 100% methanol and purified by repeat HPLC separation.

These fractions were submitted to Dr. Steve Soldin's lab for testing with the FKBP binding assay, and a mixed lymphocyte reaction for immunosuppressive activity. These procedures are described further in section **IV.2.f** and **IV.2.b**, respectively. An attempt at structural identity was made by fast atom bombardment-(FAB) mass spectrometry (MS) at the Analytical Chemistry Department, University of Alberta.

d. Investigation of rapamycin metabolites in renal transplant patient blood

Blood was drawn by therapeutic phlebotomy from a renal transplant patient undergoing therapy for polycythemia. The blood was anticoagulated with CPD-A1 and frozen at –20°C, transported on dry ice, then frozen at –70°C until used. Sixty millilitres of blood was divided into 15 aliquots of 4 mL each. They were individually acidified with 1 mL of 0.2 M HCl and extracted with two sequential additions of 8 mL diethyl ether. A reciprocating shaker was used. Ether fractions were removed, pooled and dried down under nitrogen. The residue was reconstituted with 100 µl of 65% (v/v) methanol in distilled, deionized water.

Chromatographic separation was achieved on tandem C18 60Å 4 µM 3.9 x 150 mm Waters Novapak (Millipore, Bedford MA) reverse phase columns, at a column temperature of 50°C, using a linear gradient mobile phase of 75% (v/v) methanol in 0.2% (v/v) acetic acid in deionized water at time zero, to 85% (v/v) methanol in acidified water at 30 minutes, using a flow rate of 1.1 mL/min, and a 1:10 in-line analytical splitter.

The HPLC (1090, Hewlett Packard) was used with an electrospray-interfaced (ESI) MS (Mass Selective Detector [MSD], Hewlett Packard). Selected ion monitoring was performed in positive ion mode. Under these conditions, the strongest ion signals were from sodium adducts, so ions were monitored ($[M + Na^+]$) at the following mass-to-charge ratios: *m/z* =908.6 (didemethylrapamycin),

m/z =906.6 (demethoxyrapamycin), *m/z* = 922.6 (demethylrapamycin), *m/z* = 924.6 (didemethyl, hydroxyrapamycin), *m/z* = 936.6 (rapamycin), *m/z* = 938.6 (demethyl, hydroxyrapamycin), *m/z* = 952.6 (hydroxyrapamycin), *m/z* = 968.6 (dihydroxyrapamycin), *m/z* = 970.6 (dihydrodiolrapamycin).

e. Investigation of rapamycin metabolite production by rabbit liver microsomal preparations

A New Zealand White rabbit was injected subcutaneously with phenobarbital at 60 mg/kg of body weight each day for three days to induce the CYP 450 enzymes. The rabbit was anaesthetised with standard ketamine-rompun-xylazine cocktail administered intramuscularly. The liver was harvested under aseptic conditions by abdominal dissection. The major vessels were cut and the organ removed to a basin containing ice-cold sterile normal saline. The liver was perfused with ice-cold sterile Ringer's Lactate solution through the portal vein.

The liver was minced with scissors, and put into solution using a homogenizer. The liver microsomes were isolated by standard differential centrifugation techniques according to the method of Guengerich[2]. Protein was determined by the Lowry method. Protein concentrations were estimated using a bovine serum albumin standard curve. Microsomes were resuspended in 0.1 M phosphate buffer (pH 7.4) at 0.5 mg protein/mL.

For the microsomal reactions, 320 μL of rabbit liver microsomes was pre-incubated for 3 min at 36°C with 170 μL of nicotine adenine dinucleotide phosphate- (NADPH) regeneration buffer consisting of 0.1 M phosphate buffer (pH 7.4), 10 mM $MgCl_2$, 2 mM EDTA, 0.8 mM NADP, 18 mM isocitric acid and 0.7 U/mL isocitrate-dehydrogenase. Reactions were initiated by the addition of 10 μL of substrate in 10% (v/v) ethanol in phosphate buffer. The final concentration of ethanol was 0.2% (v/v). Ethanol in control samples did not affect activity in this assay at concentrations up to 0.8% (v/v). After incubation at 36°C for 45 minutes with shaking, the reaction was terminated by the addition of 1 mL 0.1 M HCl and 6 mL diethyl ether. Samples were vortex mixed and then shaken in a reciprocating shaker for 10 minutes, followed by

centrifugation for 2 minutes at 600 *x g*. The organic layer was removed and dried under nitrogen. The residue was reconstituted in 75% (v/v) methanol in distilled deionized water and transferred to a HPLC injection vial.

Chromatographic separation was achieved on tandem C18 60Å 4 μM 3.9 x 150 mm Waters Novapak (Millipore, Bedford MA) reverse phase columns, at a column temperature of 50°C, using a linear gradient mobile phase of 75% (v/v) methanol in 0.2% (v/v) acetic acid in deionized water at time zero, to 85% (v/v) methanol in acidified water at 30 minutes, using a flow rate of 1.1 mL/min, and a 1:10 in-line analytical splitter.

HPLC- (ESI)-MS analysis was conducted as described in the previous subsection.

f. Investigation of a microbial rapamycin metabolite generation system

A filamentous bacterium was chosen for its previously demonstrated expression of CYP450 3A enzymes[3]. An *Actinoplanacete sp* (American Type Culture Collection, ATCC 53771) was grown in standard liquid fermentation medium at 27°C in an angled environmental shaker for 48-72 hours until appropriate biomass was obtained. Rapamycin was added to the fermentation slurry and incubated a further 24-40 hours. Culture and supernatant were harvested together.

The culture and supernatant were extracted with twice the volume of anhydrous diethyl ether. The ether layer was removed and dried under nitrogen, then reconstituted with absolute methanol. Chromatographic separation by HPLC and detection by ESI-MS were performed as described previously in **III.2.e**.

Fractions were collected manually. Five metabolites were chosen for isolation and purification based on their abundance, degree of separation and presence in clinical specimens as previously investigated. Corresponding fractions from multiple injections were pooled together and dried

under nitrogen. Residues were reconstituted with methanol and re-injected under similar or modified conditions for the purposes of purification.

g. Investigation of the polar Phase II metabolites of rapamycin

Human blood and urine were investigated for the presence of phase II metabolites, as were rabbit urine, fecal pellets and whole blood. Phase II metabolites are typically produced by conjugation to various substances (ie. glucuronide, sulfate, mercapturic acid, acetate) *in vivo* by liver enzymes for the purpose of detoxification, increase in water solubility and to permit excretion

Feces were first diluted and homogenized with 5 volumes of 0.1 N acetate buffer, pH 5.5. Several extraction procedures were used. Urine, feces or whole blood was precipitated with 1 volume of 30% (v/v) methanol in 0.1 N acetate buffer pH 5.5, 7.0 or 8.5. After centrifugation, the supernatant was either directly injected into the HPLC-MS or subjected to solid phase recovery for concentration on LC-18, LC-8 or LC-2 solid phase columns (Supelco). The columns were activated with 6 volumes of acetonitrile, then 1 volume of 70% (v/v) methanol in 0.1 N acetate buffer (pH 5.5). The sample was applied and washed with 10% (v/v) methanol in 0.1 N acetate buffer (pH 5.5), then eluted with 60-85% (v/v) methanol in 0.1 N acetate buffer (pH 5.5). Rabbit urine and fecal pellets were also treated with glucuronidase and aryl-sulfatase (Sigma) in an effort to demonstrate the liberation of rapamycin from a glucuronide- or sulphate-conjugated state.

Rabbit liver microsomes were used as an *in vitro* metabolite generation system, as described above. Supernatants and extracts were prepared the same way as for the blood and urine samples, in the previous paragraph. Control experiments were conducted with mycophenolic acid (MPA), a known substrate for the glucuronide conjugation reaction. Controls were evaluated for glucuronide transferase activity by measuring MPA-glucuronide conjugate by

HPLC-UV[4]. Following microsomal incubation, some controls were digested with 5U/mL glucuronidase (Sigma) to ensure specificity.

Introduction of the samples into the MS by ESI for analysis was done directly, by-passing the column, or with chromatographic separation on a single C18 60Å 4 μM 3.9 x 150 mm Waters Novapak (Millipore, Bedford MA) reverse phase column, at a column temperature of 50°C, using a linear gradient mobile phase of 45% (v/v) methanol in 0.2% (v/v) acetic acid in deionized water at time zero, to 85% (v/v) methanol in acidified water at 30 minutes and held until 50 min, using a flow rate of 1.1 mL/min. A 1:10 in-line analytical splitter was used where 10% of the flow was introduced to the MS and 90% of the flow was available for collection.

UV absorbance was monitored at 276 nm. MS parameters were similar to the microsomal experiment above. The mass range of 920-1300 amu monitored was based on predicted conjugation-type changes to rapamycin, and permitted the investigation of conjugated products of rapamycin and metabolites of rapamycin. Calculation of amus of interest was based on conjugation with amino acids, simple sugars, glucuronic acid, or sulphate.

h. Structural identification and confirmation of purity of isolated rapamycin metabolites by ESI-MS and HPLC-MS

Structures of the isolated, purified rapamycin metabolites were determined by (ESI)-MS/MS. Each metabolite was dissolved as a methanolic solution and flow injected, bypassing the HPLC column, into the MS by way of the ESI with a capillary end voltage of approximately 50eV for determination of the molecular weight of each metabolit. All detection was done in the positive ion mode. The voltage of the fragmentor and capillary exit voltages were then increased until optimal electrospray signal and fragmentation patterns were achieved for each metabolite. A mass range of 100 to 1000 amu was scanned for the appearance of ions that potentially could be assigned as characteristic fragmentation products. Fragmentation of rapamycin produced a profile of diagnostic ions. The fragmentation pattern of each metabolite was compared to that of rapamycin to localise

the site of the structural changes in the metabolites. Structures and molecular weights of the fragments were calculated manually by comparing the fragmentation pattern of each individual metabolite to that of rapamycin. Approximately 50 μg of metabolite was required for method establishment and analysis.

Initial assessment of metabolite purity was assumed on attaining a single or consistent double peak by HPLC with characteristic UV absorbance maxima at 288, 276 and 266 nm. For metabolites that eluted as two peaks after HPLC separation, purity was assured by collecting each of the two peaks and re-injecting them individually to ensure both peaks were uniform. It was presumed that the two peaks were composed of the two rotamer forms of rapamycin or of metabolite: trans and cis. Purity was further confirmed and degree of contamination estimated from mass spectrometry data. The isolated, purified metabolites in methanolic solution were flow injected into the mass spectrometer under lower voltage non-destructive conditions. A mass range of 100-1500 amu was scanned to detect ions that could not be attributed to metabolite as an estimate of purity. The metabolites were also analysed by HPLC (ESI)-MS under non-destructive conditions as described above. The areas of all non-overlapping ions were added together and used for area ratio determination of sample contamination.

i. Quantification of rapamycin metabolite stock solutions by HPLC-UV

The concentration of rapamycin metabolites was measured by HPLC, using a method modified from the procedure for rapamycin. Briefly, to 300 μL of mobile phase, 25 μL of 8 000 μg/L internal standard (DMR) was added, followed by 1-5 μL of ethanolic rapamycin metabolite stock solution. After vortexing, the mixture was separated by HPLC.

Chromatographic separation was achieved using a C18 60Å 4 μM 3.9 x 150 mm Waters Novapak (Millipore, Bedford MA) reverse phase column, at a column temperature of 50°C, isocratically at 70-75% (v/v) methanol in deionized water, using a flow rate of 0.8 mL/min. UV absorbance was monitored at 276 nm. The concentration of rapamycin metabolite was determined

by calculation of the ratio of peak heights of rapamycin metabolite compared to DMR, and read from an unextracted standard curve prepared from rapamycin. It was assumed that the molar absorptivity of the metabolites and rapamycin were equivalent, although it has not been possible to confirm this. There was not enough metabolite for gravimetric determination of the molar extinction co-efficients.

3. RESULTS

a. Urine as a source of rapamycin metabolites

Based on UV spectra, five peaks were identified as candidate metabolites and named RM1 through RM5. This is presented in Figure III-1. Four (RM1, RM2, RM3, RM4) were chosen for isolation and purification based on cleanliness of chromatography, resolution from the major CsA metabolites present in urine, consistent appearance in urine from different patients and reasonable quantity present. These candidate metabolites were submitted for binding studies with a 14 kDa and 52 kDa FKBP, where they were demonstrated to have low binding activities compared to that of parent rapamycin[5]. The immunosuppressive activity of these compounds was found to be <10% of rapamycin, as tested in the MLR using a single concentration comparison. The results of the binding study and the MLR are summarised in Table III-1.

As there was no HPLC-(ESI)-MS available at the time, structural analysis and purity evaluation was not done using this methodology. Upon further investigation of the structural character of these metabolites using FAB-MS, there were no ions in the 900-1200 atomic mass unit (amu) range demonstrated. This is the mass range where rapamycin metabolites where expected to be found. There was no reactivity with anti-rapamycin antibodies, as determined in a prototype microparticle enzyme linked immunoassay (MEIA) under development by Abbott Labs.

b. Identification of rapamycin metabolites in renal transplant patient blood

The (ESI)-MS spectrum of rapamycin is depicted in Figure III-2. This technique produced a molecular ion with a mass to charge ratio of m/z = 936.6 amu which appears consistently and is

Figure III-1 UV spectral profile of urine from a rapamycin treated patient

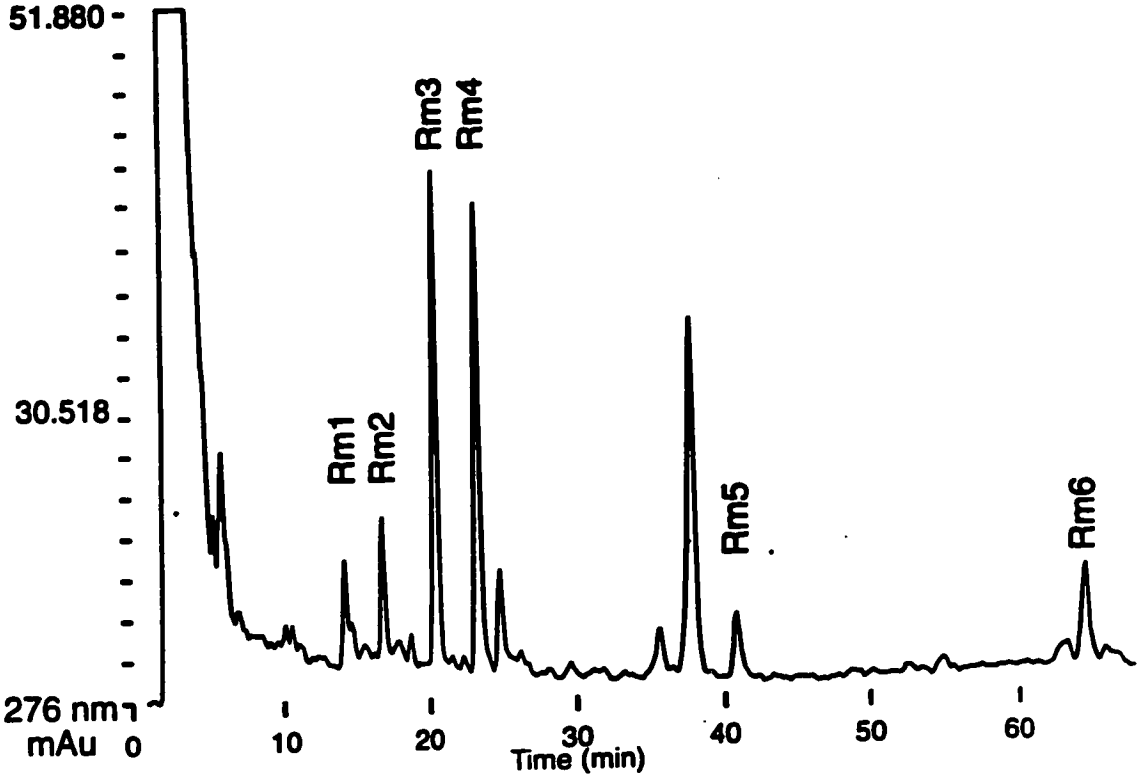

Table III-1 Immunosuppressive and immunophilin binding of four peaks isolated from the urine of rapamycin treated patients

		Immunophilin binding	
	MLR[a]	14 kDa	52 kDa
rapamycin	1.00	1.00	1.00
RM1	0.02	0.21	0.25
RM2	0.09	0.02	0.05
RM3	0.08	<0.01	<0.01
RM4	0.04	<0.01	0.03

[a] all results are reported as normailised to the activity of rapamycin

Figure III-2 ESI-MS fragmentation profile of rapamycin

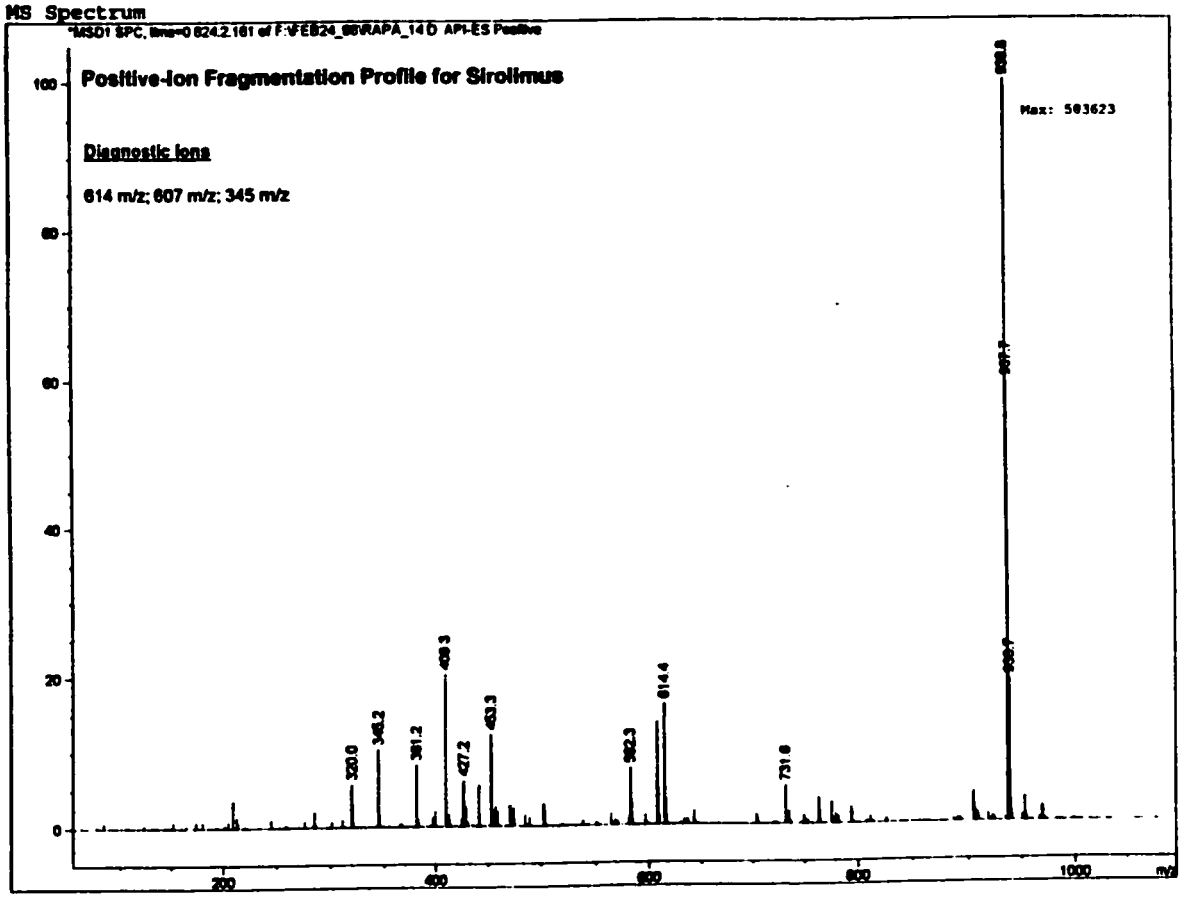

plausibly the sodium adduct of rapamycin [M + Na^+]. The presence of other minor ions corresponding to amus of other adducts is also noted, with the potassium adduct being the next most commonly seen ion, at *m/z* = 952.6 amu, and occasionally the proton adduct of *m/z* = 913.6 amu appearing at very low relative abundance as well.

The LC-MS chromatograph of a human whole blood pool with selected ion monitoring for rapamycin and metabolites is depicted in Figure III-3. Rapamycin is demonstrated in the profile and elutes near the end of the chromatographic separation, with a retention time of approximately 14 minutes, and a retention time relative to that of DMR of 0.89. Several ions corresponding to the mass of rapamycin metabolites elute before rapamycin. This is consistent with metabolic changes leading to the formation of less hydrophobic products, such as demethylation and hydroxylation. No ions corresponding to metabolite ion masses eluted in consistent, discrete peaks after rapamycin or in the solvent wash that followed each chromatographic separation.

After examination of the structure of rapamycin, it was considered likely that the drug may undergo Phase I metabolism, including oxidation (M+16), demethylation (M-15), amidase cleavage into a ring-opened product (M+1) and saturation of one or more of the double bonds in the triene structure C1-C16 with hydrogenation(M+2, M+4 or M+6) or hydration (M+32, M+64 or M+96). Based on calculation of the molecular weight of metabolites as sodium adducts, the following metabolites were detected in human whole blood: demethylhydroxy- (938.5 amu), hydroxy- (952.5 amu), dihydroxy- (963.5 amu), didemethyl- (908.5 amu), and demethylrapamycin (922.5 amu).

The metabolites present are listed in approximate descending concentration with their retention times relative to rapamycin: hydroxy- (0.54), demethyl hydroxy- (0.5), hydroxy- (0.39), demethyl- (0.54), demethyl- (0.68), and demethylrapamycin (0.86). Based on peak area ratios, the

Figure III-3 LCMS profile of rapamycin metabolites in human whole blood

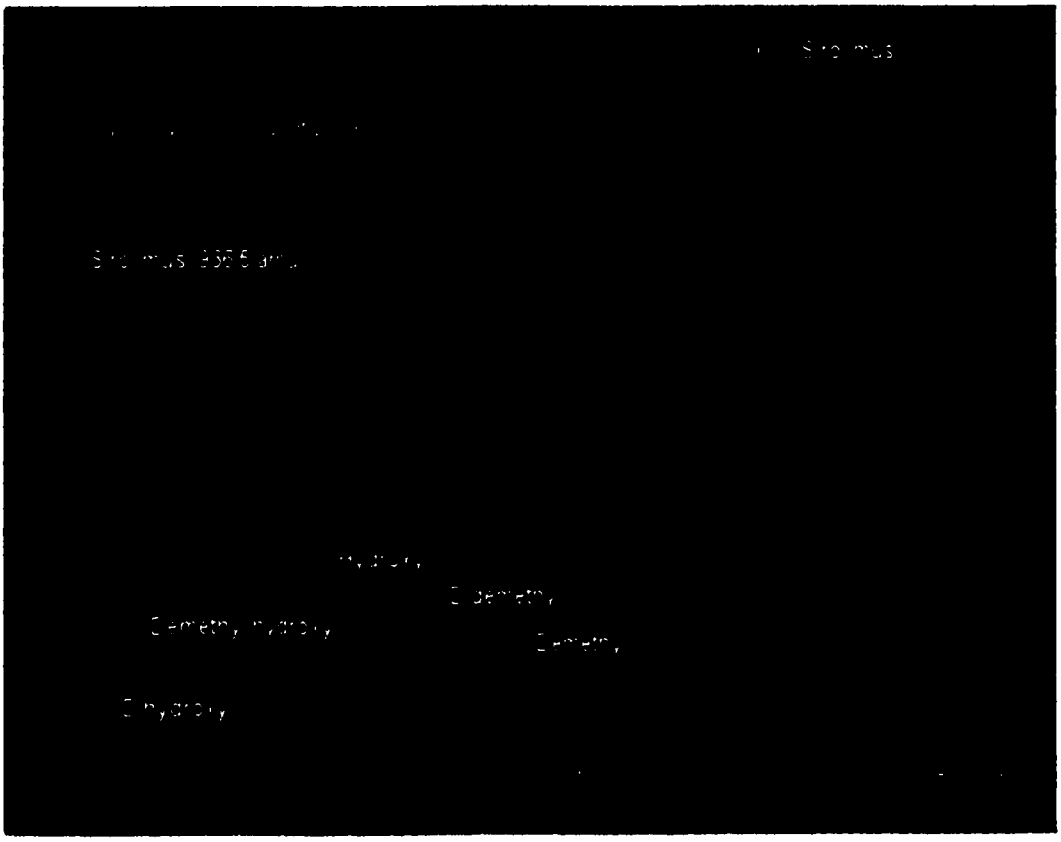

metabolites are found at concentrations estimated to each be less than 30% that of rapamycin, which is generally less than 20 μg/L.

In considering whole blood as a potential source of metabolites for further study, the feasibility was extrapolated from this small scale experiment. With a large-scale repeated extraction, a total of 100 mL of whole blood could be extracted. The gross amount of metabolite available for isolation would be less than 0.6 μg of metabolite. However, after accounting for the loss of metabolite expected with multiple extractions, separation and purification, a net yield of <0.2 μg would be expected.

c. Rapamycin metabolites from rabbit liver microsomes

The chromatograph of an extract of a rabbit liver microsomal reaction with selected ion monitoring for rapamycin and metabolites is depicted in Figure III-4. Like in the human whole blood profile, the profile from the liver microsomal reaction shows that rapamycin elutes near the end of the chromatographic separation, with a similar retention time relative to DMR as in the previous experiment. As with the metabolites found in blood, several metabolites elute before rapamycin and no metabolites appear to elute after rapamycin in this chromatographic separation.

Based on calculation of the molecular weight of metabolites as sodium adducts, the following metabolites were detected in the liver microsomal reaction: demethylhydroxy- (938.5 amu), hydroxy (952.5 amu), dihydroxy- (963.5 amu), didemethyl- (908.5 amu), and demethylrapamycin (922.5 amu).

The metabolites present are listed in approximate descending concentration with their retention times relative to rapamycin: demethyl- (0.86), hydroxy- (0.64), hydroxy- (0.54), demethyl hydroxy- (0.5), and demethylrapamycin (0.54). Based on peak area ratios, the microsomal system was found to accumulate metabolites at concentrations estimated to each be less than

Figure III-4 LCMS profile of rapamycin metabolites generated in a rabbit microsomal system

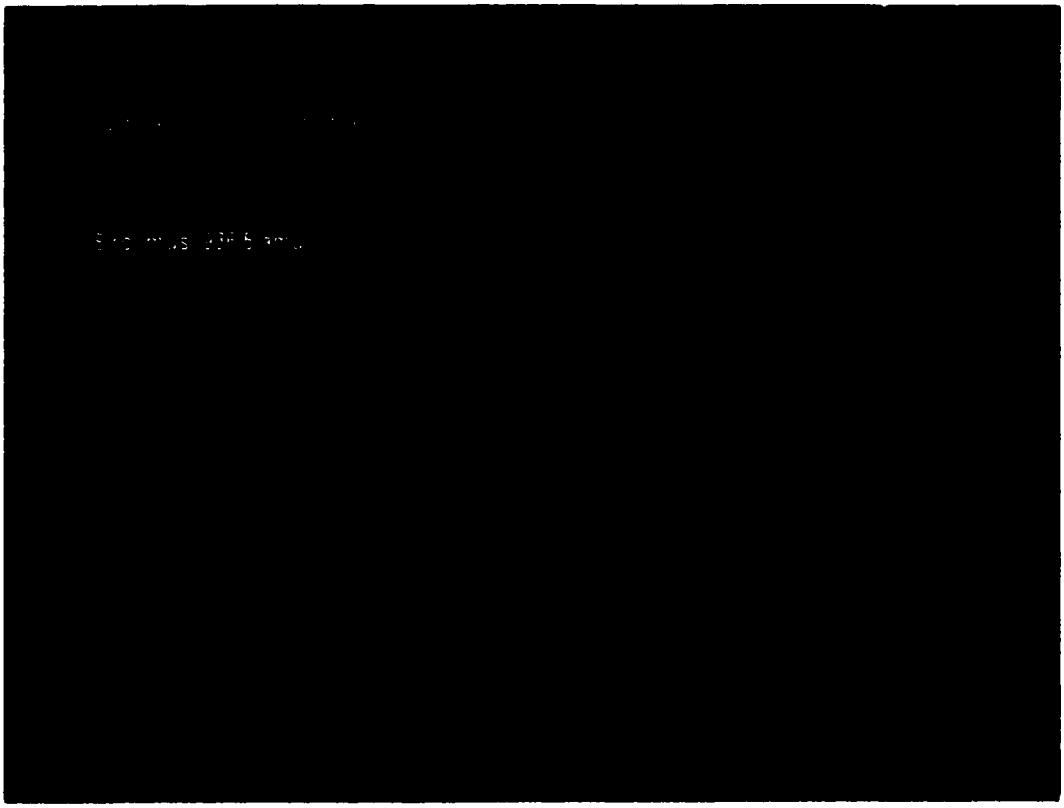

35% of rapamycin at the end of the reaction. Because of the high concentration of rapamycin present, this translates to accumulated metabolite concentrations of up to 35 μg/L for the species found at higher concentrations. Although a typical reaction was only 1 mL, a series of 20-30 replicates are feasible in a given experiment. The gross yield of an experiment, before isolation and purification was predicted to be 1 μg, and the net yield after isolation and purification predicted to be approximately 0.3 μg.

d. Microbial generation of rapamycin metabolites

In this experiment, rapamycin was incubated with a microbe for *in vitro* metabolism. The chromatograph of an extract of a microbial reaction with selected ion monitoring for rapamycin and metabolites is depicted in Figure III-5. As with the whole blood and microsomal systems, rapamycin is demonstrated in the profile and elutes near the end of the chromatographic separation (0.89 relative to DMR), with the metabolites eluting before rapamycin. With a 24 hour microbial incubation, the major accumulated metabolites, in order of decreasing concentration are: demethyl (0.86), hydroxy (0.54), dihydroxy (0.5), didemethyl (0.46), demethyl hydroxy (0.5) and demethyl (0.68).

A representative chromatograph of the extended microbial incubation is depicted in Figure III-6. With an extended microbial culture incubation (96 hours), a loss of detectable rapamycin resulted. This occurred with the concomitant formation of higher concentrations of metabolites, the appearance of more highly changed metabolite species, and the loss of late-eluting singly changed species such as demethylrapamycin (0.86). This is evident by the appearance of larger peaks eluting earlier in the chromatogram – more polar species elute earlier, and have more structural differences as compared to parent drug. This is exemplified by the appearance of tridemethylrapamycin (0.39), which was not present in either of the two other systems.

The major metabolites that accumulated after 96 hours of incubation in the microbial metabolite generation system, in descending concentration are: demethyl (0.54), hydroxy (0.54), demethyl

Figure III-5 LCMS profile of rapamycin metabolites generated in a microbial culture

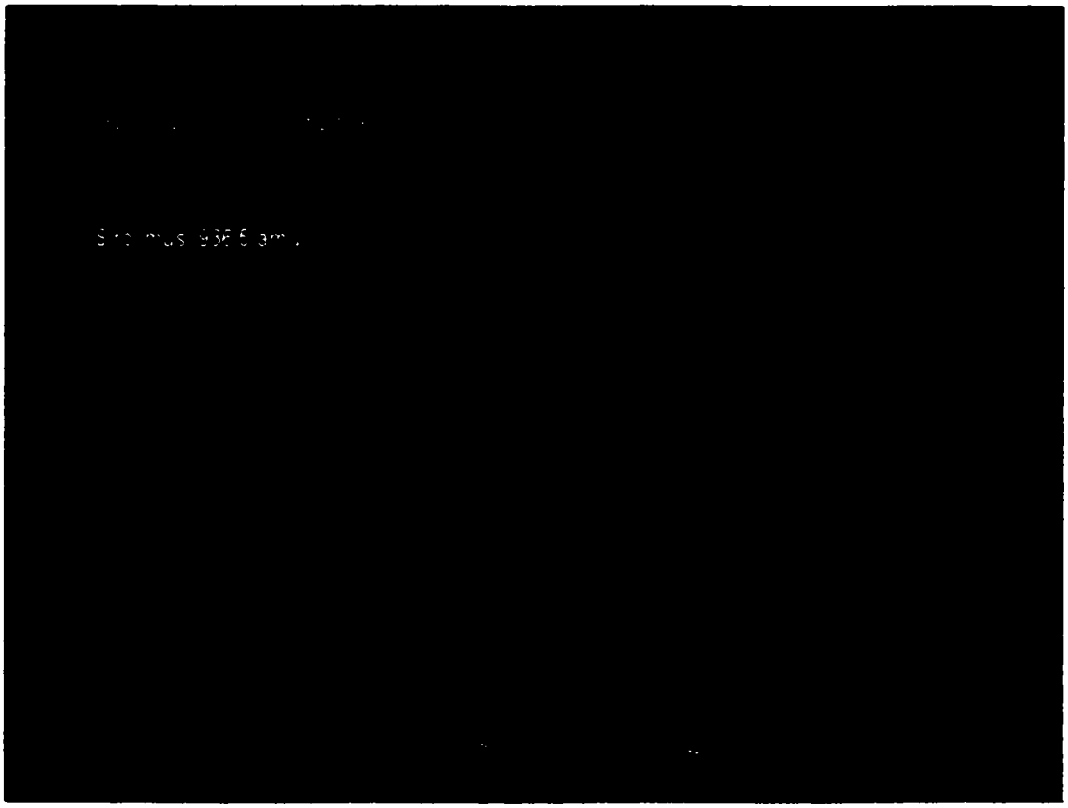

Figure III-6 LCMS profile of rapamycin metabolites generated in a microbial culture, with extended incubation time

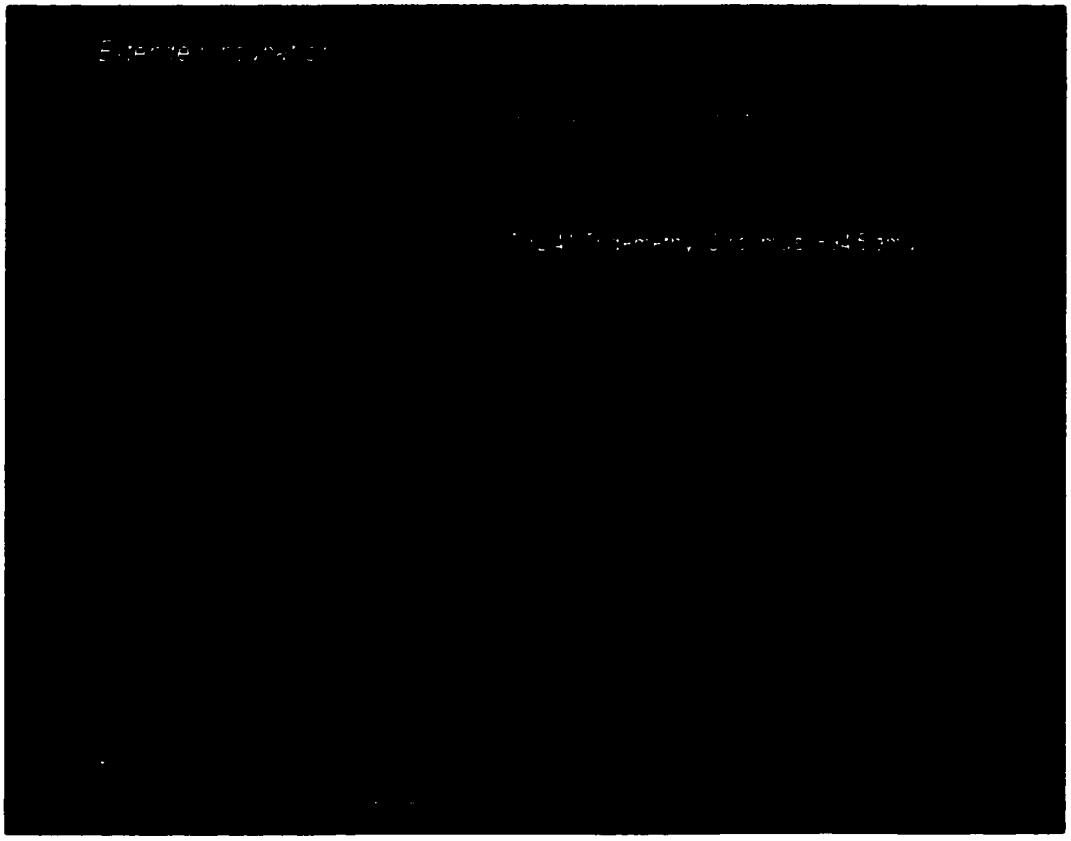

hydroxy (0.32), demethyl hydroxy (0.5), tridemethyl (0.39), dihydroxy (0.32), and demethyl (0.68).

A summary of the rapamycin metabolites identified in each of the three sources (human whole blood, rabbit liver microsomal and microbial reaction) is in Table III-2.

Based on peak area ratios, the microbial system was found to accumulate metabolites at concentrations estimated to be 25-50 μg/L for the species found at higher concentrations. The reaction would be scaled up to produce 200 mL of culture for extraction. The gross yield of an experiment, before isolation and purification was predicted to be 5-10 μg for the higher concentration metabolites, and the net yield after isolation and purification predicted to be approximately 1-3 μg.

e. Investigation of the polar Phase II metabolites of rapamycin

Phase II metabolism of xenobiotics is comprised of conjugation-type reactions where the drug is made more water soluble by the addition of polar groups to its structure. These reactions are enzymatic and involve the chemical addition of the following moieties: glucuronide (M+176), sulfate (M+80), mercapturic acid (M+162), or acetyl (M+43). Examination of the structure of rapamycin revealed the potential for Phase II metabolic conjugation, as evident by numerous available exchangable protons, hydroxyl and O-linked methyl groups.

There was no evidence found in this study to support Phase II metabolism of rapamycin occurring *in vivo* in the human or in the New Zealand White rabbit. Rigorous investigation of human urine and whole blood and rabbit blood urine and feces failed to demonstrate the presence of rapamycin or rapamycin metabolites conjugated to the above named compounds, or to amino acids or simple sugars. Rapamycin and its Phase I metabolites, as previously described, were found in whole blood, but not in urine or feces. HPLC-UV and HPLC-(ESI)-MS analysis did not identify any new characteristic UV-absorbing peaks or ions in the range

Table III-2 Rapamycin metabolite sources

Microbial Systems		Human Whole Blood		Rabbit Microsomal System	
Metabolite	RRT[a]	Metabolite	RRT	Metabolite	RRT
dihydroxy	0.26				
dihydroxy	0.34	dihydroxy	0.30-0.53	dihydroxy	0.30-0.53
dihydroxy	0.53				
demethyl-hydroxy	0.34	demethyl-hydroxy	0.30-0.53	demethyl-hydroxy	0.30-0.53
demethyl-hydroxy	0.53				
		hydroxy	0.41		
hydroxy	0.56	hydroxy	0.56	hydroxy	0.56
hydroxy	0.68	hydroxy	0.68	hydroxy	0.68
didemethyl	0.49	didemethyl	0.49	didemethyl	0.49
didemethyl	0.79				
demethyl	0.56	demethyl	0.56	demethyl	0.56
demethyl	0.71	demethyl	0.71	demethyl	0.71
39-O-demethyl	0.90	39-O-demethyl	0.90	39-O-demethyl	0.90

[a] RRT = retention time relative to DMR

of 920-1300 amu, the mass range where the conjugated products of either rapamycin or rapamycin metabolites would appear.

As an *in vitro* metabolite generating system, rabbit liver microsomes were used in an attempt to generate conjugated products. MPA, the active metabolite of mycophenolate mofetil was included as a positive control as it is a known substrate for the gucuronide conjugation reaction. It was found that MPA-glucuronide (MPAG) was formed by the liver microsomal system, and could be cleaved to free MPA with glucuronidase treatment, indicating normal glucuronide transferase activity in the rabbit liver microsomal preparation.

Although the glucuronide-transferase activity was demonstrated in the rabbit microsomal reaction, no glucuronidated products of rapamycin or rapamycin metabolites were found. Nor were amino acid- or sulfate-conjugated rapamycin or metabolite products detected. The only conjugated product found in a repeatable fashion was a glycated-rapamycin species, which was not detectable in human or rabbit samples described above.

f. Structural identification and confirmation of purity of isolated rapamycin metabolites by ESI-MS and HPLC-MS

Five metabolites initially identified and produced in the microbial reaction system were chosen for isolation and purification, based on relevance (presence in human whole blood), relative abundance, and ease of isolation. They were assigned a letter name based on the group of peaks as they are eluted from the HPLC column, then a number to subdivide the group, based on the order in which they elute in the group. For example, metabolite RC5 is a Rapamycin metabolite from group C, and is the 5th peak in this group.

After isolation and purification, the linear gradient was altered slightly to giver better peak shape. This resulted in a small change to the relative retention times of the metabolites, and they are listed with their proposed structures in Table III-3.

Table III-3 Proposed structures of five rapamycin metabolites

Fraction	Structural Alteration	RRT[a]	Proposed Structure
RC5	didemethyl	0.4	27-,39-O-didemethyl
RD4	demethyl	0.48	16-O-demethyl
RF1	demethyl	0.78	39-O-demethyl
RD1	hydroxy	0.48	(C1-C14)-hydroxy
RD3	hydroxy	0.5	(C14-C27)-hydroxy

[a] RRT = retention time relative to rapamycin

RC5: This metabolite was identified as didemethylrapamycin under non-fragmenting conditions ($[M + Na^+] = 908.5$ amu). ESI-MS was used to develop a fragmentation pattern for more specific localization of the structural changes. By increasing the voltage on the capillary exit at the threshold of the ESI chamber, additional stress in the form of extra charge is placed on the micro-droplet, which is composed of organic solvent, aqueous material, buffer and analyte. This is conducive to fragmentation of ionized particles held within the droplet as de-solvation occurs. This is presumed to occur by way of collisioninduced dissociation as ionized particles collide or explode because of stress on the surface of the droplet. The fragmentation pattern obtained by higher voltage ESI-MS of RC5 is presented as Figure III-7. The fragmentation profile was compared to that of rapamcyin, presented in Figure III-2. The molecular ion is 908.7 amu, which corresponds to RC5 as the sodium adduct of didemethylrapamycin (M – 28.1 amu). Some of the other ions found in the spectra can be assigned as fragments of RC5 based on molecular weight of the fragments of rapamycin, the known structure of rapamycin and candidate sites for the demethylation reaction. An O-linked methyl group (CH_3) represents the most likely site for demethylation. There are three O-CH_3 groups on rapamycin, C16-O-CH_3 , C27-O-CH_3 and C39-O-CH_3.

The 600.3 amu ion, found at relatively high abundance, can be assigned as the sodium adduct of a fragment of rapamycin, from C1 to C27, with the loss of one methyl (-CH_3) group and its subsequent replacement by one proton (H) (614 amu - 14 amu = 600 amu). This strongly suggests that one of the methyl groups has been lost from either the C16-O-CH_3 or from the C27-O-CH_3 site.

The 593.5 amu ion is assigned as a fragment of rapamycin from C15 to C42, with the loss of a single CH_3 group (607amu - 14 amu = 593 amu). During the fragmentation of rapamycin, it is known that this fragment loses the methyl group from C16 during the fragmentation process, with subsequent C15 to C16 double bond formation[6]. Taken together with the 600.3 amu fragment, this shows that one of the methyl groups has been lost from the C27-O-CH_3 site, and

Figure III-7 ESI-MS fragmentation of RC5

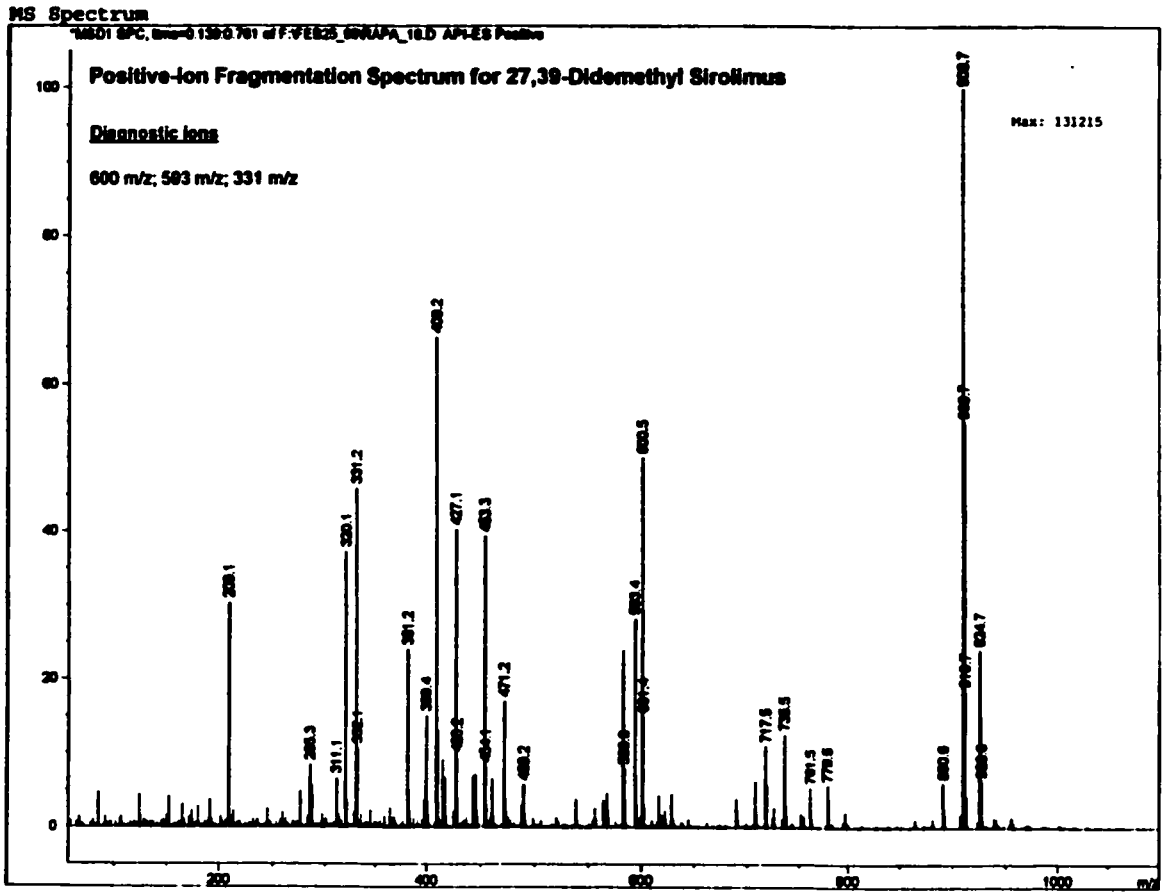

the C16-O-CH_3 group would have to be intact in this metabolite for the appropriate formation of this fragment.

The 331.2 amu fragment can be assigned as a fragment of rapamycin from C28 to C42, with the loss of a methyl (CH_3) group (345 amu - 14 amu). This indicates that the other methyl group has been lost from the C39-O-CH_3 site.

Thus RC5 is tentatively identified as 27-,39,-O-didemethylrapamycin. The structure of 27-,39,-O-didemethylrapamycin is presented in Figure III-8.

RD1: This metabolite was identified as hydroxyrapamycin under non-fragmenting conditions ([M + Na^+] = 952.6 amu). The fragmentation pattern by high voltage ESI-MS is presented as Figure III-9. The molecular ion is 952.7 amu, which corresponds to RD1 as the sodium adduct of hydroxyrapamycin. Some of the other ions found in the spectra can be assigned as fragments of RD1 based on molecular weight of the elements composing rapamycin, the known structure of rapamycin and candidate sites for the hydroxylation reaction. A non-substituted carbon in the ring represents a favorable and potential site for hydroxylation. There are many of these carbons on the main ring of rapamycin, and several on the closed six-membered ring structures of C10-C14, C2-N7 and on C33-C42.

The 345.2 amu ion, although found at only moderate abundance, can be assigned as the sodium adduct of a fragment of rapamycin from C28 to C42 intact [M + Na^+ (322 + 23) = 345.2 amu]. As there are no structural changes to this fragment, this suggests that the hydroxylation has occurred on the remainder of the structure, in the C1 to C27.

The 607.3 amu fragment, found at low abundance, can be assigned as the soduim adduct of a fragment of rapamycin from C15 to C42 and is also without structural change. During the formation of this fragment, the loss of the C16-OCH_3 group normally occurs coupled with the

Figure III-8 Structure, 27-,39-O-didemethylrapamycin

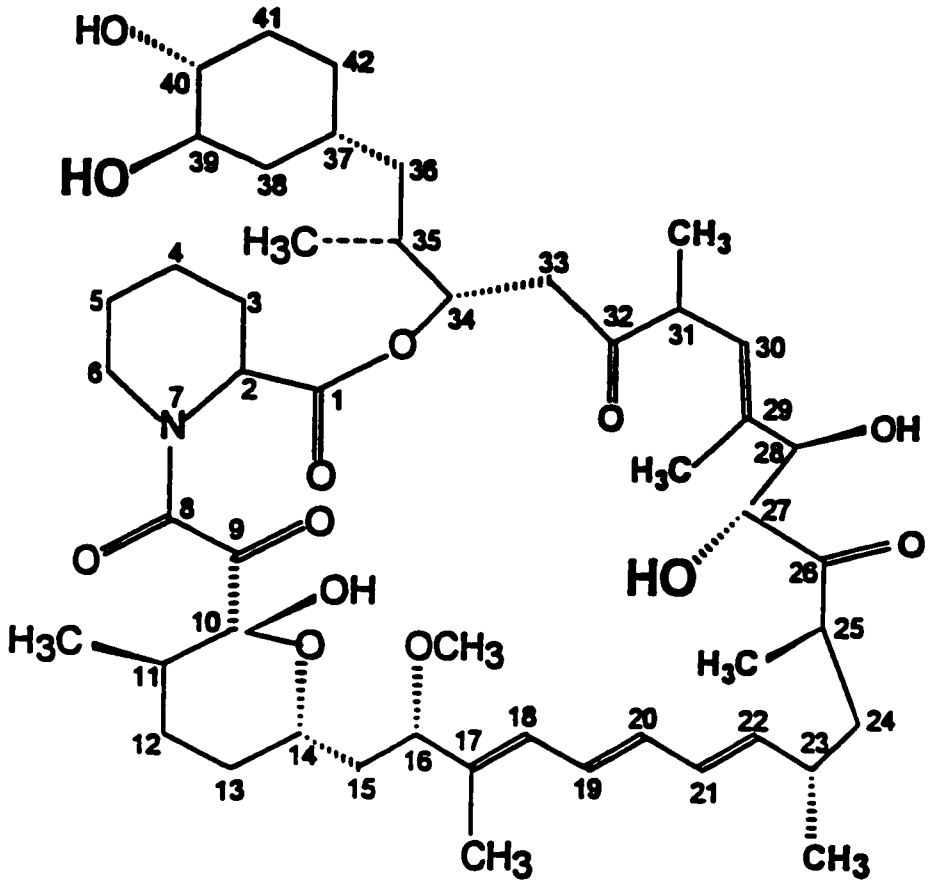

Figure III-9 ESI-MS fragmentation of RD1

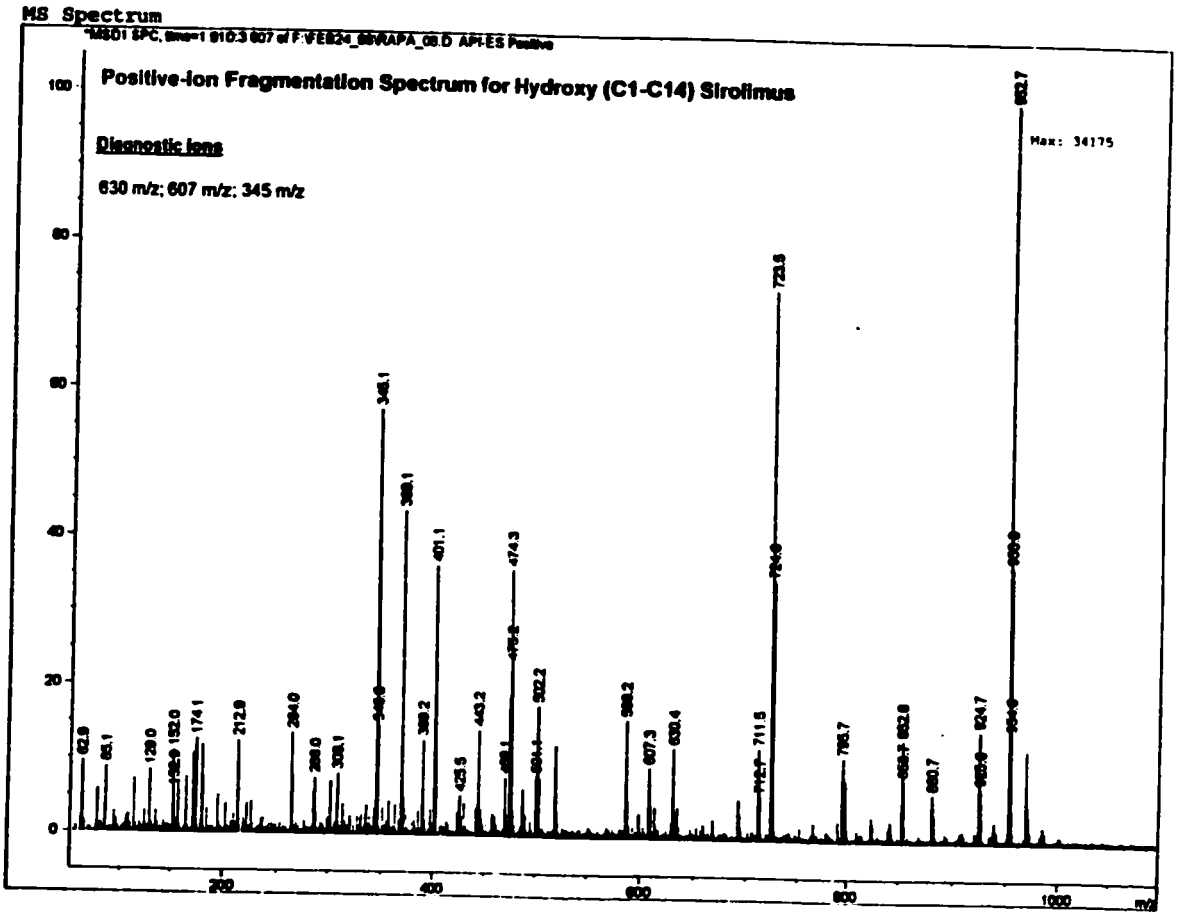

formation of a C15-C16 double bond, as discussed previously. This rules out that the hydroxylation occurred on any of these residues.

The 630.6 amu fragment can be assigned as the sodium adduct of a fragment of rapamycin from C1 to C27, with the addition of 16 amu, equivalent to a hydroxyl group. This indicates that the hydroxylation has occurred in this fragment.

Taken together, the possible sites for hydroxylation are C1 to C14. The structure of (C1-C14) hydroxyrapamycin is presented in Figure III-10.

RD3: This metabolite was identified as hydroxyrapamycin under non-fragmenting conditions ([M + Na^+] = 952.6 amu). The fragmentation pattern by high voltage ESI-MS is presented as Figure III-11. The molecular ion is 952.7 amu, which corresponds to RD3 as the sodium adduct of hydroxyrapamycin. Some of the other ions found in the spectra can be assigned as fragments of RD3 based on molecular weight of the elements composing rapamycin, the known structure of rapamycin and candidate sites for the hydroxylation reaction. A non-substituted carbon in the ring represents a favorable and potential site for hydroxylation. There are many of these carbons on the main ring of rapamycin, and several on the closed six-membered ring structures of C10-C14, C2-N7 and on C37-C44.

The 345.1 amu ion, found at only moderate abundance, can be assigned as the sodium adduct of a fragment of rapamycin from C28 to C42 intact [M + Na^+ (322 + 23) = 345.2 amu]. As there are no structural changes to this fragment, this suggests that the hydroxylation has occurred on either the C1 to C27 region.

The 623.4 amu fragment, found at low abundance, can be assigned as the sodium adduct of a frament of rapamycin from C15-C42, and with the addition of a hydroxyl (16 amu) group. During the formation of this fragment, the loss of the C16-OCH_3 group normally occurs coupled

Figure III-10 Structure, (C1-C14)-hydroxyrapamycin

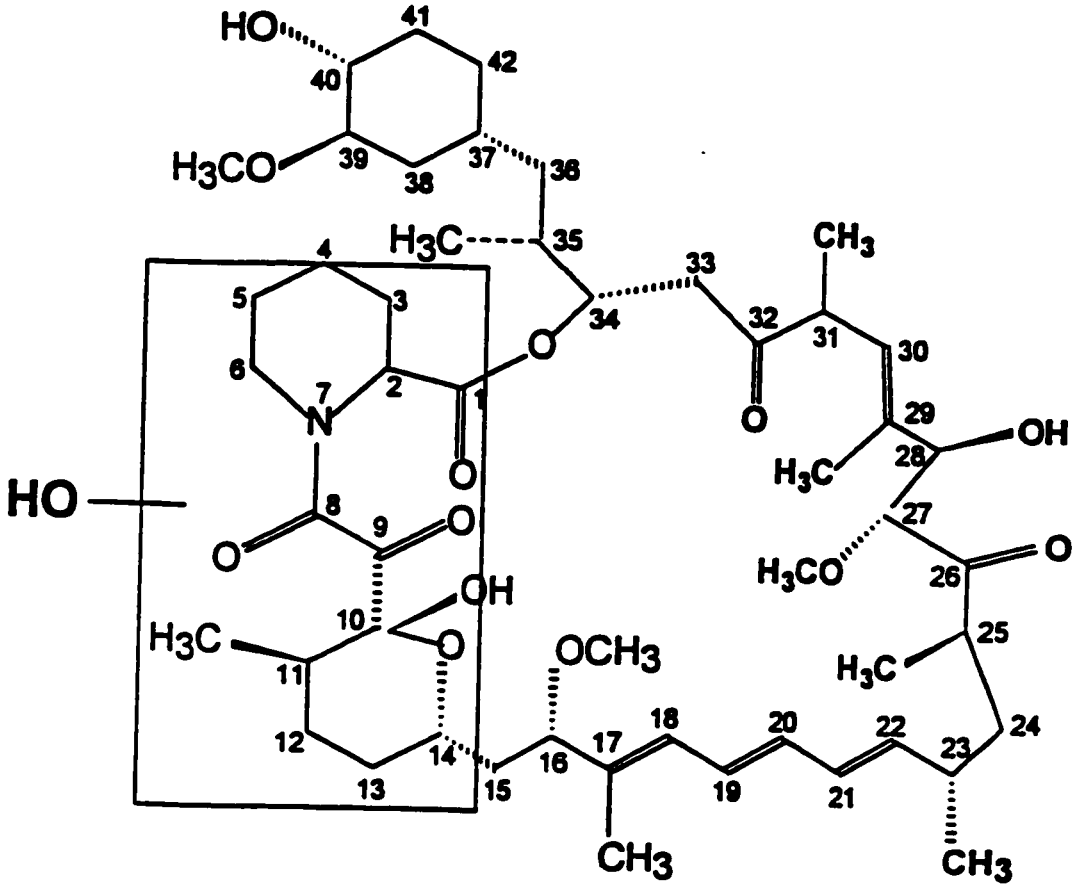

Figure III-11 ESI-MS fragmentation of RD3

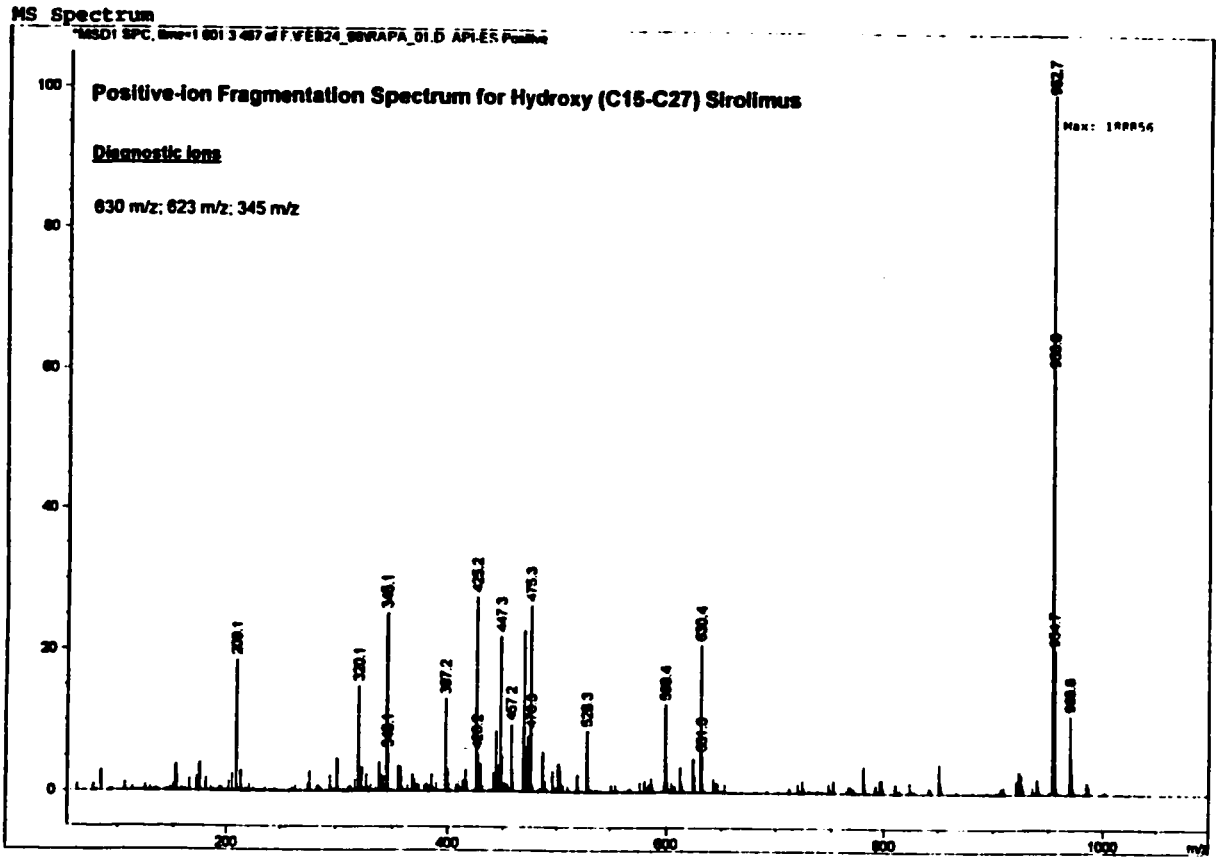

with the formation of a C15-C16 double bond. This narrows the range of sites for hydroxylation and suggests that the change has occurred in the C15 to C27 range.

The 630.4 amu ion, found at only moderate abundance, can be assigned as the sodium adduct of a fragment of rapamycin from C1 to C27, with the addition of 16 amu, or a hydroxyl group. This indicates that the hydroxylation has occurred in this fragment. Taken with the information fron the 345.1 amu fragment, as described above, the hydroxylation has occurred in the C15 to C27 region.

Taken together, the possible sites for hydroxylation are C15 to C27. The structure of (C15-C27) hydroxyrapamycin is presented in Figure III-12.

RD4: This metabolite was identified as demethylrapamycin under non-fragmenting conditions ($[M + Na^+]$ = 922.5 amu). ESI-MS was used to develop a fragmentation pattern for more specific localization of the structural changes. The fragmentation pattern obtained by higher voltage ESI-MS is presented as Figure III-13. The molecular ion is 922.7 amu, which corresponds to RD4 as the sodium adduct of demethylrapamycin. Some of the other ions found in the spectra can be assigned as fragments of RD4 based on molecular weight of the elements composing rapamycin, the known structure of rapamycin and candidate sites for the demethylation reaction. An O-linked methyl group represents the most likely site for demethylation. As previously described, there are three O-CH_3 groups on rapamycin, C16-O-CH_3 , C27-O-CH_3 and C39-O-CH_3.

The 600.3 amu ion, found at relatively high abundance can be assigned as the sodium adduct of a fragment of rapamycin, from C1 to C27, with the loss of one methyl (-CH_3) group and its subsequent replacement by one proton (H) (614 amu - 14 amu = 600 amu). This suggests that one of the methyl groups has been lost from either the C16-O-CH_3 or from the C27-O-CH_3 site.

Figure III-12 Structure, (C15-C27)-hydroxyrapamycin

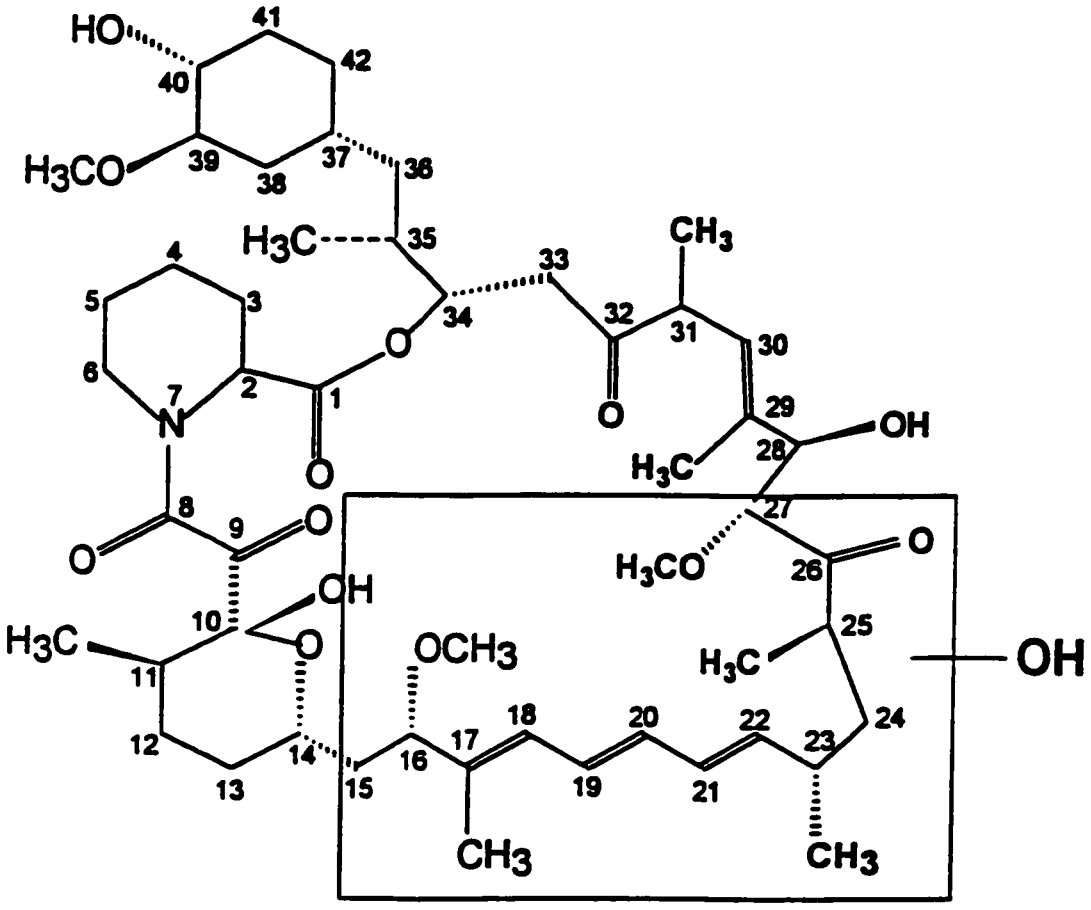

Figure III-13 ESI-MS fragmentation of RD4

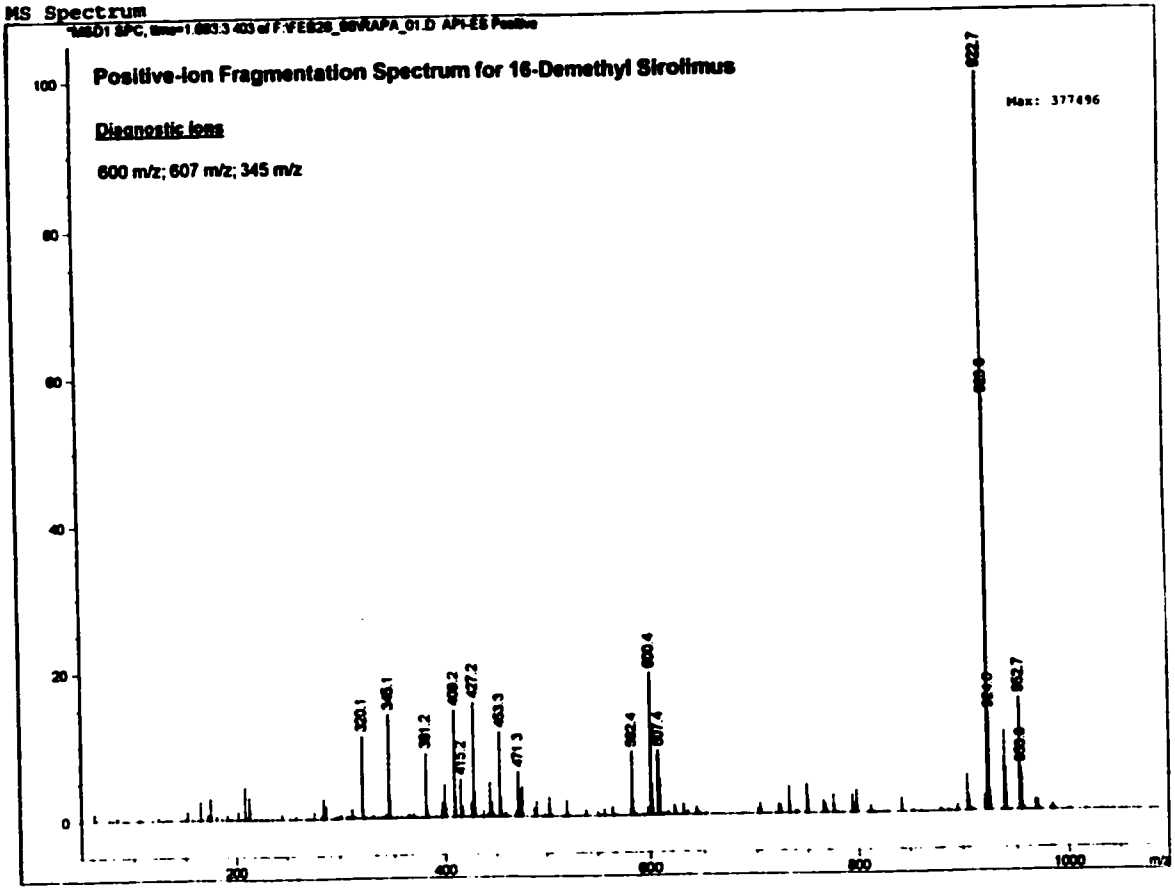

The 607.5 amu ion can be assigned as the sodium adduct of a fragment of rapamycin from C15 to C42 without structural change. This rules out that the methyl group was lost from the C27-O-CH_3 site.

The final evidence comes from the 345.1 amu fragment. It can be assigned as the sodium adduct of a fragment of rapamycin from C28 to C42 intact [M + Na^+ (322 + 23) = 345.2 amu]. As there are no structural changes to this fragment, this confirms that the 39-O-CH_3 is intact, and suggests that the demethylation has occurred in the C1 to C27 range.

Taken together, there is a strong suggestion that RD4 is 16-O-demethylrapamycin. The structure of 16-O-demethylrapamycin is presented in Figure III-14.

RF1: This metabolite was identified as demethylrapamycin under non-fragmenting conditions ([M + Na^+] = 922.5 amu). ESI-MS was used to develop a fragmentation pattern for more specific localization of the structural changes. The fragmentation pattern obtained by higher voltage ESI-MS is presented as Figure III-15. The molecular ion is 922.7 amu, which corresponds to RF1 as the sodium adduct of demethylrapamycin. Some of the other ions found in the spectra can be assigned as fragments of RF1 based on molecular weight of the elements composing rapamycin, the known structure of rapamycin and candidate sites for the demethylation reaction. An O-linked methyl group represents the most likely site for demethylation. As previously described, there are three O-CH_3 groups on rapamycin, C16-O-CH_3 , C27-O-CH_3 and C39-O-CH_3.

The 331.1 amu fragment can be assigned as the sodium adduct of a fragment of rapamycin from C28 to C42 [M + Na^+ (322 + 23) = 345.2 amu] and the loss of 14 amu, corressponding to a methyl group. This suggests that the demethylation has occurred on 39-O-CH_3.

Figure III-14 Structure, 16-O-demethylrapamycin

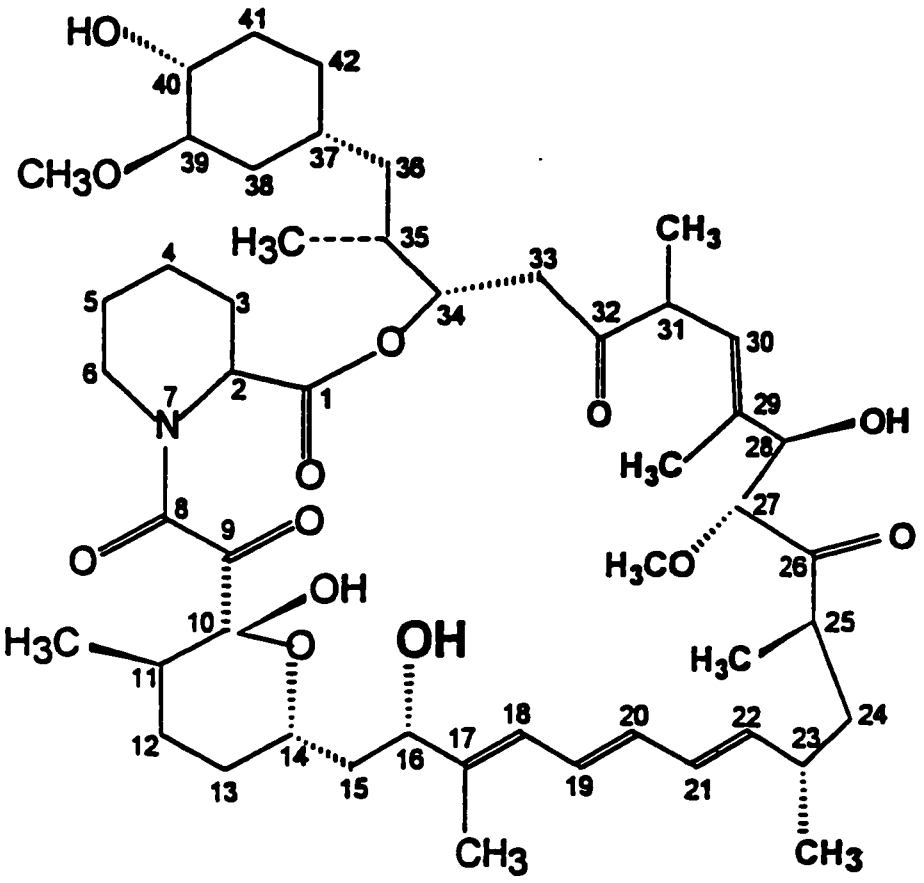

Figure III-15 ESI-MS fragmentation of RF1

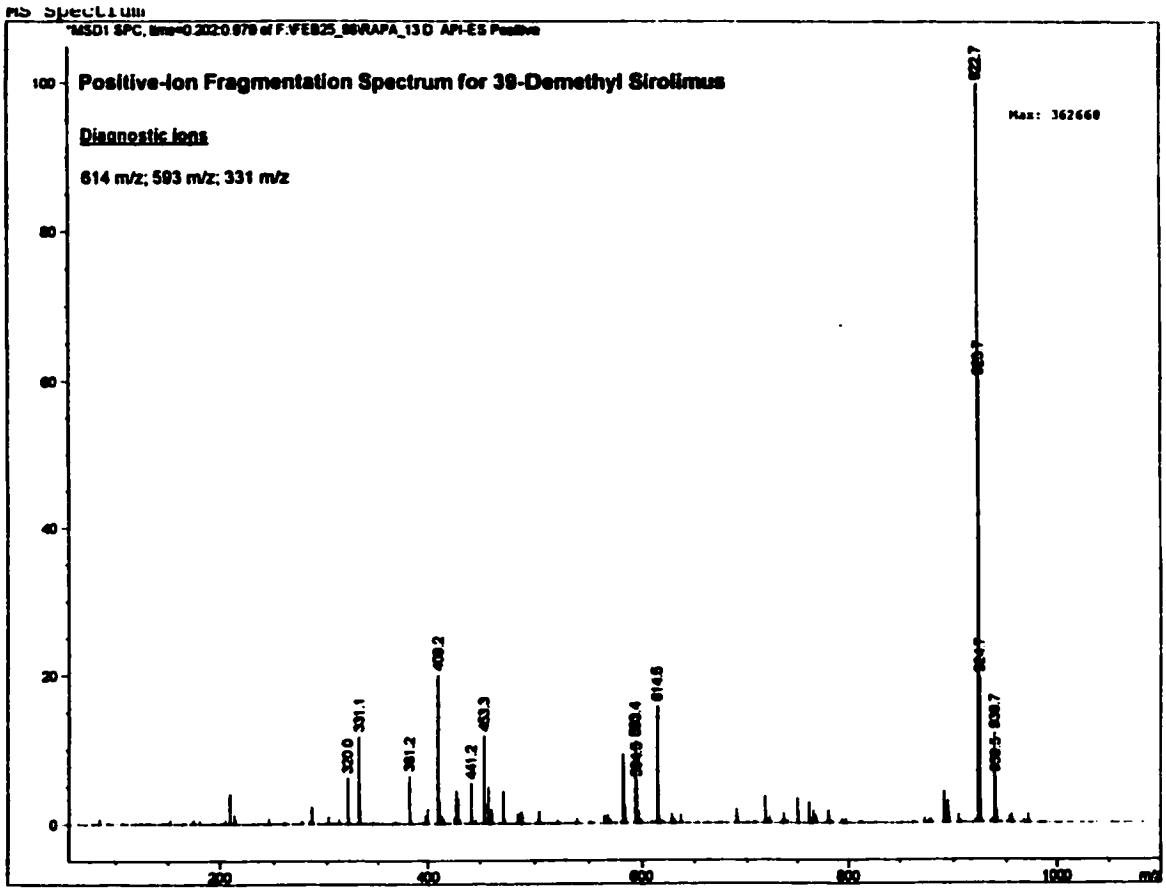

The 593.5 amu fragment can be assigned as the soduim adduct of a fragment of rapamycin from C15 to C42 with the loss of a methyl group (14 amu). As previously described, this fragment normally forms with the loss of the methyoxy group from C16 and the formation of a C15-C16 double bond. This indicates the methyl group was lost from the either the C27-O-CH_3 site or the 41-O-CH_3, and because this is a mono-demethylated metabolite, effectively rules-out C16-O-CH_3 as the site of demethylation.

The 614.5 amu fragment can be assigned as the sodium adduct of a fragment of rapamycin from C1 to C27 without structural change. This indicates that the demethylation did not occur on this fragment, and thus the C16-O-CH_3 and C27-O-CH_3 are both intact. Therefore, the structure is most likely C39-O-CH_3. The structure of 39-O-demethylrapamycin is presented in Figure III-16.

Aside from the five metabolites identified and partially characterized above, there were several other potential metabolites noted in the extracts from each of the metabolite generation systems. The basic structural alteration was identifiable by HPLC-MS, but because of technical difficulty (poor resolution or poor recovery) and small quantities of metabolite present, these metabolites were not further characterized or isolated and purified. Only well-characterized, purified metabolites were used for subsequent activity testing.

g. Metabolite Purity Assessment

Purity was determined by several methodologies. Initially purity was evaluated with HPLC-UV, with detection at 276 nm. Before proceeding, it was required that each metabolite elute as a discrete peak by HPLC. As with rapamycin and DMR, some metabolites appeared under these chromatographic conditions as two peaks, presumably rotamers of the same structure. It was proven that each of these peaks could be collected individually and resubjected to HPLC separation to again produce the two peaks. This was followed by HPLC-(ESI)-MS analysis, by adding all the non-metabolite, non-overlapping peaks together as impurites. It was found that

Figure III-16 Structure, 39-O-demethylrapamycin

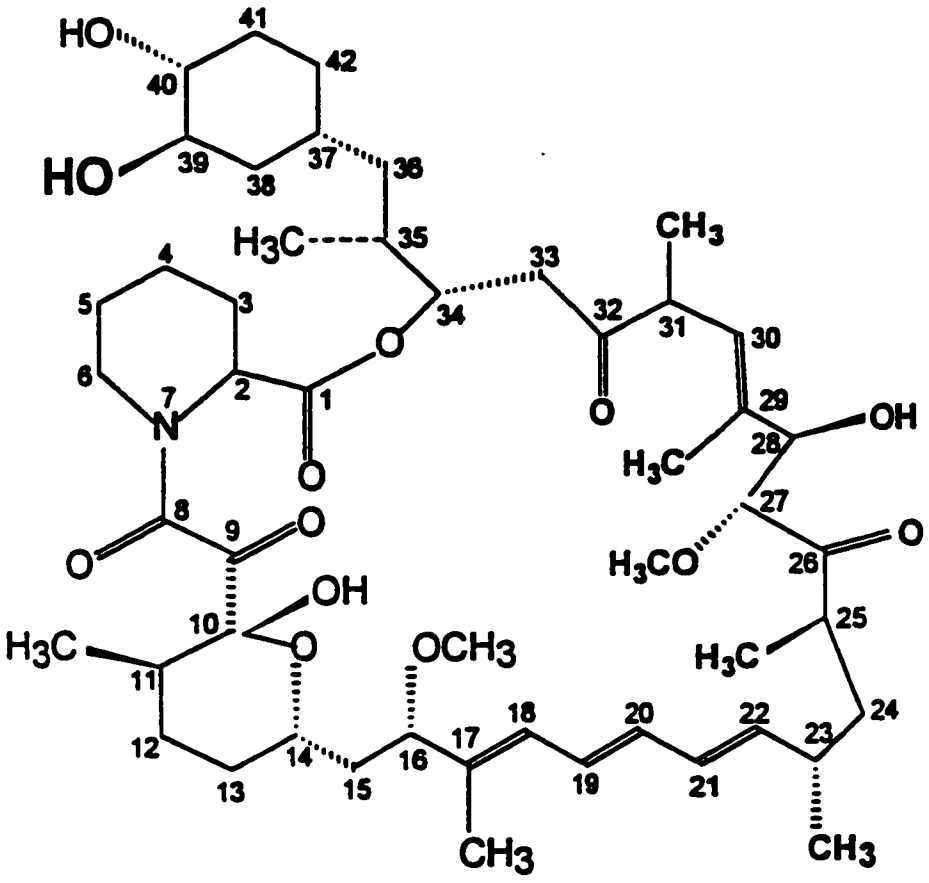

the metabolites were virtually free of contamination by rapamycin and the other metabolites, based on amu monitoring. Each metabolite had some degree of contamination with non-metabolite, non-rapamycin substances based on the calculation of all non-metabolite, non-rapamycin peaks appearing in the chromatogram. This ranged from 2-10% based on amu area calculation.

Finally, the sensitivity of the assay to detect contamination was challenged by adding increasing amounts of metabolite to rapamycin as a test, and monitoring for the appearance of the contaminating material by HPLC (ESI)-MS. The principle of this method is based on the fact that different compounds appear as molecular ions of differing mass. As previously stated, rapamycin appears by ESI-MS as a sodium adduct, *m/z* = 936.5. If it was contaminated with hydroxyrapamycin, a second molecular ion of 952.5 amu would appear in the mass spectra. The absolute cutoff for detection of metabolite contamination of rapamycin ranged from 0.06 ug/L of contaminant for RD1 and 0.08 ug/L of contaminant for RC5, in a 10 ug/L sample of rapamycin. A similar experiment using DMR and rapamycin revelaled that rapamycin was detectable at 0.07 μg/L rapamycin in 10 μg/L DMR. As in the mass spectra where purity was assessed, there was no measurable contamination of the metabolites by rapamycin, DMR or other rapamycin metabolites. The samples were >99% free of contamination from other metabolites or rapamycin. This represents <1% contamination by other rapamycin metabolites or by rapamycin.

h. Quantification of rapamycin metabolites by HPLC

The amounts of rapamycin metabolites as estimated by HPLC are presented in Table III-4.

Table III-4 Amounts of purified rapamycin metabolites isolated

Rapamycin Metabolite	Amount Isolated (μg)
27-,39-O-didemethyl	334
16-O-demethyl	726
39-O-demethyl	249
(C1-C14)-hydroxy	488
(C14-C27)-hydroxy	685

4. DISCUSSION

In order to study the activity of the metabolites of rapamycin, it was necessary to first find a source of these metabolites. It was also necessary that the metabolites be isolated and purified from that source before activity testing could commence. Before conclusions can be reached regarding rapamycin metabolites and their role in immunosuppression and toxicity, it is manditory that they be measureable, of known structure, and of appropriate quantity and purity.

There were several products detected by HPLC-UV in human urine that resembled rapamycin metabolites. The UV spectra of these products approximated that of rapamycin, with similar absorbance peaks in the 266, 276 and 286 nm range. They were isolated and tested for immunosuppression in the MLC assay and for binding to the 14- and 52- kDa FKBP. Unfortunately, structural evaluation by FAB-MS was not available until after these studies were completed, and it appears these substances are likely small molecules (<900 amu) that may or may not be related to rapamycin. They may be small cleavage products of rapamycin, or may be other substances that contain a triene-structure, accounting for the characteristic UV absorbance.

It was surprising that rapamycin and rapamycin metabolites were not isolated from human urine or rabbit feces or urine. Metabolites of both CsA and tacrolimus are excreted in the bile and urine[7, 8]. Based on this information, it was thought that rapamycin and/or metabolites would be similarly excreted in the urine or feces. It remains possible that the metabolites of rapamycin may be susceptible to degradation in the bile and urine, and thus may be broken down rapidly by chemical or microbial processes and excreted as small molecular weight products which were not predicted or detected.

Rapamycin and several of its metabolites were detectable in human and rabbit whole blood using HPLC-(ESI)-MS. This technique has a major advantage over HPLC-UV in that a molecular weight range or selected masses are measurable for each peak as it elutes from the

HPLC system and is analyzed by the MS. When choosing compounds for further studies, this enables decisions to be made on the basis of appropriate molecular weight, rather than spectral absorption character, which is a scan of the absorption of a particular wavelengths of light by electrons in characteristic chemical groups. UV absorbance at a given wavelength suggest that the chemical group is present in the compound, but does not give a definitive identity to the compound itself. Using MS in conjunction with UV detection decreases the likelihood of chosing an irrelevant compound for further study.

There were hydroxylated, dihydroxylated, demethylated, didemethylated, demethyl-hydroxylated-rapamycin metabolites and rapamycin demonstrated in the blood of a renal transplant patient. For some metabolites, there was more than one peak in the profile with a mass that corresponded to a single structural change. This could be accounted for by the presence of multiple rapamycin metabolites with one type of structural change at several different sites on the molecule. For example, there were at least three peaks for hydroxylated species detected. These could all represent different hydroxyrapamycin species. All structural modifications were determined by calculating the alteration in amu, as compared to rapamycin, but metabolites were not fully characterized or structural changes localized in these rapamycin-metabolites because of the small amount of recoverable metabolite present in whole blood.

A similar rapamycin metabolite profile was found after incubation of rapamycin in the rabbit liver microsomal system. Essentially the same rapamycin metabolites were produced in this system that were found in human whole blood (hydroxylated, dihydroxylated, demethylated, didemethylated, demethylhydroxylated metabolites from rapamycin), but in varying absolute and relative amounts. Again, multiple peaks for various metabolites were noted, but structural changes were not further investigated because of small metabolite yield in the microsomal metabolite generation system.

The microbial culture produced the most promising results for metabolite generation. Essentially the same rapamycin metabolites were produced in the microbial system as were found in blood and as were produced in the micosomal system. The amounts of rapamycin metabolites present in the microbial system varied from the other two systems. Hydroxylated, dihydroxylated, demethylated, didemethylated, demethylhydroxylated metabolites and rapamycin were all found in the microbial culture at 24 hours. When the incubation was extended to 40 hours, the degree of hydrophilicity of the metabolites increased, as did the degree of change to the structure of rapamycin, with more multiply changed species appearing. In this system, a novel metabolite was produced, tridemethylrapamycin, which was not demonstrated in any of the other systems.

Because this microbial system was easily manipulated and possessed the potential for the greatest amount of metabolite production, it was chosen for the production of rapamycin metabolites. One of the specific aims of this study was to isolate, purify, and characterize rapamycin metabolites for subsequent activity testing. The rapamycin metabolites that were chosen from all those produced were ones that were found in all systems tested: microbial, microsomal and in the human whole blood. This was done to ensure only biologically relevant metabolites were further investigated.

Five rapamycin metabolites were isolated and purified from the microbial system. Two were hydroxylated species RD1and RD3, two were demethylated species RD4 and RF1, and RC5 was a didemethylated metabolite. This partial characterization was based on molecular weight measurements as determined by HPLC-(ESI)-MS. Upon further investigation using high voltage (ESI)-MS for fragmentation, the demethylated metabolites were further characterized as 16-O-demethylrapamycin (RD4), 39-O-demethylrapamycin (RF1) and 27-,39-O-didemethylrapamycin (RC5). The site of hydroxylation of the other two metabolites was localized into regions of the molecule: (C1-C14) hydroxyrapamycin (RD1) and (C15-C27) hydroxyrapamycin (RD3).

The ability of this HPLC-(ESI)-MS to definitively identify the exact site of alteration is limited by the numerous sites on rapamycin that are available for change by metabolic processes. High-voltage ESI-MS was used in this study to localize structural changes for some metabolites, through the alteration of the characteristic fragmentation pattern produced by rapamycin. However, because fragment production only allows for the localization of the structural change to a given fragment, if there are multiple sites on the fragment available for structural change, the exact sit of alteration is not identifiable. This makes full characterization of the hydroxylated rapamycin metabolites particularly elusive.

Other investigators have explored *in vivo* metabolism of rapamycin, with detection of rapamycin metabolites in human blood[9], rat plasma[10] and rat bile[11]. *In vitro* experiments have been reported using rat bile[10], microsomes from rat liver[12,13], pig liver[14] human liver[6,12,15]and purified CYP enzymes[12]. There are no published reports of systems transgenic for CYP enzymes or microbial systems used for rapamycin metabolite investigation, although novel changes to the structure of rapamycin have been reported with microbial manipulation of the producing bacterium[16].

HPLC-UV has been used for the investigation of metabolite formation, without structural elucidation[12]. Additionally, combinations of HPLC-MS, HPLC-MS/MS and MS alone have been used by several other investigators both in rapamycin metabolite identification and structural investigation[9,11-13,15,17]. FAB, another fragmenting MS technique, has also been used with some success to evaluate rapamycin metabolite structure[10,13-15]. HPLC-(ESI)-MS is acceptable for the determination of the molecular weight of the unknown compound, and in several instances, with modifications to the basic procedure, useful for localization of structural alterations through analysis of charge-induced fragmentation. The fragmentation patterns obtained from both techniques are directly comparable.

Several metabolites of rapamycin have been reported and partially or fully characterized. Metabolites well characterized from microsomal reactions are: 39-O-demethylrapamycin [6,14,15], 12-hydroxyrapamycin[6], 16-O-demethylrapamycin[6], all of which agree with the present study. Also isolated and characterized from microsomal reactions was a ring-opened degradation product, 34-hydroxyrapamycin[6], which was not noted in our work.

Additionally, other metabolites were found in lower abundance and not fully characterized by other investigators, possibly corresponding to some of the metabolites that were characterized and described here. Of note were two more hydroxylated metabolites, plus di, tri- and tetra-hydroxylated rapamycin metabolites with sites of hydroxylation all being in the C10-C27 range[6]. Novel rapamycin metabolites were produced in microsomal reactions, but have not yet been confirmed in biological specimens. These include the tri- and tetra-hydroxylated metabolites, a rapamycin tris-epoxide metabolite[18], and both 3,4- and 5,6-dihydrodiol rapamycin metabolites[13].

A report exists in the literature of the measurement of total hydroxy-, demethyl-, dihydroxy- and didemethylrapamycin in whole blood from renal transplant patients, but without characterization or indication of how many different species of each were present, and without specific metabolite standardisation[9]. This will be discussed in section V: Metabolite quantification by LCMS.

Other mechanisms for the identification of rapamycin metabolites could potentially include the use of other specroscopic techniques. To date, the most success in characterization of rapamycin metabolites has been with multiple and tandem techniques, such as HPLC-(ESI)-MS followed by MS/MS. These have been successful in identifying the site of one of the hydroxylated rapamycin metabolites (12-hydroxyrapamycin[6]) where as in the present study, the site of hydroxylation is only available as a range for both hydroxylated metabolites investigated here by HPLC-(ESI)-MS and high voltage ESI-MS. It is possible that with MS/MS analysis, these structures could be fully elucidated and by using MS analysis with different detection

techniques, the structures of the metabolite and metabolite fragments can potentially be confirmed or more specifically elucidated. This includes using time-of-flight detection for exact mass deretmination and using an ion trap detector that may be more sensitive in detecting small fragments. Another technique for metabolite elucidation is the use of derivitization to eliminate a specific site as a metabolic target or to trace a fragment of interest.

The use of nuclear magnetic resonance (NMR) has assisted in the identification of several metabolites of CsA[8], and for the characterization of two ring-opened degradation products of rapamycin[10]. However, with the study of CsA, NMR was most effective in localizing changes to individual amino acids. This is not helpful for studying rapamycin as it is not peptide-based, but a macrolide lactone $C_{51}H_{79}NO_{13}$[19]. Consequently, in our experience, the ^{1}H spectra of rapamycin is very complex and difficult to resolve. This is partially due to the tautomeric nature of rapamycin. In solution, rapamycin appears as a mixture of cis and trans rotamers, with rotationcentred on the amide bond at position N7. This means that for many functional groups in the molecule, two chemical shifts appear on the spectra, further complicating the interpretation. The ^{13}C NMR spectra would be more useful for detecting sites of specific chemical changes, particularly with sophisticated two or three dimentional experiments. Unfortunately, the low isotopic prevalence of ^{13}C makes the technique less sensitive than ^{1}H NMR, and more than 5 mg of rapamycin was required for a single 500 mHz HETCOR two-dimentional ^{13}C NMR experiment conducted. This experiment consisted of a 4 hour data collection period and resulted in the total destruction of the sample in the process of analysis, likely due to heat instability. The same was found for DMR, where 6 mg of sample was required for the HETCOR two-dimentional ^{13}C NMR experiment, again with destruction of the sample. As rapamycin metabolites were only isolated in amounts of less than one milligram, these techniques were not reasonable to attempt.

Perhaps in the near future, NMR technology will advance and permit a higher degree of structural elucidation and resolution for these low-resonance compounds.

X-ray crystallography is another technique that could be used for characterization of rapamycin metabolites. Although it has not yet been applied to this problem, investigation of FK506 structure and binding to FKBP12 has been evaluated with this technique[12,20]. Through computer-assisted mathematical modelling, this technique could enable the elucidation of the three-dimentional structure of the metabolites, including delineation of functional group changes and locations. Further, through the use of nuclear Overhauser effect dynamics, the through-space interactions of the functional groups of FK506 in intra- and inter-molecular bonding when complexed to FKBP have been determined[12,20]. Hydrogen bonding sites have been localized and regions of FK506 that are directly involved in formation of the immunophilin complex have been determined. This could be done like-wise for rapamycin and its metabolites, perhaps lending a better understanding of the importance of functional group alterations first in FKBP binding, then in abrogation or modulation of immunosuppression. X-ray crystallography is, however, a technique that is limited by the amount of compound available for analysis; it is doubtful that in this study sufficient rapamycin metabolites were generated for this type of analysis.

One major crticism of published reports of rapamycin metabolite structure and activity is the lack of proof of purity of the isolated samples. It is of utmost importance that for the testing of activity of a compound that the compound be of extremely high purity and quality. Contaminating substances can have an inhibiting or enhancing effect on activity, and every effort must be made to properly prove purity of the compound. In the current study, determination of the sensitivity of the purity assay was made, in order to assign a purity value to the compounds of interest. A rigorous test was performed, and a high degree of purity could be assigned as the individual metabolite stocks were >99% free of contamination by other rapamycin metabolites and rapamycin itself. In contrast, none of these such studies was reported in the literature when the activity of isolated metabolites was determined[13,15]. Further, one investigator was able to measure the rapamycin metabolites gravimetrically using a semi-mico balance, but concurrently

failed to report purity assessment methods and specifications[13,14]. Both are necessary to fully evaluate purity.

From a clinical perspective, it is valuable to determine the immunosuppressive and toxic effects of rapamycin metabolites. Rapamycin therapy is undertaken at a given dose in order to produce a favorable clinical result. To date, little monitoring of rapamycin has been conducted clinically, as many of the studies have been completed on a fixed dose regimen. It is well known that under these conditions, there is a variety of favorable and deliterious outcomes. This may be due in part to variability in rapamycin level, in combination with variability in rapamycin metabolite levels. It is desirable to monitor rapamycin levels for patients on immunosuppressive therapy, and to establish if the monitoring of rapamycin metabolites is appropriate. If rapamycin metabolites are found to have toxic or immunosuppressive activities, therapeutic and monitoring strategies may be directly affected. It may be necessary to measure the concentrations of active metabolites in evaluating of the overall biological effect of rapamycin therapy.

In an effort to develop an automated method for the measurement of rapamycin, the likely candidate methodologies include receptor-binding and antibody-based assays. These both need to be tested rigorously for specificity to parent rapamycin, and to rule out cross reactivity with metabolites or other drug-like substances. This is not possible without purified, well-characterised metabolites.

The ultimate goal of rapamycin treatment is to deliver maximal immunosuppression while accepting the minimum risk of toxic and undesirable side effects. Knowledge of rapamycin metabolism and the specific biological effects of rapamycin metabolites will assist in therapeutic monitoring of the drug. This in turn, will afford better dosing of rapamycin through more appropriate evaluation of immunosuppression and risk of side effects. The first step in assessing these activities is to obtain reliable, pure and characterized metabolites. It seems

unneccessary to reiterate that this requirement be met before assigning activity and further investigating these compounds. The investigations presented in the following chapters are dependent on the correct concentration, correct structure and highest degree of purity in the rapamycin metabolites isolated here.

5. REFERENCES

1. Yatscoff RW, Faraci C, Bolingbroke P. Measurement of rapamycin in whole blood using reverse-phase high-performance liquid chromatography. Ther Drug Monit 1992; 14:138-41.

2. Guengerich FP. Microsomal enzymes involved in toxicology -- analysis and separation. Hays AW, ed. Principles and methods of toxicology. New York, NY: Raven Press, 1982: 609-37.

3. Chen TS, Arison BH, Wicker LS, *et al.* Microbial bioransformation of immunosuppressive compounds. I. Desmethylatin of FK506 and immunomycin (FR900520) by Actinplanes sp. ATCC 53771. J Antibiot 1992; 45:118-123.

4. Shipkova M, Niedmann PD, Armstrong VW, *et al.* Simultaneous determination of mycophenolic acid and its glucuronide in human plasma using a simple high performance liquid chromatography. Clin Chem 1998; 44:1481.

5. Goodyear N, Napoli KL, Murthy J *et al.* Radioreceptor assay for sirolimus. Clin Biochem 1996; 29:457-60.

6. Streit F, Christians U, Schiebel H-M, Meyer A, Sewing K-F. Structural Identification of three metabolites and a degradation product of the macrolide immunosuppressant sirolimus (rapamycin) by electrospray-MS/MS after incubation with human liver microsomes. Drug Met Dist 1996; 24:1272-8.

7. Copeland K.R., Yatscoff RW. Comparison of the effects of cyclopsorine and its metabolites on the release of prostacyclin and endothelin from mesangial cells. Transplantation 1992; 53:640-5.

8. Maurer G, Loosli HR, Schreier E, Keller B. Disposition of cyclosporin in several animal species and man. I. Structural elucidation of its metabolites. Drug Met Dispos 1984; 12:120-6.

9. Streit F, Christians U, Schiebel H-M *et al.* Sensitive and specific quantification of sirolimus (rapamycin) and its metabolites in blood of kidney graft recipients by HPLC/electrospray-mass spectrometry. Clin Chem 1996; 42:1417-25.

10. Wang PC, Chan KW, Schiksnis RA, Scatina J, Sisenwine SF. High performance liquid chromatographic isolation, spectroscopic characterization, and immunosuppressive activities of two rapamycin degration products. J Liquid Chrom B 1994; 17:3383-92.

11. Wang PC, Lim HK, Chan KW, Scatina J, Sisenwine SF. Isolation of ten metabolites from the bile of rats receiving rapamycin (sirolimus) intraveneously. ISSX Proc 1995; 8:136.

12. Sattler M, Guengerich FP, Yun C-H, Christians U, Sewing K-F. Cytochrome P-450 enzymes are responsible for biotransformation of FK506 and rapamycin in man and rat. Drug Met Dispos 1992; 20:753-61.

13. Nickmilder MJM, Latinne D, Verbeeck RK, Janssens W, Svoboda D, Lhoest GJJ. Isolation and identification of new rapamycin dihydrodiol metabolites from dexamethasone-induced rat liver microsomes. Xenobiotica 1997; 27:869-83.

14. Nickmilder MJM, Latinne D, De Houx J-P, Verbeeck RK, Svoboda D, Lhoest GJJ. Isolation and identification of a C39 demethylated metabolite of rapamycin from pig liver microsomes and evaluation of its immunosuppressive activity. Clin Chem 1998; 44:532-8.

15. Christians U, Sattler M, Schiebel H-M *et al.* Isolation of two immunosuppressive metabolites after *in vitro* metabolism of rapamycin. Drug Met Dispos 1992; 20:186-91.

16. Nishida H, Sakakibara T, Aoki F *et al.* Generation of novel rapamycin structures by microbial manipulation. J Antiobiot 1995; 48:657-66.

17. Kiplinger JP, Guadliana MA. Structural analysis of rapamycin and related compounds using $[M+Li]^+$ ions generated by liquid secondary ion mass spectrometry. Org Mass Spectrom 1994; 29:445-53.

18. Lhoest G, Zey T, Verbeeck RK *et al.* Isolation from pig liver microsomes, identification by electrospray tandem mass spectroscopy and in vitro immunosuppressive activity of a rapamycin tris-epoxide metabolite. J Mass Spec 1999; 34:28-32.

19. McAlpine JB, Swanson SJ, Jackson M, Whittern DN. Revised NMR assignments for rapamycin. J Antibiot 1991; 44:688-90.

20. Van Duyne GD, Standaert RF, Schreiber SL, Clardy J. Atomic structure of the rapamycin human immunophilin FKBP-12 complex. J Am Chem Soc 1991; 113:7433-4.

IV. ACTIVITY OF RAPAMYCIN METABOLITES

1. RATIONALE

Patients who are treated with a xenobiotic drug change the drug into metabolites that potentially have less activity and are easier to excrete. With hydrophobic drugs, like rapamycin, this is associated with an increase in water solubility. At the onset of this study, it was presumed that as patients are exposed to rapamycin, they subsequently make and are thus exposed to various rapamycin metabolites. These metabolites could have residual immunosuppressive and/or toxic activity. The activities of rapamycin metabolites remain poorly defined, and the clinical significance of these metabolites is unknown. The aim of this study was to test the immunosuppressive and toxic activity of the five rapamycin metabolites that were identified, isolated and described in the previous chapter. The relative contribution of rapamycin metabolites to immunosuppression and toxicity was investigated using *in vitro* cellular proliferation and growth assays and binding studies.

2. MATERIALS AND METHODS

a. Source of drugs and specimens

Rapamycin and DMR were gifts from Wyeth-Ayerst Inc. (Princeton, NJ). Rapamycin metabolite stocks were prepared from the purified samples described in section III. Fresh heparinized whole blood was procured by venipuncture from apparently healthy volunteers in the lab.

b. Mixed Lymphocyte Reaction

Human peripheral blood lymphocytes were isolated for the mixed lymphocyte reaction (MLR) from heparinized blood using density gradient centrifugation[1]. Briefly, the blood was diluted 3:2 (v/v) with sterile normal saline and layered over an equal volume of Ficoll-paque (Amersham Pharmacia Biotech, Uppsala, Sweden) in sterile centrifuge tubes and centrifuged at room temperature for 30 minutes at 400 x *g*. The mononuclear cell layer was removed and transferred to a fresh tube for washing. The cells were washed twice with sterile saline by

centrifugation at 250 x *g*. RPMI medium (Gibco Life Technologies, Gaithersburg MD) supplemented with 10% (v/v) heat-inactivated fetal bovine serum (Hyclone Laboratories, Logan UT), 1% (w/v) glutamine, 1% (w/v) pyruvate and 1% (w/v) HEPES (all Gibco Life Technologies, Gaithersburg MD) was used for a third wash at 150 x *g*, which was used to decrease platelet contamination of the mononuclear cell culture.

Cells were inspected and viability was determined by trypan blue dye exclusion under light microscopy. Mononuclear cells were resuspended in complete RPMI at 1×10^6 apparently viable cells/mL. Two-way, primary mixed lymphocyte cultures were carried out in 96 well, round bottomed culture plates with 1×10^5 cells in 100 μL media per well from each of two donors. Drug or drug metabolite was added to wells at various concentrations, dissolved in ethanol. The concentration of ethanol in all wells, including controls was 0.5% (v/v). Culture plates were incubated at 37°C in 5% (v/v) CO_2, and humidified air, in a water-jacketed incubator. After 120 hours, 0.6 μCi ^{3}H-methyl-thymidine (Amersham Pharmacia Biotech, UK, 25Ci/mmol), was added to each well for a further 18 hour incubation.

The cells were harvested with a semi-automatic cell harvester (Skatron) onto glass microfibre filters, dried and counted in fluor (ScintiSafe 50%, Fisher Scientific, NJ) for β-particle emission by liquid scintillation counting (Taurus, Micromedic Systems). Counting efficiency was 56%. Experiments were done in quadruplicate on six different days. The data were background corrected and replicate wells were averaged and expressed as a percentage of inhibition of proliferation by drug:

$$\% \text{ inhibition} = \left(\frac{\text{cpm in drug presence}}{\text{cpm in absence of drug}} \right) \times 100$$

The dose of drug required to produce a median effect was calculated. The median effect (ED_{50}) is defined as the point at which 50% of the reaction is inhibited and 50% of the reaction is

unaffected. Based on Michalis-Menton kinetics and using a modified Hill plot, the median effect equation is constructed[2]. It is modified from the dose-response curve:

$$\frac{Fa}{Fu} = \left(\frac{D}{Dm}\right)^m$$

where Fa is the fraction of the system that is affected (percent inhibition of ^{3}H-thymidine incorporation/100), Fu is the fraction of the system that is unaffected (1-Fa), D represents the drug concentration, Dm is the concentration of drug required for ED_{50} and m is a slope co-efficient describing the sigmoidal nature of the dose-response curve. This graphic representation is non-linear; the plot of Fa/Fu versus log D results in a sigmoid curve. It is necessary to convert the equation in logarithmic fashion to linearize the relationship:

$$\log\left(\frac{Fa}{Fu}\right) = m \log D - m \log Dm$$

This plot redefines m as the slope of the line, and log Dm as the X-intercept when the median effect is achieved: Fa = Fu = 0.5 or log (Fa/Fu) = 0. Linear regression was performed, regression analysis and regression statistics were completed for each plot. Several criteria were employed, including the requirement that $r^2 \geq 0.75$ to ensure the data fit the median-effect principle. Experiments were done in quadruplicate on four different days, using different combinations of donor lymphocytes each time.

c. Endothelin/Prostacyclin release assays

The ability of rapamycin and its metabolites to affect the secretion of vasoactive substances was investigated using cell culture. Normal human mesangial cells (NHMC), a renal cell line (Clonetics, East Rutherford, NJ) was plated in 96 well, flat bottom plates at a capacity of 2×10^3 cells per well and grown for 48 hours until nearly confluent. Mesangial cell basal medium (Clonetics) was used for all culture purposes with serum supplement for culture growth, and without serum for incubations. The cells were inspected using an inverted microscope for

growth consistency, before proceeding with the experiment. Each well was gently washed twice with 200μL of serum and antibiotic-free medium over thirty minutes. Drug or metabolite was added to each well at a potentially toxic concentration of 200μg/L, diluted in serum and antibiotic-free basal medium. Alcohol concentration was kept constant in all wells at 0.05% (v/v) ethanol. Cells were incubated with drug for 24 hours, at which time the supernatant was sampled and the cells washed twice with serum and antibiotic-free medium. The mesangial cell basal medium was replaced for a second 15 minute incubation. Supernatants were pooled from replicate wells at the 24 hour and the 24 hour + 15min time points and frozen at –20°C until analysed for vasoactive substance production and release. This experiment was done in quadruplicate on three different days.

Endothelin-1 (ET-1) was measured by competitive radio-immune assay (RIA) using a high sensitivity commercial kit that measured ET-1,2 (Amersham Pharmacia Biotech, UK). Standards of synthetic ET-1 were prepared at concentrations ranging from 0.5-58.2 fmol/mL in assay buffer (0.02M borate, 0.1% (w/v) NaN_3, pH 7.4). The primary antibody was rabbit anti-ET-1 and the secondary detection reagent was donkey anti-rabbit serum coated onto magnetized polymer particles. The tracer was [^{125}I]-synthetic ET-1 (1μCi/mL) in assay buffer. Supernatants and controls were used undiluted and unextracted. All reagents were equilibrated to room temperature before use. Briefly, samples or controls were incubated in 12 x 75mm polystyrene tubes with primary antibody for 4 hours at 5°C, then with tracer for an additional 16 hours at 5°C, then with secondary detection reagent for 10 minutes at room temperature. Separation was achieved by putting the tubes into a magnetic separator base for 15 minutes at room temperature. Unbound tracer was decanted, and the pellets were counted for gamma scintillation (Crystal). All standards, controls and unknowns were run in duplicate and averaged.

Standard curves were constructed by plotting $\%B/B_0$ versus standard concentration, where %B is the percent radioactivity bound for each sample, and B_0 is the amount of radioactivity bound by the zero standard. Results were corrected for non-specific binding. Unknowns were calculated from the standard curve after regression analysis and regression statistics were calculated. Unknowns from the three experiments were averaged and Student's paired t-tests done to test for statistical significance in ET-1 secretion, comparing the results of each drug or metabolite group to that of the media control.

6-Keto-$PGF_{1\alpha}$ was measured by competitive RIA using a high sensitivity commercial kit that measured 6-keto-$PGF_{1\alpha}$ (Amersham Pharmacia Biotech, UK). Standards of 6-keto-$PGF_{1\alpha}$ were prepared at concentrations ranging from 0.31-40.00 pg/mL in assay buffer (0.05M phosphate, 0.1% (w/v) NaN_3, 0.05% (w/v) bovine serum albumin, pH 7.3). The primary antibody was rabbit anti-6-keto-$PGF_{1\alpha}$ and the secondary detection reagent consisted of donkey anti-rabbit serum coated onto magnetized polymer particles. The tracer was 6-keto-$PGF_{1\alpha}$ [^{125}I]iodotyrosine methyl ester (0.2μCi/mL) in assay buffer with 5% (v/v) ethanol. Supernatants and controls were used unextracted and diluted by a factor of three with assay buffer, as recommended in the product literature. All reagents were equilibrated to room temperature before use. Briefly, samples or controls were incubated in 12 x 75mm polystyrene tubes with primary antibody and tracer for 18 hours at 5°C, then with secondary detection reagent for 10 minutes at room temperature. Separation was achieved by putting the tubes into a magnetic separator base for 15 minutes at room temperature. Unbound tracer was decanted, and the pellets were counted for gamma scintillation (Crystal Counter). All standards, samples and unknowns were run in duplicate and results averaged.

Standard curves were constructed by plotting $\%B/B_0$ versus standard concentration, where %B is the percent radioactivity bound for each sample, and B_0 is the amount of radioactivity bound by the zero standard. Results were corrected for non-specific binding. Unknowns were

calculated from the standard curve after regression analysis and regression statistics were calculated. Unknowns from the three experiments were averaged and the Student's paired t-tests done to test for significant differences in 6-keto-$PGF_{1\alpha}$ secretion, comparing the results of each drug or metabolite group to that of the media control.

d. Rapamycin Immunoassay

Candidate metabolites from urine were submitted to Abbott Labs Inc (Abbott Park, IL) for determination of cross-reactivity in a rapamycin microparticle enzyme immunoassay (MEIA) that was under development at the time.

When the MEIA was released for supervised institutional testing, rapamycin metabolites were tested for cross-reactivity. Spiked samples were prepared by taking purified, identified rapamycin metabolites or rapamycin parent, diluting them each in methanol and adding to pooled whole blood. The concentration of methanol was kept constant at 0.05% (v/v) and the blood was equilibrated for 4-18 hours at 5°C before analysis. In some instances, samples were frozen for 2-3 days before analysis. The metabolite-supplemented blood samples were analysed for cross-reactivity in the automated Rapamycin MEIA (Abbott Diagnostics Inc, Abbott Park, IL) at the Department of Laboratory Medicine and Pathology, University of Alberta Hospital on an Abbott IM_X analyzer. Theoretical values for the supplemented blood samples were checked for accuracy and purity by HPLC (ESI)-MS and HPLC-UV.

For the immunoassay, the manufacturer's directions were followed. Briefly, 100 μL of whole blood was treated with 30 μL commercial solubilizer and 300 μL commercial precipitation reagent. After vigorous mixing and centrifugation at 12 000 *x g* for 5 minutes, the clear supernatant was decanted and used for the automated analysis. If the result was beyond the linear limit of the assay (5-30 μg/L), as suggested by Abbott, the sample was diluted 1:2 or 1:4 with pooled whole blood before extraction.

e. Cross-reactivity Determination

Cross-reactivity was calculated from the value obtained in the MEIA and the theoretical spiked value using the following equation:

$$\left(\frac{\text{metabolite measured as rapamycin}}{\text{concentration of metabolite added}} \right) \times 100 = \text{percent cross-reactivity}$$

f. Minor immunophilin binding study

Samples of rapamycin and isolated metabolites were submitted to the laboratory of Dr. S.J. Soldin at the National Children's Health Center for testing in an immunophilin binding assay using 5 – 8, 14, 37 or 52 kDa proteins with rapamycin and FK506 binding properties [3].

The 5 – 8, 14, and 52 kDa proteins were isolated from calf thymus. Fresh tissue was homogenized in buffer (3 mM EDTA, 1.2 mM EGTA, 100mg/L PMSF, 1mM DTT, 5mM potassiun phosphate and 0.05 mg/L pepstatin, pH 6.8) and ultracentrifuged at 100 000 x *g* for 90 minutes. The cytosol was then subjected to repeat isoelectric focusing using the Biorad Rotofor™ system. The pH 6.5 to 7.5 fractions were pooled and NaCl was added to a final concentration of 1M to dissociate the ampholytes. Following dialysis overnight, the protein was further separated by molecular weight using several molecular weight cut-off filters: a 30 kDa filter (Macrosep, Pall filtration Corp, Northborough, MA), or a 10 kDa (Snakeskin, Pierce, Rockford, IL). This was followed by molecular sieving with Sephadex G50 (Pharmacia Biotech) after equilibration with 5mM phosphate buffer and 1 mM DTT. One milliliter fractions were screened for FK506 binding activity. Pooled fractions with binding activity were subsequently concentrated with 3 kDa membrane filters (Macrosep, Pall Filtration Corp., Northborough, MA). The 5-8 kDa protein was used at homogeneity and the 14 kDa used at >80% purity as evaluated by visualization on silver stained SDS-PAGE.

The 37 kDa protein was isolated from Jurkat Tcells as previously described [4]. Cells were lysed by snap freezing in liquid nitrogen and thawing three times, then suspended in buffer containing 3 mM EDTA, 1.2 mM EGTA, 0.1% Triton X-100 and 0.5% ∃-mercaptoethanol. This was

followed by sonication for 2-3 minutes. Protease inhibitors (pepstatin 0.05 mg/L and PMSF 100 mg/L) were added followed by ultracentrifugation at 100 000 x *g* for 60 minutes. The supernatant was separated by isoelectric focussing and partially purified with a 30 kDa molecular weight cut-off membrane filter as described in the preceding paragraph. The 37 kDa protein was purified with weak cation exchange HPLC to >95% purity as evaluated by silver staining of SDS-PAGE.

For the binding assay, a series of standards and controls containing various concentrations of rapamycin and several concentrations of metabolites were diluted in methanol. The tracer employed was [^{3}H]-dihydro-FK506 (Amersham, Buckinhamshire, UK), as the binding site of rapamycin and FK506 are believed to be identical, and labelled rapamycin was not readily available. Triplicates of standard, control or metabolite were added to 25 μL of tracer (150 000 dpm) in ethanol, 200 uL of binding buffer (5 mM phosphate buffer, 0.25% (v/v) Tween-20, pH 6.8) and binding protein diluted in binding buffer to a final volume of 375 μL. The amount of protein used per tube was 20.6 μg of 37 kDa protein, 34.4 μg of the 14 kDa protein, 24.0 μg of 5 – 8 kDa protein, and 15.0 μg of the 52 kDa protein. Following a 30 minute, room temperature incubation, free and bound tracer were separated on Sephadex LH-20 columns (Pharmacia Biotech, Piscataway, NJ, USA), equilibrated with LH-20 buffer (20 mM TRIS buffer, 5 mM β-mercaptoethanol, 0.05% sodium azide, pH 7.2), and eluted with 1.4 mL of LH-20 buffer. The eluent contained the bound fraction, and was measured in 10 mL of Optima Gold Scintillation cocktail (Packard Instruments, Downers Grove, IL, USA) on a Beckman LS500 TD liquid scintillation counter with an efficiency of 55%. Non-specific binding was estimated with 1250 μg/L of unlabelled rapamycin which was shown to displace >95% of tracer from binding sites.

For whole blood samples, extraction was necessary. A 200 μL aliquot of whole blood was added to 2 mL of methanol and vortexed for 5 minutes. This was followed by incubation at room temperature for 5 minutes, and centrifugation to pellet the cellular debris. The methanol

was removed and dried under nitrogen in a warm water bath. The tracer and buffers were added directly to these tubes for the binding assay, as described above, except the amount of 5 – 8 kDa protein was increased to 44 μg per tube.

To determine the reactivity of metabolites in the assay, standard curves were constructed using various concentrations of rapamycin in methanol and in whole blood. Single concentrations of rapamycin metabolite were processed as described above, and read from the standard curve for rapamycin. The measured response for metabolite at a given concentration was compared to the standard response of rapamycin, and these values were used to calculate a percent cross-reactivity. Bias was calculated by using the following formula:

3. RESULTS

a. Mixed Lymphocyte Reaction

The immunosuppressive activity of rapamycin metabolites was determined using this *in vitro* model. All experiments were conducted in quadruplicate, on four different days. The results of these experiments are summarised below. Figure IV-1 depicts one of the obtained dose response curves for rapamycin and the five metabolites over a broad range of concentrations in the MLR. For each metabolite, the concentration required to inhibit the MLR is greater than the required concentration of rapamycin. Table IV-1 gives the mean concentrations of metabolites and rapamycin required for 50% inhibition of [^{3}H]-thymidine uptake (ED_{50}) in this assay system. The ED_{50} results for the metabolites are also described as a proportional response, as compared to the ED_{50} of rapamycin, and the relative potency of each metabolite is also included in Table IV-1. As there was some variation in response, Figure IV-2 shows the scatter of results obtained in the MLR experiments for rapamycin and the five metabolites tested, which is indicative of inter-individual variability of response, as well as inherent error and imprecision in the assay.

Figure IV-1 A single MLR profile: rapamycin and five metabolites

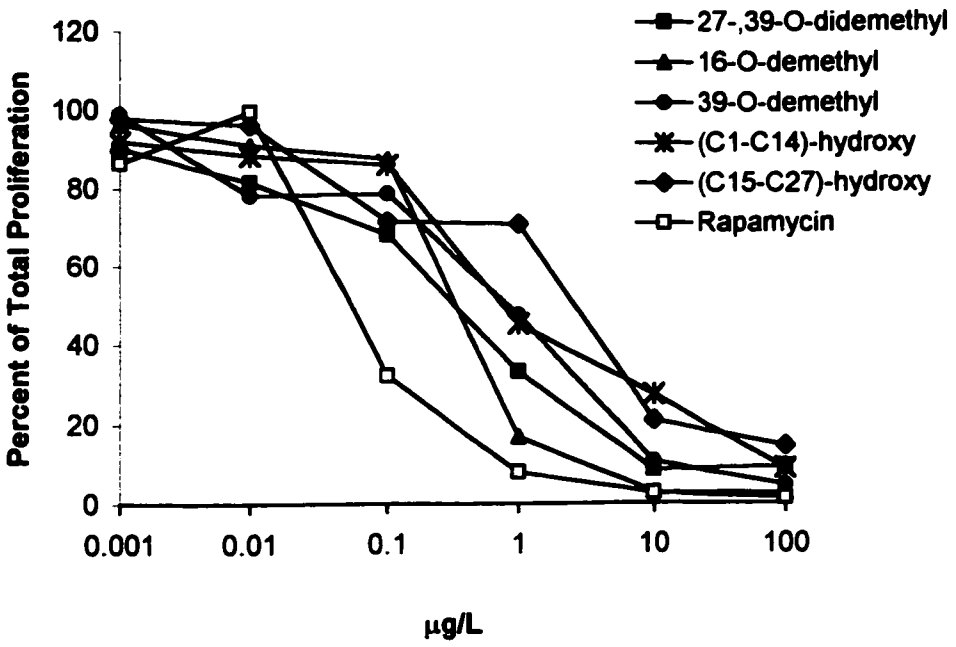

Table IV-1 Immunosuppressive activity of rapamycin and five metabolites by MLR

Compound	ED_{50} (μg/L)	Potency
rapamycin	0.48 (0.23)[a]	1.000
27-,37,-O-didemethyl	5.90 (1.94)	0.080
16-O-demethyl	2.85 (1.14)	0.173
39-O-demethyl	4.68 (2.42)	0.105
(C1-C14)-hydroxy	467.5 (257.1)	0.001
(C15-C27)-hydroxy	252.5 (102.4)	0.002

[a] Resuts are expressed as mean (SD)

Figure IV-2 Summary of rapamycin and metabolite MLR ED_{50}

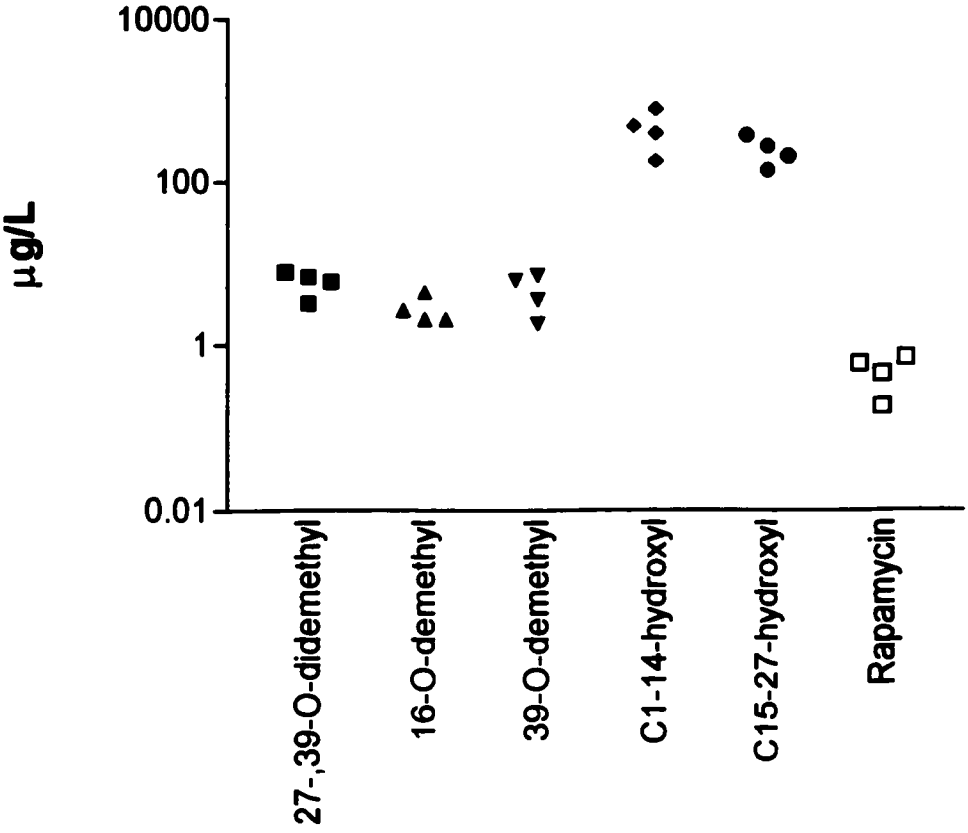

Each point represents the ED_{50} obtained in a single experiment, using 4 different donor combinations.

The immunosuppressive activity of the demethylated metabolites more closely approximated that of rapamycin, demonstrating an average of 8% and 17% of the activity of rapamycin in the MLR. This is distinct from the hydroxylated metabolites, as each has less than 1% of the immunosuppressive activity of rapamycin. The potency of the metabolites tested in the MLR was 16-O-demethyl > 39-O-demethyl > 27,39-O-didemethyl > (C15-C27)-hydroxy > (C1-C14)-hydroxy.

b. Endothelin/Prostacyclin release assays

The release of ET and 6-keto-$PGF_{1\alpha}$, the stable metabolite of prostacylin (PGI_2) from mesangial cells was evaluated by RIA. Normal Human Mesangial cells were cultured in the presence of drug or drug metabolite, and the supernatant was sampled to evaluate the secretion of vasoactive substances. A summary of the results of the ET-1 secretion is depicted in Figure IV-3. As compared to the media and ethanol controls, there is no significant difference at each time point between the drug groups, as calculated using the Mann-Whitney Rank Sum Test. Neither is there a difference within each drug or metabolite group as compared at 15 minutes and 24 hours post-exposure, using the Wilcoxon Signed Rank Test.

In an effort to bring significance to the experiment, it was decided to correct for the protein content in each series of wells used in these experiments. Although the wells of the culture plates used in this experiment were examined visually, and they appeared relatively consistent in cell density, an attempt was made to measure the amount of protein in each well as an estimation of the consistency in cell density. After trypsinization, the cells were removed from the 96 well plates, pooled and transferred to a secondary container, where they were solubilized, precipitated, concentrated and analyzed by the Lowry protein assay method. Unfortunately, the results were below the limit of detection, so the protein correction was not performed. In pilot experiments, cells were trypsinized out of the wells and enumerated manually. The variability of cell plating density at similar culture intervals (n=6),

Figure IV-3 ET-1 Production in NHMC

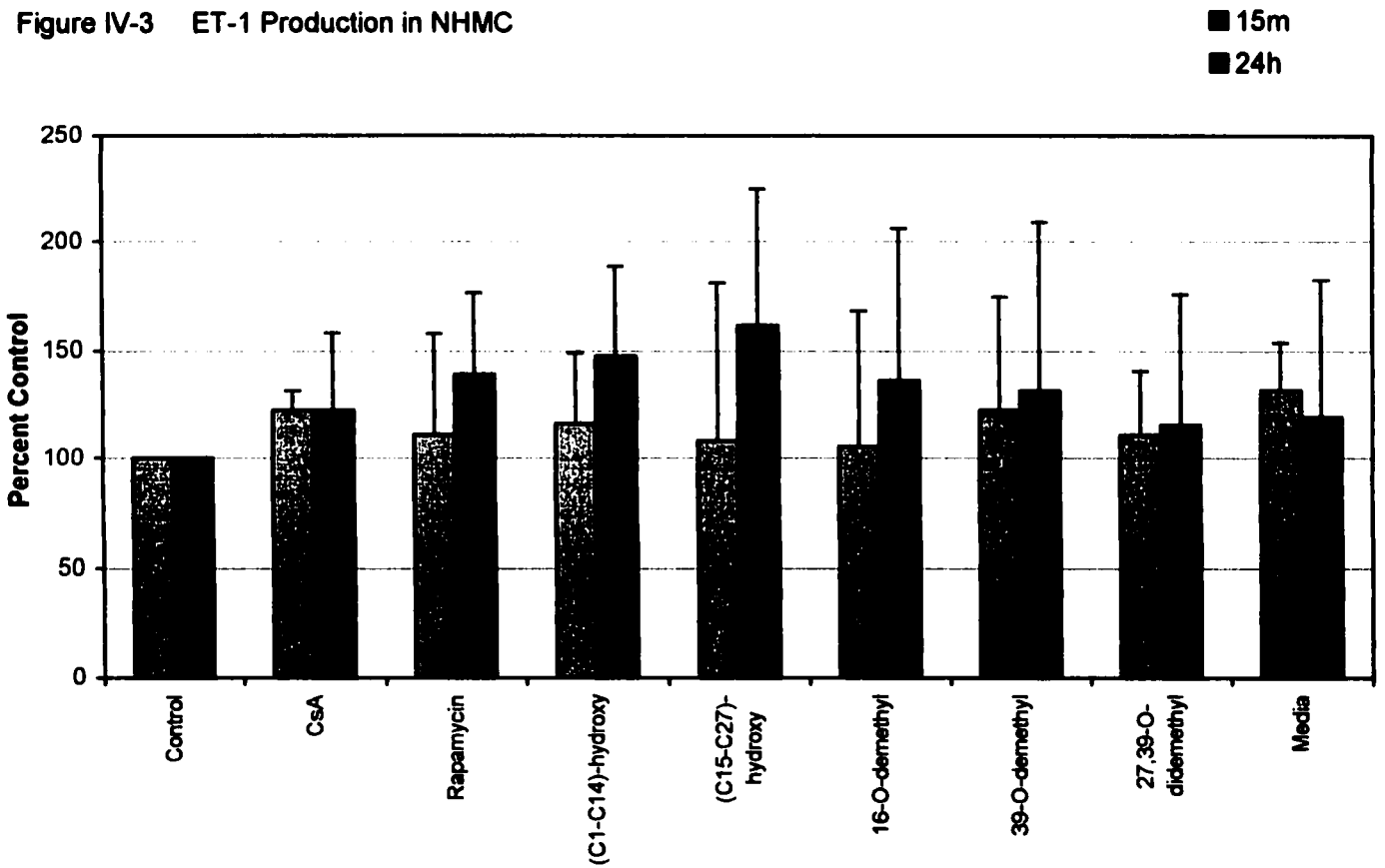

Results are presented as mean +/- SD. Four experiments were done in quadruplicate on different days.

and are expressed as coefficient of variation was 13% (15 minutes) to 22% (24 hours) for the passage previous to the one used in this experiment.

The effect of rapamycin and metabolites on the secretion of secreted 6-keto-$PGF_{1\alpha}$ was also inconclusive. The mesangial cells used in the experiment failed to secrete a measurable amount of 6-keto-$PGF_{1\alpha}$ in the conditions used. The addition of rapamycin, metabolite or cyclosporine did not increase this secretion to measurable levels.

c. Rapamycin Immunoassay

The putative metabolites isolated from urine were the first substances submitted for testing in the immunoassay for cross-reactivity. There was minimal binding of these substances in this assay, as depicted in Table IV-2. After further investigation, it was determined that there was a lack of compelling evidence to prove that the substances isolated from the urine as described in the previous chapter were derived from or directly related to rapamycin. There was minimal cross-reactivity with anti-rapamycin antibodies as tested in by MEIA, lack of appropriate MS evidence for a mass in the correct range for rapamycin metabolites, and low activity in the FKBP binding assay, as described in the following section.

The characterised and purified metabolites isolated from the microbial culture system were spiked into blood, extracted by standard procedure and tested in the MEIA. The immunoassay results are summarised in Table IV-3, with the theoretical ("spiked") values, HPLC determined values for rapamycin and HPLC-MS values for rapamycin and metabolites. The results of this pilot study are difficult to interpret. When introduced to whole blood alone, the metabolites have cross-reactivity ranging from not detectable to 95.5%, virtually the same response as for rapamycin. The cross-reactivity of rapamycin and metabolites in this assay when tested alone was rapamycin > 39-O-demethyl > 27, 39-O-didemethyl > (C1-C14)-hydroxy > 16-O-demethyl > (C15-C27)-hydroxy. When introduced to whole blood together with rapamycin, the metabolites may have a modulating effect on the immunoassay. In several instances, the reactivity of the

Table IV-2 Urine substance cross-reactivity by MEIA

	Cross-reactivity (%)	Level Tested (μg/L)
rapamycin	100	50
M1	<10	50
M2	9	100
M3	6	100
M4	<10	50

Table IV-3 Rapamycin metabolite cross-reactivity in the rapamycin immunoassay (MEIA)

	Theoretical		HPLC	HPLC-MS		IMX	
	rapamycin µg/L	metabolite µg/L	rapamycin µg/L	rapamycin µg/L	metabolite µg/L	rapamycin µg/L	Reactivity %
CsA patient	0	0	<3	<0.2	<0.2	1	
rapamycin	50	0	47.5	49.2	<0.2	48.4	96.8
(C1-C14)-hydroxy	0	20	<3	<0.2	19.6	2.3	11.5
(C15-C27)-hydroxy	0	20	<3	<0.2	20.7	<1.5	0
16-O-demethyl	0	20	<3	<0.2	21	2.2	11
27,39-O-didemethyl	0	20	<3	<0.2	19.7	3.1	15.5
39-O-demethyl	0	20	<3	<0.2	19.4	19.1	95.5
DMR	0	20	<3	<0.2	20.1	<1.5	0
(C1-C14)-hydroxy	50	20	45.1	48.6	19.9	30	64.0
(C15-C27)-hydroxy	50	20	52.2	49.7	20.5	51.6	101.3
16-O-demethyl	50	20	51.6	50.6	20.6	49.2	96.3
27,39-O-didemethyl	50	20	51.2	51.2	19.4	38.8	75.8
39-O-demethyl	50	20	49.1	50.7	19.4	43.2	86.6
DMR	50	20	47.1	50.4	19.5	33.6	68.9
DMR	20	10	19.1	19.3	9.6	21.5	112.0

samples spiked with both rapamycin and metabolite was lower than would be expected if rapamycin was introduced alone. However, this effect was not consistent, as when DMR was tested with rapamycin at two concentrations, it gave differential results. At a high concentration, DMR appeared to cause inhibition of the reactivity of rapamycin in the assay, but when used at a lower concentration, the rapamycin cross-reactivity result was very close to what was expected for rapamycin alone: the inhibition was no longer apparent. Specifically, when DMR was tested alone, there was no detectable cross-reactivity, when tested at 20μg/L with 50μg/L rapamycin, there was 32.8% loss of reactivity, and when tested at 10μg/L DMR with 20μg/L rapamycin, there was +4.5% cross-reactivity in the immunoassay.

d. Minor immmunophilin binding assay

The results of the binding studies undertaken with three minor immunophilins are summarized in Table IV-4. There is a variable amount of cross-reactivity of the various metabolites tested using the four immunophilins. Cross-reactivity varied from <10 % for all metabolites when used at concentrations of <2.5 μg/L to a maximum observed cross-reactivity of 47.2% for (C15-C27) hydroxy-rapamycin when extracted from whole blood at 11.8 μg/L. Additionally, there appeared to be a concentration dependency on the cross-reactivity as observed in the assay, with higher concentrations of metabolite giving higher percent cross-reactivity. Unfortunately, the metabolites were not all tested at the same concentrations, nor was a full range of concentrations included for each metabolite, which may have increased our understanding and enabled more complete interpretation of the metabolite behaviour in this assay.

Table IV-4 Immunophilin Binding of Rapamycin Metabolites

Metabolite	5-8 kDa WB extract[3]	5-8 kDa methanolic[3]	14 kDa methanolic[3]	37 kDa methanolic[3]	52 kDa WB extract[19]
16-O-demethyl	34[a]	44.8	<10	21.6	20
39-O-demethyl	25.2	33.6	<10	15.2	21.2
27,39-O-didemethyl	29.2	37.6	<10	23.2	13.6
(C1-C14)-hydroxy	<10	<10	<10	<10	<10
(C15-C27)-hydroxy	47.2	46.4	18	20	26

[a] % Cross-reactivity in immunophilin binding assay at 25 μg/L

4. DISCUSSION

Sparse data regarding rapamycin metabolites were available at the onset of this study. These experiments were planned before any data regarding the human toxicity and efficacy of rapamycin were available. The investigation was initiated in an attempt to either reveal or rule-out negative effects that may overlap current immunosuppressive regimens. The specific objective of these experiments was to evaluate the immunosuppressive potency of the newly identified metabolites and define some of the toxic effects of rapamycin and its metabolites.

As a measure of immunosuppressive activity, the ability of rapamycin and metabolites to inhibit the MLR was evaluated. Although an imperfect test of immunosuppression, there is some degree of correlation of *in vitro* IC_{50} and ability of a drug to suppress the allo-immune response *in vivo*. *In vitro* activity in the MLR is higher than *in vivo* activity to suppress allograft rejection in many experimental models for CsA, FK506 and rapamycin. It is speculated that this may be attributed to a given drug's whole blood distribution. In whole blood, these hydrophobic drugs are mostly sequestered in the cellular component and bound to intracellular binding proteins. The free-fraction of drug (non-protein bound) in the plasma is relatively small[5, 6]. Using classical pharmacological theory, the free fraction of drug is the pharmacologically active proportion. This can be interpreted in this instance to mean that the proportion of drug that is in red blood cells (RBC), which is the vast majority of rapamycin in whole blood, is merely a depot, or yet inactive fraction. Only the free drug would be available for transport into the target cell (lymphocyte) for inhibition of cellular processes. Using this explanation, the *in vitro* experiments will overestimate the "real" potency of an agent, compared to *in vivo* data, if there are fewer depot binding sites in the system. As these *in vitro* experiments are done in tissue culture medium, not whole blood, this is likely the case. This is why activities are expressed as a percent or proportion of that of parent rapamycin, instead of only as an absolute value.

The metabolites of rapamycin all displayed some ability to inhibit the MLR, with potencies ranging from <1% to 18% as compared to parent drug. The hydroxylated metabolites showed

the greatest loss of activity in this assay, as compared to the demethylated metabolites. This is not surprising, as a hydroxylation event could contribute to an altered charge localization or electron density, resulting in decreased affinity for the binding of either the FKBP or mTOR. In comparison to other immunosuppressive drugs, rapamycin metabolites have a moderate degree of activity in the MLR. In general, metabolites of CsA have far less ability to inhibit the MLR. Metabolites of FK506 have been difficult to evaluate, but it is clear that certain metabolites have high immunosuppressive activity, while others have negligible activity in the same assays. That 16-O-demethylrapamycin demonstrated 18% activity compared to parent drug is noteworthy, and may indicate that metabolites of rapamycin are contributing to overall or net immunosuppression in a small but measurable fashion. The other metabolites of rapamycin have negligible immunosuppressive activity in the MLR, and thus need to be discriminated from rapamycin for the purposes of therapeutic drug monitoring.

Because current immunosuppressive therapy consists of CsA-or tacrolimus based immunosuppression, one of the major toxic side effects to be addressed is renal vascular impairment. This was the major focus of toxicity investigation in the current study. Although the mechanism of CsA-related immmunosuppression is not fully understood, there are several theories. One is that CsA disrupts kidney calbindin function, leading to loss of divalent cations in the urine through lack of ionic re-uptake in the proximal tubule[7]. Another hypothesis on renal side-effects revolves around the ability of CsA to alter vasoactive substance production/secretion and thus change renal hemodynamics. Vasoconstriction is mediated by endothelin and antagonized by prostanoids. There is some evidence that CsA exposure decreases PGI2 release in mesangial cell culture, with CsA metaboiites retaining some activity in this assay [8]. There is similar evidence for induction of ET-1 release by the CsA metabolites AM1, AM9 and AM1c9 *in vitro* [8] and by CsA *in vivo* [9, 10].

The current study was conducted to evaluate the effect of rapamycin and its metabolites on the CsA induced mode of renal effects. Evaluation of the effect of rapamycin on cultured

endothelial cell secretion of vasoactive substances revealed that rapamycin did not increase the secretion of ET-1 as tested here. Neither CsA alone, in combination with rapamycin or its metabolites provided evidence of increased ET-1 production with drug exposure, as compared to controls. Experiments evaluating the effect of drug and/or drug metabolite on production and secretion of PGI_2 were inconclusive, as the amounts of 6-keto-$PGF1_{1\alpha}$ (as a measure of PGI_2) produced were not present in measurable amounts in the RIA chosen for the experiment. The possibility remains that due to lack of expertise, conditions were not achieved for adequate cellular production of vasoactive substances or response to drugs in these experiments. Although these experiments were planned and executed using concentrations of parent drug (rapamycin and CsA) approaching the maximum expected concentration in the pharmacokinetic profile, this still failed to provoke a measurable change in either ET-1 or 6-keto-$PGF1_{1\alpha}$ secretion. This is unfortunate, as this activity has not been evaluated for rapamycin metabolites in other studies.

It may be unnecessary to test the activity of rapamycin in vasoactive substance production, as it has since become apparent that rapamycin alone does not produce increases in systemic blood pressure or in renal arterial pressure as is found with CsA treatment[11]. Further, the vaso-relaxing effect of rapamycin may be partially due to its ability to inhibit smooth muscle migration and stress-induced proliferation[12], as demonstrated in animal models of artherosclerosis and arterial injury. Future studies should be directed into this area, instead.

Evaluation of the cross-reactivity of rapamycin metabolites in a semi-automated immunoassay under development and tested at the University of Alberta Hospitals Clinical Laboratory yielded results that were difficult to interpret. A clear pattern of cross-reactivity with the antibody based assay, or inhibition of antibody binding in these conditions was impossible to tease from the data obtained. Some metabolites produced a seemingly differential effect, with cross-reactivity demonstrated at high concentrations alone, but a failure to produce an additive effect when tested in combination with rapamycin.

Metabolites could compete for antibody binding with rapamycin, or could be inactive in this regard. Functional group changes on drug metabolites can have local or more global structural effects. Alteration in stereochemical configuration and alteration in cis-trans ring structure may themselves have significant implication in altering immunophilin or mTOR binding. Increased steric hindrance, for example, with Phase II metabolism (conjugation reactions) may disrupt binding dynamics by making some interactions non-permissible; this is not necessarily relevant to the study of rapamycin. Similarly, though perhaps less drastic, semi-localized or localized changes affecting available protons for hydrogen binding, or altering electron-rich areas for proton reception could also result in loss of binding activity, as with hydroxylation events. However, changes that are restricted to the local environment are expected with demethylation of rapamycin, as this appears to occur at O-linked sites, leading to a somewhat isolated phenomenon, and less drastic effect than with hydroxylation events.

Further experimentation with the MEIA using a wider range of concentrations of metabolites, though warranted, were not performed due to the withdrawal of the assay from development by the proprietary company. Full concentration curves of metabolite alone and in combination with a constant amount of rapamycin could produce reactivity curves and permit calculation of an affinity constant of the antibody for the metabolite, through depiction of the Langmuir plot and construction of a binding isotherm. This would have been very important to determine if the assay was going to be used for determination of rapamycin in patient blood samples. Any appreciable cross-reactivity of the antibody with non-parent-drug substances, including drug metabolites, endogenous drug-like substances and other xenobiotics with similar chemical structures would produce a positive bias in the assay, translating to falsely high results. Conversely, if a multiple binding-site assay was used (i.e. a sandwich immunoassay), metabolites could produce differential effects. If the antibodies were not specific for parent rapamycin, and also bound metabolites with similar, increased or slightly decreased affinity, this would produce a positive result and cross-reactivity. If only one of the antibodies was specific

for parent, but the other was able to bind rapamycin metabolites, this could result in a situation where rapamycin metabolite could disrupt rapamycin-antibody sandwich formation through non-specific binding if that binding was saturable in assay conditions.

For the immunophilin binding assays, the cross-reactivity of the metabolites varied from undetectable [<10% at 25 μg/L for (C1-C14) – hydroxy] to significant [47.2 % at 25 μg/L for (C15-C27) – hydroxy]. The cross-reactivity was decreased by approximately 25% in spiked, extracted whole blood samples, as compared to methanolic samples. This may reflect on extraction efficiency. The 14 kDa immunophilin produced the lowest degree of cross-reactivity with the metabolites, and the 5-8 kDa immunophilin the greatest. None of the immunophilins tested were able to detect binding with the (C1-C14)-hydroxyrapamycin metabolite at 25μg/L.

The immunophilin thought to be critical for rapamycin action is the 12 kDa FKPB, which possesses rotamase activity[13]. The immunophilins used in the present study have only been partially characterised by Davis and associates[14]. None of the minor immunophilins tested here display rotamase, cAMP-dependant kinase activity or protein kinase C activity. The 5-8 kDa immunophilin is able to inhibit calcineurin phosphatase activity. The 37 kDa immunophilin displayed glycerol-3-phosphate dehydrogenase activity, and is able to inhibit calcineurin phosphatase activity. The 52 kDa immunophilin was untestable in the calcineurin phosphatase assay because of possible impurity in the preparation. The 5-8 kDa immunophilin may be a novel protein or may be a sub-unit of the 52 kDa immunophilin[14]. None of these minor immunophilins have been tested for mTOR binding or inhibition.

As a measure of pharmacological response, target protein binding can be an important measure of overall activity. With rapamycin, it is known that a complex between drug and free binding protein FKBP must occur, presumably first, before binding to the cytosolic protein target mTOR. Although two binding events must occur before rapamycin can exert its biological effects, a study of binding to each protein alone is also important to understand the relationship

of binding dynamics to pharmacological efficacy. In predicting the loss of activity caused by a given metabolic change to a drug molecule, function may be considered relative to binding of accessory protein or target. A decrease in binding of either protein could result in a drastic decrease in downstream activity for the metabolite. This decrease in activity could be less drastic in the demethylated metabolites because a demethylation event would putatively have less charge-distribution effect on the whole molecule, including less effect on ring tension and triene conjugation, as is important for maintaining trans-isomer formation for FKBP binding. It was expected that any changes to moieties that are directly involved in accessory protein binding would have drastic effects on immunosuppressive activity, with the prediction that multiple changes could result in more drastic loss of function. Of particular interest is (C1-C14)-hydroxyrapamycin, which is structurally altered in the FKBP binding region, displays decreased FKBP binding will all the proteins described in this study, and retains <1% of immunosuppressive activity as tested by the MLR.

As extrapolated from x-ray crystallography of the binary complex of FKBP12-FK506[15] and observed in ternary complex (rapamycin-FKBP12-FRAP)[16] experiments, the main regions of rapamycin involved in FKBP binding are: C1 to C12 and C28 to C42 and for mTOR capture are C16 to C31. The formation of 5 hydrogen bonds with conserved aromatic residues on FKBP12[17,18] and hydrophobic interactions between rapamycin and both FKBP12 and FRAP are important for complex formation[16]. For example, the stereochemistry and placement of C23 appears to be important, as the auxiliary methyl group is found very deeply buried in FRAP when the ternary complex is formed[16]. The methyl is able to take this position, avoiding contact with Phe 2108 and sliding into the groove formed with Leu2031, as a result of a slight deformation and partial loss of conjugation in the triene that results from hydrophobic interactions between C19 and C22, and other hydrophobic residues on FRAP. It can be easily understood how hydroxylation on a residue in close proximity to C23 or the triene could prevent these hydrophobic interactions and alter effective complex formation. The (C15-C27) hydroxylated metabolite follows this pattern, disrupting much of the immunosuppressive activity

that was found in rapamycin. The (C15-C27) hydroxylated metabolite demonstrates less than 1% activity in the MLR, likely a result of disrupted mTOR/FRAP binding, although it retains significant (47%) FKBP binding activity with the minor immunophilins as the aspect of the molecule involved in immunophilin binding is intact. This is an excellent example of how FKBP12 (or other immunophilin) binding activity could be intact, but immunosuppressive activity lost or abrogated if FRAP binding was altered instead.

There is more to be investigated as to the relative importance of given inter-molecular interactions, as loss of a single interaction does not always result in severe loss of activity. The C16-O-demethylated metabolite retains 18% activity in the MLR, while retaining up to 44% activity in the FKBP minor immunophilin binding assay. This is the most pharmacologically active metabolite tested here. According to the x-ray crystallography data, the 16-O-methyl group interacts with aromatic groups on FRAP, such as Thr2098 and Tyr2105[16]. One explanation is that the hydrophobic interaction mediated by this methyl group may be less important to the overall tertiary structure of rapamycin, leading to only small effects on protein binding activity, and thus on immunosuppression. Another possibility is that this interaction may not be critical to alteration of FRAP function. FRAP structural alterations and inhibition may still be permitted with binding of this metabolite, and pharmacologic effects may still occur, though in a more limited fashion.

In summary, the metabolism of rapamycin to hydroxylated and demethylated forms could affect binding to the FKBP and mTOR respectively, by alteration to residues that are directly involved in binding, or by preventing certain interactions from occurring. If we had access to well characterised antibodies, perhaps they could be used in elucidation of exact chemical sites of modification for the hydroxylated rapamycin metabolites that are only partially characterised. Conversely, in the future, cross-reactivity with well characterised metabolites could be used to characterise antibodies raised to rapamycin, rapamycin analogues or immuno-conjugates.

The results gained in these experiments indicate that metabolites of rapamycin have little immunosuppressive activity. No apparent renal vascular activity was demonstrated. Toxic activity of these metabolites should be examined in a system to evaluate the more pertinent effects on blood lipids and platelet function and production. Cross-reactivity in immunoassay needs to be further investigated if another commercial assay is to be developed. Immunophilin binding by metabolites appears to be only partially related to pharmacologic activity, necessitating further study in this area.

5. REFERENCES

1. Boyum A. Isolation of leukocytes from blood and bone marrow. Scand J Clin Invest 1968; 21(suppl 97):77.

2. Chou TC. Derivation and properties of Michalis-Menton type and Hill type equations for reference ligands. J Theor Biol 1976; 39:253.

3. Davis D, Murthy J, Gallant-Haidner HL, Yatscoff RW, Soldin SJ. Minor immunophilin binding of tacrolimus and sirolimus metabolites. Clin Biochem 2000; 33:1-6.

4. Murthy JN, Goodyear N, Soldin SJ. Identification of a 37 kDa tacrolimus, sirolimus and cyclosporine binding immunophilin possessing glyceraldehyde-3-phosphate dehydrogenase activity from Jurkat T cell line. Clin Biochem 1997; (30):129-33.

5. Yatscoff RW, LeGatt D, Keenan R, Chackowsky P. Blood distribution of rapamycin. Transplantation 1993; 56:1202-6.

6. Brattstrom C, Sawe J, Tyden G *et al.* Kinetics and dynamics of single oral doses of sirolimus in sixteen renal transplant recipients. Ther Drug Monit 1997; 19:297-406.

7. Yang CW, Kim J, Kim YH *et al.* Inhibition of calbindin 28kDa expression by cyclosporin A in rat kidney: the possible pathogenesis of cyclosporin A-induced hypercalciuria. J Am Soc Nephrol 1998; 9:1416-26.

8. Copeland K.R., Yatscoff RW. Comparison of the effects of cyclopsorine and its metabolites on the release of prostacyclin and endothelin from mesangial cells. Transplantation 1992; 53:640-5.

9. Kon V, Suguira M, Ignamami T, Harview BR, Ichikowa I, Hoover RI. Role of endothelin in cyclosporine-induced glomerular dysfunction. Kidney Int 1990; 37:1487-91.

10. Greiff M, Loertscher R, Shohuib SA, Stewart DJ. Cyclosporine-induced elevation in circulating endothelin-1 in patients with solid organ transplants. Transplantation 1993; 56:880-4.

11. Olyaei AJ, de Mattos AM, Bennett WM. Immunosuppressant-induced nephropathy: pathophysiology, incidence and management. Drug Safety 1999; 21:471-88.

12. Braun-Dullaeus RC, Mann MJ, Von der Legen HE, Morris RE, Dzau VJ. Cell cycle protein expression in proliferating vascular smooth muscle cells is transiently regulated through mTOR and p70S6 kinase. Circulation 1997; 96:47-51.

13. Schreiber SL. Chemistry and biology of the immunophilins and their immunosuppressive ligands. Science 1991; 251:283-7.

14. Davis DL, Murthy JN, Soldin SJ. Biochemical characterization of the minor immunophilins. Clin Biochem 2000; 33:81-7.

15. Van Duyne GD, Standaert RF, Karplus PA, Schreiber SL, Clardy J. Atomic structure of FKBP-FK506, an immunophilin-immunosuppressive complex. Science 1991; 252:839-42.

16. Choi J, Chen J, Schreiber SL, Clardy J. Structure of the FKBP12-rapamycin complex interacting with the binding domain of human FRAP. Science 1996; 273:239-42.

17. Van Duyne GD, Standaert RF, Schreiber SL, Clardy J. Atomic structure of the rapamycin human immunophilin FKBP-12 complex. J Am Chem Soc 1991; 113:7433-4.

18. Van Duyne GD, Standaert RF, Karplus PA, Schreiber SL, Clardy J. Atomic structures of the human immunophilin FKBP-12 complexes with FK506 and rapamycin. J Mol Biol 1993; 229:105-24.

19. Davis DL, Murthy JN, Napoli KL *et al*. Comparison of steady-state trough sirolimus samples by HPLC and a radioreceptor assay. Clin Biochem 2000; 33:31-6.

V. RAPAMYCIN METABOLITE QUANTIFICATION BY LCMS

1. RATIONALE

Therapeutic monitoring of immunosuppressive drugs currently consists of measurement of single drug species concentrations in whole blood or in plasma. This is based on the assumption or proven knowledge that the drug of interest is present predominantly in active form, which is usually unchanged, and referred to as "parent" drug. As demonstrated in the previous sections, rapamycin is biotransformed into several detectable product metabolites. As some of these metabolites have negligible toxic and immunosuppressive activity, and others retain but a small degree of activity, we suggest that rapamycin could be monitored by an assay that is specific for parent drug. This is necessary until one or more of the metabolites are proven to be clinically significant. However, the true contribution of rapamycin metabolites is not only dependent on absolute activity, but also on the relative concentrations present. Further, knowledge of the relative amounts of metabolite present will facilitate structure-targetted design of immunoassay- or receptor-based technology for the specific measurement of rapamycin in complex biological matrices and mixtures of drugs and drug metabolites.

Because of the small concentrations of rapamycin metabolites present, and the low molar absorptivities of these compounds, HPLC with UV detection was found to be unsuitable for rapamycin metabolite quantification in biological specimens. A method for the determination of rapamycin and its metabolites in whole blood specimens was developed and validated for clinical and research use.

2. MATERIALS AND METHODS

a. LC-MS quantitative assay for rapamycin and five metabolites

Internal standard, 25 μL of 4000 μg/L DMR, was added to 1 mL EDTA anti-coagulated whole blood which was acidified with 1mL 0.1M acetic acid. After brief vortex mixing, 8 mL of diethyl ether was added and liquid/liquid extraction was facilitated by shaking (Eberbach) at 100 rpm

for 20 minutes. After centrifugation, the ether layer was removed and evaporated to dryness. The residue was reconstituted with 150 μL 80% methanol/water (v/v) and put in a sonicating water bath for 5 minutes to ensure full reconstitution from the vial. After centrifugation to pellet any insoluble matter, the supernatant was transferred to an autosampler vial for LC-MS analysis. Electrospray MS parameters were set as described in the previous chapter, with selected ion monitoring for the detection of hydroxylated, demethylated, didemethylated and dihydroxylated metabolites. A 100 μL injection was made and HPLC separation was achieved on a C18 Waters Novapak column (4.6 x 150 mm, 5μm, Milford, MA) at 0.6 mL/min, using a linear 60-80% (v/v) methanol/water gradient, followed by a brief wash at 95% methanol and 4 column volumes of re-equilibration at 60% (v/v) methanol/water.

Rapamycin parent was routinely measured in the laboratory by a HPLC-UV method. The internal standard, 25 μL of 8000 μg/L DMR, was added to 1 mL EDTA anti-coagulated whole blood and basified with 1mL 1.33% (w/v) K_2CO_3. After brief vortex mixing, 8 mL of diethyl ether was added and liquid/liquid extraction was facilitated by shaking (Eberbach) at 100 rpm for 20 minutes. After centrifugation of the resulting emulsion, the ether layer was removed and evaporated to dryness. The residue was reconstituted with 300 μL 80% methanol/water (v/v) and vortex mixed briefly. After centrifugation to pellet any insoluble matter, the supernatant was transferred to an autosampler vial for LC-UV analysis. A 100 μL injection was made and separation was achieved by HPLC on a C18 Waters Novapak column (4.6 x 150mm, 5μm, Milford, MA) at 40°C and a flow rate of 0.6 mL/min, using isocratic methanol at 84% (v/v). Absorbance was monitored at 278 nm.

b. Standardisation and quality control preparation

Standards for rapamycin were prepared by adding methanolic rapamycin to pooled EDTA anti-coagulated whole blood obtained from the Red Cross from their donor testing programme. Standards were used for instrument calibration and were made in a large batch and frozen in

individual portions for up to 5 months at –70°C or –80°C before analysis. Standards used for rapamycin metabolite quantification and response factor determination were made fresh daily by adding methanolic metabolite solution to fresh, pooled whole blood. Internal Quality Control (QC) samples for rapamycin were made from a separate stock drug solution, and prepared in large batches by adding methanolic rapamycin to pooled EDTA treated whole blood. The QC samples were frozen in individual portions for up to 3 months at -70°C or –80°C before analysis. Both standards and QC samples were analysed fresh and frozen for similarity and continuity with the previous batch before being included in the testing regimen. The concentration of methanol in all standards and QC samples was 0.1% (v/v).

c. Assay validation

The extraction procedure and HPLC-MS method was evaluated for recovery of drug and drug metabolite from whole blood by comparing the peak area of extracted, unextracted and blank extracts of whole blood all spiked to the same level. Standards were used to construct a standard curve using a linear regression curve-fit and a $1/x^2$ weighting scheme. Accuracy of the standards was evaluated by re-reading the standards as unknowns from the curve using the regression equation. Accuracy and precision of the QC were evaluated by extracting and measuring replicates both within a day (intra-assay) and between days (inter-assay) and reading the values from the standard curve.

A method comparison was performed by analysing a series of samples both by LC-UV and LC-MS. Samples were collected from patients taking rapamycin for immunosuppression for liver transplantation for analysis of rapamycin by LC-UV. After routine analysis by LC-UV, these samples were stored frozen at –20°C for 1-5 days, then at –70°C or –80°C for up to two years before analysis by LC-MS.

d. Rapamycin metabolite standardisation

Metabolites were extracted in replicates of six, at four concentrations on three separate days. The response ratio of each metabolite was calculated relative to that of rapamycin. This response ratio was used to calculate the concentration of metabolite in clinical specimens based on the standard curve of rapamycin.

e. Data manipulation

Statistical calculations, some curve regression and graphing were done using Graph Pad Prism, version 3.0 software (Graph Pad Software, San Diego, CA). Standard curve construction for LC-MS analysis was done using HP Chemstation software with the linear weighting option enabled.

3. RESULTS

a. Recovery determination

Results of the recovery experiments are summarised in Table V-1. Calculation of overall extraction recovery, as compared to unextracted samples was lower than expected, at 44.9 +/- 2.7 % for rapamycin and 50.2 +/- 4.4 % for the internal standard DMR (mean +/- SD, n=18). As the relationship between signals produced by extracted and unextracted samples was not consistant for rapamycin, metabolites and IS, another approach was investigated. Blank blood was extracted in parallel with rapamycin spiked whole blood. The blank extracts were then spiked with methanolic rapamycin to 100% of the level of the extracted samples. When analysed immediately after the extracted and unextracted samples, these spiked samples provided more predictable, consistent comparison with the extracted samples for the purpose of calculation of percent recovery. Using the blank samples spiked post-extraction for comparison, the recovery was calculated at 76.3 +/- 6.9 % for rapamycin and 76.9 +/- 6.5 % for DMR (mean +/- SD, n=12). The overall variability in recovery was 8.7 % CV for rapamycin and 8.5 % CV for the internal standard, DMR as measured here, at the 5.0 μg/L level, in 12 replicates over a three day period.

Table V-1 Percent recovery of rapamycin and DMR by LC-MS

Rapamycin	mean(%)	SD	%CV	n
Extracted/Unextracted	44.9	2.7	6.0	18
Extracted/Spiked Extract	76.3	6.9	9.0	12
DMR				
Extracted/Unextracted	50.2	4.4	8.8	18
Extracted/Spiked Extract	76.9	6.5	8.5	12

b. Rapamycin standard curve and quality control

An analytical run or "batch" was defined as a group of standards, QC samples and unknown samples prepared for analysis by extraction in a single day, and analysed by LC-MS within 40 hours of extraction. Quality control samples were run both at the beginning and end of each batch, and standards and unknowns run individually in sequence between.

After graphic representation and regression analysis, assay acceptability was evaluated by examining the standard curve and QC data. In the course of this study, 18 LC-MS analytical runs were completed and independently standardised, and 29 to 32 QC samples per level were analysed. A typical standard curve is depicted in Figure V-1 with its linear regression equation. Standards were read back from the standard curve, using the regression equation to calculate the curve-fitted value for each. The summary of the curve-fit data for the standards is summarised in Table V-2. Outlying points were omitted and the curve refitted. It was required that standards be within 40% of their nominal value for the standards ranging in concentration from 0.1 to 0.5 μg/L and within 30% of their nominal value for other standards (1.0 μg/L to 75 μg/L) in order to be included in the standard curve regression, and that a minimum of five standards be included in the regression calculation for acceptance of the standard curve. Only 6 of 195 standards were omitted on the basis of excessive deviation from theoretical mean. All curves were constructed from 8 to 12 standards and each was acceptable. Certain standards were, on occasion, not run if a smaller linear range was required for the analysis of the unknown samples in the batch. For example, if only trough samples were run, a standard curve from 0 – 30 μg/L was used, and if PK profiles were included in the run, a curve from 0 – 75μg/L was used. Although the limit of detection was 0.05 μg/L (defined as 3x background), the limit of quantification was defined by the boundaries of the standard curve at all times, usually 0.1 μg/L.

Figure V-1 Rapamycin analysis by LC-MS: standard curve

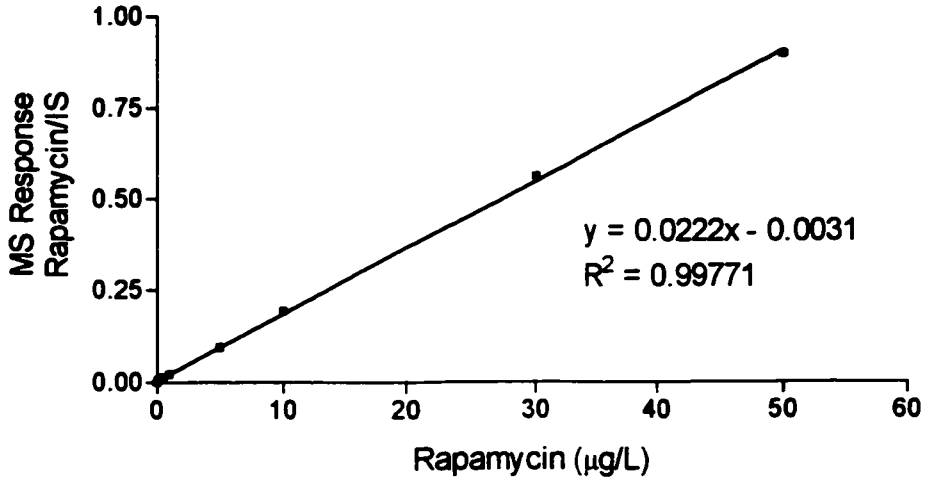

Table V-2 Compiled calculated standard curve parameters: LC-MS rapamycin assay

Parameter	n[a] (%)	Mean (SD) (μg/L)	%CV[b]	Range (μg/L)
μg/L Standard				
0.1	16 (88)	0.10 (0.04)	23.4	0.06-0.2
0.3	18 (94)	0.30 (0.11)	23.6	0.20-0.63
0.5	18 (89)	0.53 (0.14)	12.4	0.27-0.97
1	18 (100)	1.04 (0.10)	9.7	0.83-1.18
3	16 (100)	3.18 (0.33)	10.2	2.43-3.84
5	17 (94)	5.05 (0.44)	4.1	3.47-5.65
10	18 (100)	9.92 (0.67)	6.7	8.72-10.87
20	15 (100)	19.71 (0.85)	4.3	18.15-21.29
30	17 (100)	30.4 (0.72)	2.4	29.17-32.03
40	14 (100)	39.25 (1.62)	4.1	37.59-43.77
50	18 (100)	51.12 (2.72)	5.3	47.93-60.73
75	9 (100)	73.76 (2.39)	3.2	69.47-78.31
Slope	18	0.022		0.0182-0.041
y-intercept	18	0.002		-0.005 to 0.006
R^2	18	0.9990		0.9973-0.9998

[a] Total number of calibrators analysed (percentage of calibrators acceptable)
[b] CV = coefficient of variation

Instrument calibration and QC stability was assessed by running QC samples when freshly extracted, after the standard curve, and at the end of an analytical run, approximately 24 to 34 hours later. The results of a comparison of 14 pairs of QC samples are depicted in Table V-3.

Using the paired Student's t-test, it was found that there was not a significant difference in any of the three levels of quality control samples run immediately at the beginning of an analytical run or held for delayed analysis (P=0.6, 0.8, 0.3). Although there is no difference in the means of the QC run, in the delayed samples there was a higher degree of imprecision, as indicated by higher %CVs. This may illustrate that for this complex analytical method, although a 40 hour total run time is acceptable, it is challenging the limit of analytical acceptability.

Quality control specimens were extracted in tandem with the standards and unknowns for analysis for the purpose of ensuring each analytical run was valid. Within-day precision was evaluated by extracting and analysing six replicates at each of four levels of QC material. Imprecision varied intra-day from 2.3% at the 48.1 μg/L level, to 15.0% at 0.28 μg/L rapamycin and is summarised in Table V-4 with the between-day (Inter-day) cumulative QC data for the LC-MS assay. QCL, QCM and QCH are pools that were used for both HPLC-UV and LC-MS determination. QC4, 5 and 6 are dilutions of the above noted QC pools, and were run by LC-MS only. There were from 29 to 32 QC samples run per level, and this varied based on resource limitations and technical failure. Overall for LC-MS, there were only 10 QC samples of a total of 179 that were excluded because of failure to fall within 20% of the nominal value of the QCL, QCM and QCH, and of 30% of the nominal value for QC4, QC5, and QC6. Additionally, several Westgard rules were also used. For the detection of a trend in the mean the 10x rule was used, and to detect a rapid unexpected shift in the mean, the 2x rule was used for QC interpretation.

Table V-3 LC-MS assay for rapamycin: 40 hour on-instrument quality control stability

	Immediate Analysis			Delayed Analysis		
	QCL	QCM	QCH	QCL	QCM	QCH
mean (μg/L)	7.9	23.7	55.2	8.1	23.9	56.9
SD	0.4	1.5	3.7	1.0	3.2	7.1
%CV	5.1	6.3	6.7	12.3	13.4	12.5
n	14	14	14	14	14	14
P[a]	0.55	0.83	0.30			

[a] paired t-test, immediate analysis versus delayed analysis

Table V-4 Rapamycin by LC-MS: Quality control results

A. INTRA-DAY ANALYSIS

	QCA	QCB	QCC	QC6 X 2
mean (μg/L)	19.19	48.08	2.55	0.28
SD	0.62	1.09	0.23	0.04
%CV	3.23	2.27	9.08	15.04
n	6	6	6	6
range	18.72-20.22	46.75-48.66	2.20-2.83	0.21-0.31

B. INTER-DAY ANALYSIS

	QCL	QCM	QCH	QC4	QC5	QC6
mean (μg/L)	8.05	24.01	56.51	0.74	2.49	0.58
SD	0.82	2.90	6.70	0.14	0.29	0.10
%CV	10.19	12.08	11.86	18.92	11.65	17.24
%error	0.63	-3.96	2.75	-7.50	-0.40	5.45
n	32	30	30	29	29	29
range	6.78-10.26	18.48-32.4	46.75-76.12	0.43-0.95	1.90-2.99	0.43-0.84
Mean+/-2SD	6.41-9.69	18.21-29.8	43.11-69.91	0.46-1.02	1.91-3.07	0.38-0.78
Mean+/-3SD	5.59-10.51	15.31-32.7	36.41-76.61	0.32-1.19	1.62-3.36	0.28-0.88

No additional QC samples were excluded, nor any analytical runs rejected on the basis of failing to meet these stringent Westgard rules. A retrospective analysis was completed at the end of the 18 analytical runs, and no additional values were excluded based on post-hoc testing using the measured mean +/- 3SD range for QC acceptability. Greater than 95% of results fall within 2 SD of the mean. Prospectively, limits were established where an analytical run was accepted and unknowns were calculated from the standard curve if 4 of 6 QC samples for LC-MS were acceptable according to these standards. In fact, all analytical runs were accepted, because at most only one QC sample per run was excluded per run on this basis.

The LC-UV method was used concomitantly in the laboratory for rapamycin parent drug level determination in clinical samples. The cumulative results of the QC data for the LC-UV assay for the same time-period are summarised in Table V-5. Overall accuracy for the LC-MS assay was higher than for the LC-UV assay, as was imprecision.

c. Method comparison, LC-UV and LC-MS

A method comparison was conducted by correlating 83 samples collected from 7 liver transplant patients (2 to 18 samples per patient) as previously described. Only one sample was excluded from the correlation because of unacceptable and erratic background when analysed by LC-MS. There was insufficient quantity for repeat extraction and analysis. The results of the correlation of 82 samples as analysed by LC-UV and LC-MS is presented in Figure V-2. Using an unweighted correlation, the correlation co-efficient (R^2) was 0.9829 with a standard error of the estimate of 1.474, the slope 0.9895 +/- 0.015, and the y-intercept of 0.54 +/- 0.36. The results of the bias analysis are depicted in Figure V-3 as a Bland-Altman plot. The median and inter-quartile range for the LC-UV and LC-MS assays are 19.3 μg/L (16.00-24.80) and 19.18 (15.93-24.57), respectively. The average difference between the two methods was 0.31 μg/L, with LC-UV being higher than LC-MS. The equation for the regression line is –0.0019, the y-intercept 0.3519, with a low regression statistic of <0.001 and a standard error of the estimate of 1.479. There was not a significant deviation from a zero slope. Further, there was no significant

Table V-5 Rapamycin by LC-UV: Cumulative quality control data

	QCL	QCM	QCH
mean (μg/L)	7.87	22.64	56.73
SD	1.02	2.48	5.28
%CV	13.0	10.9	9.3
%error	-1.6	-9.4	3.1
n	64	68	66
range	4.4-9.8	17.6-29.1	42.1-69.5
Mean+/-2SD	5.8-9.9	17.7-27.6	46.2-67.3
Mean+/-3SD	4.7-10.9	15.2-30.1	40.9-72.6

Figure V-2 Method comparison: HPLC-UV versus HPLC-MS

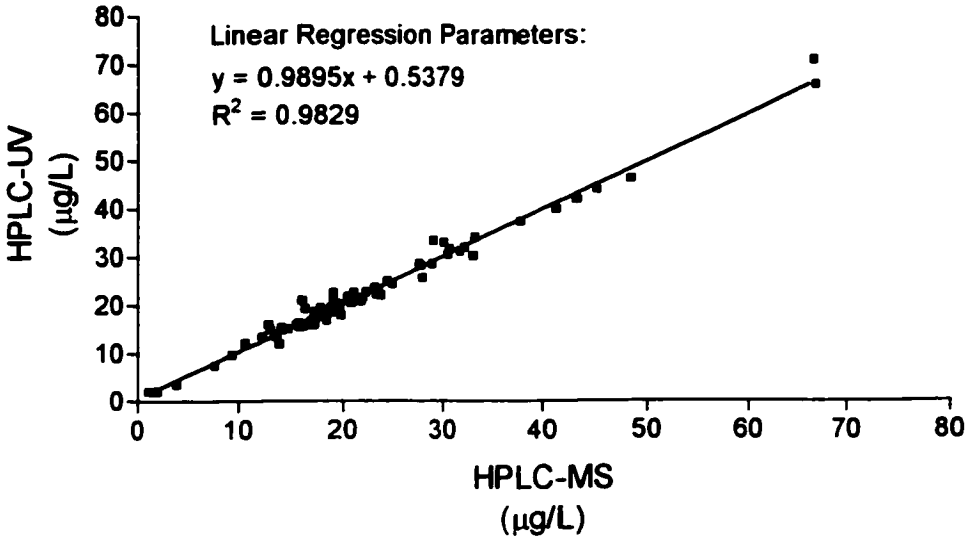

Correlation of 82 whole-blood rapamycin concentrations obtained using HPLC-UV and HPLC-MS.

Figure V-3 Bland-Altman Bias Plot of HPLC-UV versus HPLC-MS rapamycin analysis methods

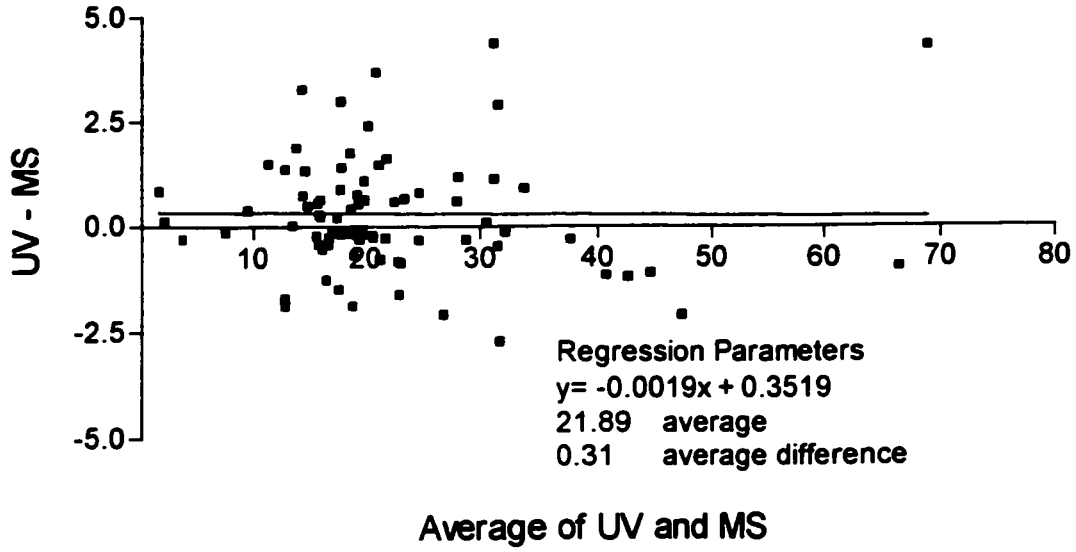

Difference in rapamycin concentration measured by HPLC-UV and HPLC-MS versus the average concentration measured in 82 whole blood trough samples from liver transplant recipients

difference between the two data sets, as analysed by a non-parametric two-tailed paired Wilcoxan signed rank test (P=0.2). The pairing was effective, as tested by the Spearman Approximation (P<0.0001).

To calculate the percentage bias, or overestimation due to one analytical method, the Bland-Altman bias evaluation technique was used[1]. It is depicted in Figure V-4. The average percentage bias for HPLC was 2.8% +/- 11.0% (mean +/- SD) with a linear regression revealing a bivariate correlation coefficient (R^2) of 0.0609 and a standard error of the estimate of 10.73. The slope was significantly non-zero (P=0.03) at –0.242 +/- 0.1063 with a y-intercept of 8.07 +/- 2.596.

These results indicate an acceptable correlation exists between the two analytical methods over the range tested (5-75 μg/L), without significant bias or concentration-dependent bias between the two analytical methods.

d. Extrapolated rapamycin metabolite response curves

The slope response of each of five rapamycin metabolites over the standardisation range was compared to that of rapamycin. Extracted spiked whole blood specimens were analysed by LC-MS in replicates of six on three separate days. This is depicted in Figure V-5. The relative response of each metabolite was initially evaluated for divergence from that of rapamycin by constructing a P statistic with a 2-tailed ANCOVA-like approach to compare the means of the slopes[2]. It was found that the difference between the slopes was extremely significant (P<0.05), and so it was not possible to compare the differences in the intercepts. As the slopes were so different from each other, and the variability in response for each metabolite ranged only from 2.9 to 8.7% CV for eighteen determinations done over three days, it was decided that it would be suitable to use a relative response ratio for calculation of individual metabolite levels in unknown specimens using the rapamycin standard curve. The Relative Response was calculated by dividing the slope of rapamycin by the slope of the metabolite to attain a

Figure V-4 Bias in rapamycin determination by HPLC-UV versus HPLC-MS

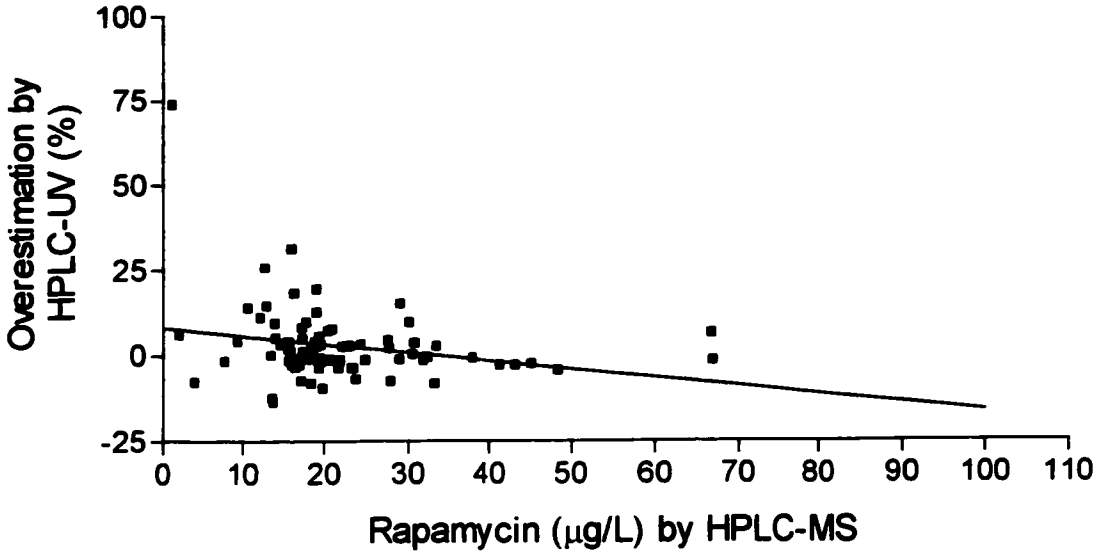

Figure V-5 Rapamycin metabolite slope response by LC-MS

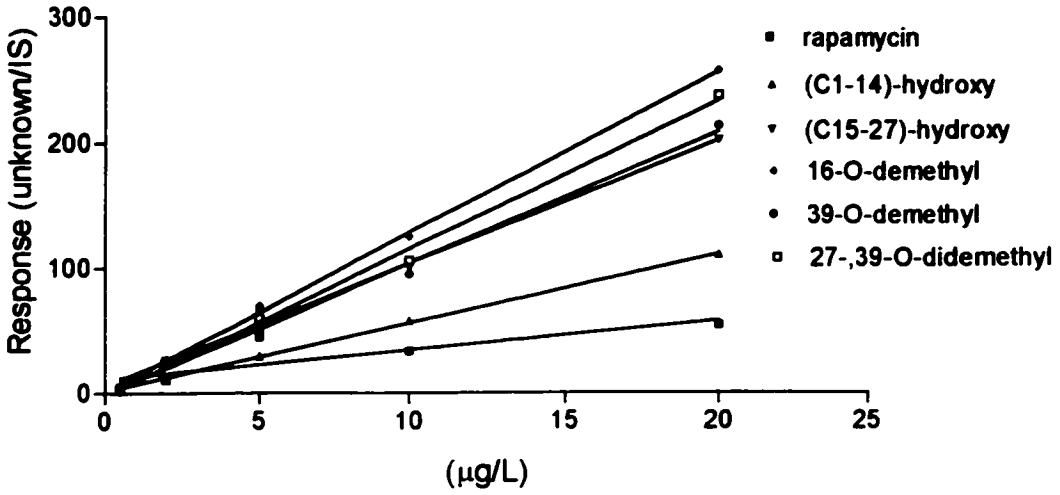

metabolite-specific factor. This factor was multiplied with the slope of rapamycin to attain a corrected slope for the metabolite response for a given run, and would be used as a surrogate standardisation for determination of rapamycin metabolites in all subsequent analytical runs.

5. DISCUSSION

The motive behind monitoring drug levels is to optimise drug therapy in individual patients. The requirement for therapeutic drug monitoring (TDM) is determined by examining the relationships between drug dose, biological (pharmacokinetic) disposition, clinical or pharmacologic efficacy and undesirable effects. As a result of these inter-relationships, there are several instances where TDM is particularly useful: (1) the drug level or pharmacokinetic parameter correlates to clinical efficacy and/or toxicity; (2) efficacy or toxicity are difficult to measure clinically; (3) disease state or patient status alters drug disposition; (4) there is a weak or unpredictable correlation between drug dose and efficacy; (5) there is significant inter-individual pharmacokinetic variability; (6) drug interactions are possible; or (7) when non-compliance is a risk. For rapamycin therapy in transplant patients, all seven situations are pertinent.

Rapamycin was approved in the USA by the Food and Dug Administration for use in prevention of organ rejection in renal transplant recipients on September 15, 1999. Although approved in this patient population for use with CsA and corticosteroids, there have also been instances of release drug by the regulatory agencies for compassionate reasons, specifically for use in individual patients with other indications and other drug combinations. The licence for use of rapamycin in combination was granted without specific obligation or requirement for therapeutic drug monitoring of rapamycin. However delineation of TDM recommendations was specific for pediatric patients, those with suspected or known hepatic impairment, cases where CYP 3A4 inducers or inhibitors are also given, and for patients where CsA is markedly reduced or discontinued. The patients treated at the University of Alberta Hospitals centre who were converted to the rapamycin therapeutic regimen all met one or more of these criteria, and were

all monitored closely from the date of conversion for adequate rapamycin levels and clinical response.

One of the basic requirements for appropriate therapeutic monitoring of any drug is to use a well-defined and validated method to determine the drug levels. The implemented assay system should be an analytical method that is validated over the clinically relevant range of concentrations, with acceptably low levels of analytical variation and a high degree of precision. If multiple centres are conducting analysis for the same analyte, there should be a good correlation between the methods for the purpose of equivalent monitoring. Most of the methods published in the literature for the analysis of rapamycin and described herein have met analytical testing parameters suggested for TDM of drugs, and specifically, TDM of rapamycin[17].

The methods that were either available or under development for TDM of rapamycin were HPLC-UV, HPLC-MS, HPLC-MS/MS, the FKBP radio-receptor binding assay (IBA, previously described), and the experimental semi-automated micro-particle enzyme immunoassay (MEIA, previously described). These methods are compared in Table V-6.

Preparation of samples for analysis consisted of either extraction of the compound of interest into an organic layer, or precipitation of the blood proteins with salt and organic solvent. Some of the extraction procedures and all of the precipitation procedures also used solid-phase extraction to further purify and concentrate the sample prior to analysis. None of these techniques has an obvious advantage over the others in terms of recovery or specificity, and all appear to be acceptable for the analysis of rapamycin.

Detection of rapamycin in these various analytical methods did vary somewhat. For LC-UV, detection was uniform at the wavelength of maximum absorbance, 278 nm. Analysis of rapamycin by MEIA was particularly unique, as it relied on the formation and detection of a fluorescent product using a specialised instrument, the IM_X. The immunophilin binding assay

Table V-6 Rapamycin methodology comparison

		LC-UV	LC-UV	LC-UV	LC-UV	LC-UV	LC-MS-MS	MEIA	IBA	LC-MS	LC-MS
Sample Volume	(mL)	1.0-2.0	0.25-1.0	1.0	1.0	1.0	0.5	0.15	0.2-0.4	1.0	1.0
Internal Standard		DMR	BME[a]	DMR	DMR	DMR	DMR	none	^{3}H-diOH-FK506	none	DMR
Extraction Method		L/L[b]	L/L	L/L then SPE[d]	L/L	L/L	ppt[c] then SPE	ppt	ppt	ppt on-line SPE	L/L
LOD/LOQ[g]	(μg/L)	0.5 LOD	1.0 LOQ	0.4 LOD	5.0 LOQ	2.5 LOQ	0.25 LOD	3 LOQ	1.0 LOD	0.4 LOQ	0.1 LOQ
Range	(μg/L)	1-250	1-50	1-50	5-350	2.5-150	0.25-100	3-30	2.5-40	0.4 – 100	0.1-75
Imprecision Intra-assay	%CV(μg/L)	8.1 (10) 1.9 (50)	6.4 (3) 4.2 (75)	NR[e]	3.8 (15) 3.1 (235)	14.4 (7.5) 13.2 (60) 12.0 (120)	NR	NR	NR	4.6 (5) 3.9 (25) 3.2 (100)	15.0 (0.3) 9.1 (2.5) 2.3(55)
Inter-assay	%CV(μg/L)	14.4 (10) 5.6 (50)	11 (4) 13.0 (32)	9.8 (5) 5.6(40)	4.5 (15) 4.1 (235)	13.0 (7.5) 5.7 (60) 2.6 (120)	9.2 (0.5) 6.9(20.0) 5.9(75)	10.7(5) 9.6(11) 7.5(22)	12.9 (2.5) 9.2 (7.5) 5.9 (20.0)	9.5 (5) 8.3 (25) 7.8(100)	16.7 (0.6) 11.5(2.5) 11.9(55)
Recovery	%	35	94	45	82	88-106	99.5-103	99-106		87 – 106	76
Reference		7	8 9	10	11	12	13	5	3 14 15	16	current study
Specific for rapamycin?		YES	YES	YES	YES	YES	YES	metabolite XR[f]	some metabolite XR	YES	YES

[a] BME = β-estradiol-3-methyl ester

[b] L/L = liquid/liquid extraction

[c] ppt = precipitation

[d] SPE = solid phase extraction

[e] NR = not reported

[f] XR = cross reactivity

[g] LOD/LOQ = limit of detection/limit of quantitation

relies on the competitive binding of a protein target and measured free radioactivity. All MS and MS/MS techniques relied on an electrospray interface and one required the use of post-column flow-splitting prior to MS/MS analysis. For the LC-MS analysis of rapamycin, the detection of rapamycin-adduct formation was done using selected or single ion monitoring at 936.6 (Na^+) or 931 (NH_2^+). This depended on the adduct formed, which was in turn dependent on various parameters of the method used (buffer presence, ion mode) and probably was also due in part to the instrumentation used. For LC-MS/MS, single ion monitoring of intact parent ion at m/z 931 and daughter ion formation at 864.6 was conducted for the most specific detection of rapamycin with the least extraneous signal.

For its ability to definitively exclude interference and to sensitively detect rapamycin, LC-MS/MS should be considered the reference methodology, or "Gold Standard", against which other methods can be compared. The LC-UV and LC-MS or LC-MS/MS detection methods were sufficiently sensitive and specific for detection of rapamycin alone. However, the IBA displays a degree of cross-reactivity with rapamycin metabolites, as described in Chapter 2. The cross-reactivity was <10% to 26%[3], which obviously requires further study and examination to determine the clinical relevance. The experimental MEIA displays an even greater degree of cross-reactivity with rapamycin metabolites as tested, as alluded to by the preliminary experiments conducted in conjunction with the University of Alberta Hospitals laboratory and described in Chapter 2. It has since been published that the MEIA demonstrates a metabolite cross-reactivity varying from 50% (uncharacterised hydroxyrapamycin) to 127% (41-O-demethyl rapamycin)[4]. The MEIA also has an overall significant positive bias in clinical specimens that is dependent on concentration, hematocrit and time post-transplant[5].

The limit of detection and imprecision of the LC-MS method for rapamycin developed and described in the current study is comparable or slightly lower than the LC-MS and LC-MS/MS methods in the literature. The linear range of the current study was designed to be smaller than the other published methods (0.1-75 μg/L versus the maximum range of 0.25-250 μg/L)

because of analytical requirements in our lab, but this could easily be expanded to accommodate future requirements. In our lab, two LC-MS units were used for rapamycin and metabolite determination. These were shared instruments, used by multiple users to measure several very different compounds, and used for developmental/experimental and research grade assays. Each time a rapamycin and metabolite assay was to be run, complete change-over of columns, solvents and MS parameters was necessary. The standards and QC samples were run as soon as possible after change-over because of resource limitations, and this may have introduced some unexpected variability. These are possible explanations for the high inter-assay CV, and may be lowered significantly if dedication of an instrument to the analysis of rapamycin and metabolites in the lab was possible.

There are also contrasts between these methods regarding availability and expertise required for execution of the various analytical procedures, and accessibility of the testing platform. LC-UV analysis of rapamycin is a likely candidate for implementation in many clinical laboratories. Although it is a difficult method to establish, the HPLC equipment required to do the assay for rapamycin is likely to be found in most analytical and clinical labs with esoteric or toxicology testing capabilities. Less common is the LC-MS equipment, as MS detectors are expensive, not widely available and require a higher degree of expertise to operate effectively. The MEIA is not yet clinically available, and it has recently been removed from clinical development because of problems with the producing company. Although it requires a specific instrument for testing (the Abbott IM_X), the instrumentation is frequently found in clinical labs that have a TDM component. The MEIA is potentially a very simple and fast (high through put) assay, and would be welcome in many testing sites. For the immunophilin binding assay (IBA), a major disadvantage is its use of radioactivity. The use of radio-isotopes is no longer desirable, as clinical laboratories are switching to other detection methodologies for measurement of low concentration and complex bio-analytes where possible. Also, IBA is not yet commercially available in kit form, and establishing this assay would be costly and complicated. The substrate for this assay is ^{3}H-dihydroxy-FK506, which is not commercially available. Neither is

its precursor available; dihydroxy-FK506 or the protein immunophilins necessary for binding. Not all labs have the expertise or facilities to isolate and purify drug metabolites or proteins. Also, it is very expensive to custom radio-label the competitive substrate, contributing to an unattractively high start-up cost. However, the method is simple to follow and relatively fast, and a liquid scintillation counter is usually available in an esoteric clinical lab, so it would be a fairly accessible test if the materials were made available.

At the time of writing of this document, the only acceptable methods for measurement of rapamycin metabolites were HPLC-MS and HPLC-MS/MS. A summary of these methods is presented in Table V-7.

Detection of rapamycin metabolites was done using mass-to-charge ratios of parent ion for MS detection and parent and daughter ion formation (MS/MS), and was similar to the detection of rapamycin as described above. Separation was uniformly achieved using HPLC.

Standardisation of these assays for the determination of rapamycin metabolites is, of course, problematic. Rapamycin metabolites are not readily available pure and in sufficient quantities for the routine standardisation of these methods. Ideally, each metabolite should be available for extraction, construction of a standard curve and analysis of quality control samples for each and every run. As I did not possess enough metabolites to do this, I compromised by establishing relative response ratios (Figure V-5) for each metabolite as compared to rapamycin and proved that the variability in these response ratios was suitably low. As there were considerable differences in the slopes of the assay for each metabolite, only the metabolites for which standards existed were measured using this method. Streit and associates describe another assay methodology where the slopes of the standard curves for the two metabolites tested were not significantly different from that of rapamycin; they extended this assumption to metabolites not specifically tested and quantified uncharacterised metabolites on this basis[6]. It

Table V-7 Rapamycin metabolite methodology comparison

		LC-MS-MS	LC-MS
Sample Volume	(mL)	1.0	1.0
Internal Standard		Acetyl-sirolimus	DMR
Extraction Method		precipitation, then SPE	liquid/liquid
LOD/LOQ	(µg/L)	LOQ 0.25	LOQ 0.2
Range	(µg/L)	0.25-250	0.2-75
Imprecision (Rapamycin)	Intra-assay %CV (µg/L)	12.5 (1.0) 5.9 (15) 11.4 (40)	15.0 (0.3) 9.1 (2.5) 2.3(55)
	Inter-assay %CV (µg/L)	19.5 (1.0) 9.3 (15) 14 (40)	16.7 (0.6) 11.5(2.5) 11.9(55)
Recovery	%	88	76
Metabolites measured		39-O DM DM OH	39-O-DM 27-O-DM 13,27-O-diDM C1-C14 OH C15-C27 OH
Metabolite standardisation		Equivalent slopes	Slope Ratio
Reference		[6]	Current Study

appears that metabolite response is either method- or platform-dependent, but should be determined for each metabolite and equivalency should not be accepted based on assumption.

Otherwise, the in-house developed method (LC-MS) and the one described in the literature (LC-MS/MS) compare to one another favourably in terms of recovery, imprecision and sensitivity. Although they differ in sample preparation and detection mode, they are very similar in analysis technique and in the analytical results produced – ideally, a correlation study where the two methods are directly compared should be completed.

Although expensive and requiring expertise, LC-MS and LC-MS/MS remain the only methods for adequately quantifying rapamycin metabolites to date. Because of the specialised nature of the analysis, instrumentation, and expertise required, it is unlikely that clinical labs will offer rapamycin metabolite levels for routine analysis in the near future. Perhaps in the future, dynamic immunophilin, receptor-based or antibody-based assays will be developed that can discriminate between rapamycin and its various metabolites and provide determination of multiple metabolites as well as rapamycin. It is predicted that these assay methodologies could be more easily adapted for clinical use.

In summary, the LC-MS method developed and evaluated here compared favourably to the in-house LC-UV method used for the determination of rapamycin in whole blood specimens. The sensitivity, accuracy, and precision is suitable for routine rapamycin determination. The analytical parameters are similar to, or exceed those of published methods to date.

This LC-MS method can also be used for the determination of the five rapamycin metabolites described in the previous chapter, by virtue of their response relative to that of rapamycin. Although this novel approach is not shared by other investigators conducting rapamycin metabolite measurement, it appears to be sufficient for the estimation of these particular rapamycin metabolites under the conditions described here.

5. REFERENCES

1. Bland JM, Altman DG. Statistical methods for assessing agreement between two methods of clinical measurement. Lancet 1986; i:307-10.

2. J Zar. Biostatistical Analysis. Chapter 18 . 2nd edition edition. Prentice-Hall, New York, 1984.

3. Davis D, Murthy J, Gallant-Haidner HL, Yatscoff RW, Soldin SJ. Minor immunophilin binding of tacrolimus and sirolimus metabolites. Clinical Biochemistry 2000; 33:1-6.

4. Jones K, Saadat S, Lee T *et al.* An immunoassay for the measurement of sirolimus. Clin Ther 2000; 22:B49-B61.

5. Salm P, Taylor PJ, Pillans PI. The quantification of sirolimus by high-performance liquid chrmatography-tandem mass spectrometry and micro particle enzyme immunoassay in renal transplant recipients. Clin Ther 2000; 22:B71-B85.

6. Streit F, Christians U, Schiebel H-M *et al.* Sensitive and specific quantification of sirolimus (rapamycin) and its metabolites in blood of kidney graft recipients by HPLC/electrospray-mass spectrometry. Clin Chem 1996; 42:1417-25.

7. Yatscoff RW, Faraci C, Bolingbroke P. Measurement of rapamycin in whole blood using reverse-phase high-performance liquid chromatography. Ther Drug Monit 1992; 14:138-41.

8. Napoli KL, Kahan BD. Sample Clean-up and high-performance liquid chromatographic techniques for measurement of whole blood rapamycin concentrations. J Chrom B Biomed Appl 1994; 645:111-20.

9. Napoli KL, Kahan BD. Routine clinical monitoring of sirolimus (rapamycin) whole-blood concentrations by HPLC with ultraviolet detection. Clin Chem 1996; 42:1943-8.

10. Svenssön JO, Brattstrom C, Sawe J. Determination of rapamycin in whole blood by HPLC. Ther Drug Monit 1997; 19:112-6.

11. Holt DW, Lee T, Johnston A. Measurement of sirolimus in whole blood using high-performance liquid chromatography with ultra violet detection. Clin Ther 2000; 22(Suppl B):B38-B48.

12. Maleki S, Graves S, Becker S *et al.* Therapeutic monitoring of sirolimus in human whole-blood samples by high-performance liquid chromatography. Clin Ther 2000; 22:B25-B37.

13. Taylor PJ, Johnson AG. Quantitative analysis of sirolimus (rapamycin) in blood by high-performance liquid chromatography-electrospray tandem mass spectrometry. J Chrom B Biomed Appl 1998; 718:251-7.

14. Goodyear N, Napoli KL, Murthy J *et al.* Radioreceptor assay for sirolimus. Clin Biochem 1996; 29:457-60.

15. Goodyear N, Napoli KL, Murthy J *et al.* Radioreceptor assay for sirolimus in patients with decreased platelet counts. Clin Biochem 1997; 30:539-43.

16. Kirchner GI, Vidal C, Jacobsen W *et al* . Simultaneous on-line extraction and analysis of sirolimus (rapamycin) and ciclosporine in blood by liquid chromatography-electrospray mass spectrometry. J Chrom B Biomed Appl 1999; 721:285-94.

17. Yatscoff RW, Boeckx R, Holt DW *et al.* Consensus guidelines for therapeutic drug monitoring of rapamycin: report of the consensus panel. Ther Drug Monit 1995; 17:676-80.

VI: CANINE PORTAL AND SYSTEMIC PHARMACOKINETICS OF RAPAMYCIN

1. RATIONALE

The disposition of rapamycin and the dynamic formation of its metabolites after an oral dose has not been investigated. Rapamycin metabolism has only been described partially using *in vitro* models. The role of the intestine and liver in the metabolic fate of rapamycin and the production of metabolites has yet to be investigated.

The differences in portal and systemic pharmacokinetic parameters of rapamycin was investigated at acute and chronic dosing intervals, using a canine model to determine if rapamycin is suitable for immunosuppression of liver and pancreatic islet cell grafts.

2. MATERIALS AND METHODS

a. Surgical Procedure

Six healthy mongrel dogs (20-25 kg) were used for this study done in conjunction with A.M.J. Shapiro and Ergeng Hao (Department of Surgery, University of Alberta). Catheters were surgically placed in the portal vein and the carotid artery and subcutaneously-tunnelled to the back of the neck. This permitted chronic blood sampling from non-restrained, non-sedated animals. These silastic catheters were prepared using techniques modified from O'Brien and colleagues[1]. Briefly, two catheters of 0.062" internal diameter and 0.125" outer diameter (Silastic, Dow Corning, Midland, MI) were cut to 70 cm length. For the purpose of anchoring the catheters into the tissue, double velour Dacron cuffs (Meadox, Oakland, NJ) were trimmed to 2 cm in diameter and placed 15 cm from the external end of each catheter with medical grade elastomer glue (Silastic, Dow Corning, Midland, MI). To secure the catheters within the blood vessels and prevent withdrawal from the point of ligation, a lip of silicone glue was constructed at 10 cm and 15 cm each from the internal end of the portal and carotid catheters, respectively. Several 1 mm perforations were made in the distal end of the catheters, to reduce the likelihood of occlusion of the catheter against the wall of the vessel during blood sampling. Catheters were sterilized using ethylene oxide gas.

After an overnight fast, each dog was anaesthatised with an intra-muscular (IM) injection of acepromazine (1 mg), meperidine (12 mg) and atropine (2.5 mg). Endotracheal intubation was necessary for maintainence of general anasthesia with halothane inhalation. Phrophylactic antibiotic was administered (cloxacillin, 1g, IM) and continued daily at 500 mg IM for three days.

The right side and dorsal neck was shaved and prepared for surgery and the catheters were pre-flushed with heparinized saline (100 iU/mL). A dorsal midline incision was made in the neck and two subcutaneous pockets were made by blunt dissection to accommodate the catheters. A second incision was made on the right side of the neck to expose the right common carotid artery. The artery was occluded proximally and distally, and arteriotomy made, and the catheter was guided centrally towards the heart until the silicone anchor bead was reached. The catheter was secured with 3/0 silk ties, permanently occluding the vessel and preventing bleeding or dislodgement at the entry site. The catheter was aspirated and flushed with heparinized saline to confirm patency and adequate placement, then delivered to the external dorsal neck site and capped with a luer-lock hub (PRN Adaptor, Deseret Medical Inc., Sandy, UT).

The portal catheter was delivered externally through the dorsal neck pocket and tunnelled with a 100 cm tunnelling device to the right flank. An incision was made in the right flank to the level of the peritoneum. A small hole was made into the peritoneum and the catheter threaded into the peritoneal cavity. The lateral incision was closed with 2/0 Vicryl (muscle) and 3/0 vicryl (skin). A separate midline abdominal incision was made and deepened through the linea alba, to access the peritoneal cavity. After removal of the extra-peritoneal fat pad using cautery, a self-retaining Balfour retractor was placed to provide maximal access to the main portal vein. The gastroduodenal vein was used for the insertion site for the catheter, which was placed so the end was located just proximal to the portal bifurcation. It was secured with 3/0 silk ties and aspirated and flushed with heparinized saline to confirm patency and adequate placement

before closing. The abdomen was closed *en masse* with running 2/0 prolene reinforced with 3/0 vicryl subcuticular skin closure.

After extubation, animals were transferred to heated cages. Analgesia was given as required using buprenorphine (Schering, Toronto, ON) subcutaneously (0.1 – 0.2 mg/kg). Fluid balance was maintained intra-operatively with Ringer's lactate solution (75 mL/h) and by subcutaneous bolus post-operatively. Free access to water was given on day 1, and regular standard diet thereafter. A recovery period of 14 days was allowed before initiation of the oral immunosuppressive regimen. All animals were cared for by personnel of the Health Sciences Laboratory Animals Services of the University of Alberta under direct supervision of a veterinarian in compliance with the guidelines of the Canadian Council on Animal Care. All animals were sacrificed humanely upon completion of the study.

Catheters were flushed daily with 0.9 % (w/v) saline followed by a heparin-saline "lock" mixture (1000 iU/mL) to maintain patency. The heparin was increased to 10 000 iU/mL one week post surgery to reduce the chances of thrombosis. Catheters were cleaned and maintained every 3-4 days by replacing the PRN adapters, fully aspirating the heparin-saline locks, flushing with 0.9% saline followed by a sterilizing solution of ACD with formaldehyde (0.4% w/v anhydrous citric acid, 1.32 % w/v sodium citrate dihydrate, 1.47 % w/v dextrose mono-hydrate, 1.5% formaldehyde) to fill the catheter dead space. The sterilizing solution was left for 5 minutes, aspirated, and the catheter re-flushed with 0.9 % saline and locked with heparin-saline. Non-constricing neck bandages were used to prevent the animals from damaging the external catheter tips.

b. Pharmacokinetic Study

After 14 days of recovery, the animals received immunosuppressant for five sequential days, with pharmacokinetic studies on days one and five. A 14 day wash-out period was instituted between treatment periods. Rapamycin was given orally by mouth at 2.5 mg/kg/d in a non-

aqueous liquid formulation provided by Wyeth Ayerst Research, (Princeton, NJ). Paired blood samples were drawn from both catheters at 0.5, 1, 2, 4, 6, 8, 12 and 24 hours post dose, as appropriate. The catheters were flushed with saline between sampling periods, and 10 mL of blood was withdrawn prior to each sample for the purpose of ensuring the sample was neither contaminated nor diluted with saline or heparin-saline. Whole blood samples were collected into EDTA and stored at 4°C for 3-5 days, then frozen at –70°C for two years. Portal blood was collected separately from the carotid blood, which was considered a distinct systemic sample at each timepoint.

c. Drug and Metabolite Analysis

Rapamycin was measured by HPLC-UV (described in the previous chapter) within two days of sample collection. Rapamycin metabolites were measured by HPLC-MS (described in the previous chapter) after storage for two years at –70°C.

d. Pharmacokinetic and Statistical Analysis

The PK parameters were calculated using Win-Nonlin v.1.0, Standard edition. A non-compartmental model was used, with the linear trapezoidal rule for AUC calculation and uniform weighting throughout. Statistical analysis was conducted to demonstrate differences between acute and chronic dosing, and between portal and systemic PK parameters and drug levels. This was done using either the repeated measures ANOVA, and the Bonferroni's Multiple Comparison post-hoc test, or the Friedman non-parametric test with Dunn's post-hoc analysis as appropriate. Prism Graph Pad software was used for graphing and statistical calculation. A p value of less than 0.05 was considered statistically significant.

3. RESULTS

a. Rapamycin Pharmacokinetics

The 24-hour PK profiles for rapamycin in the canine model are shown in Figure VI-1. Only five of the six experiments were completed, as patency of one catheter was not maintained in one

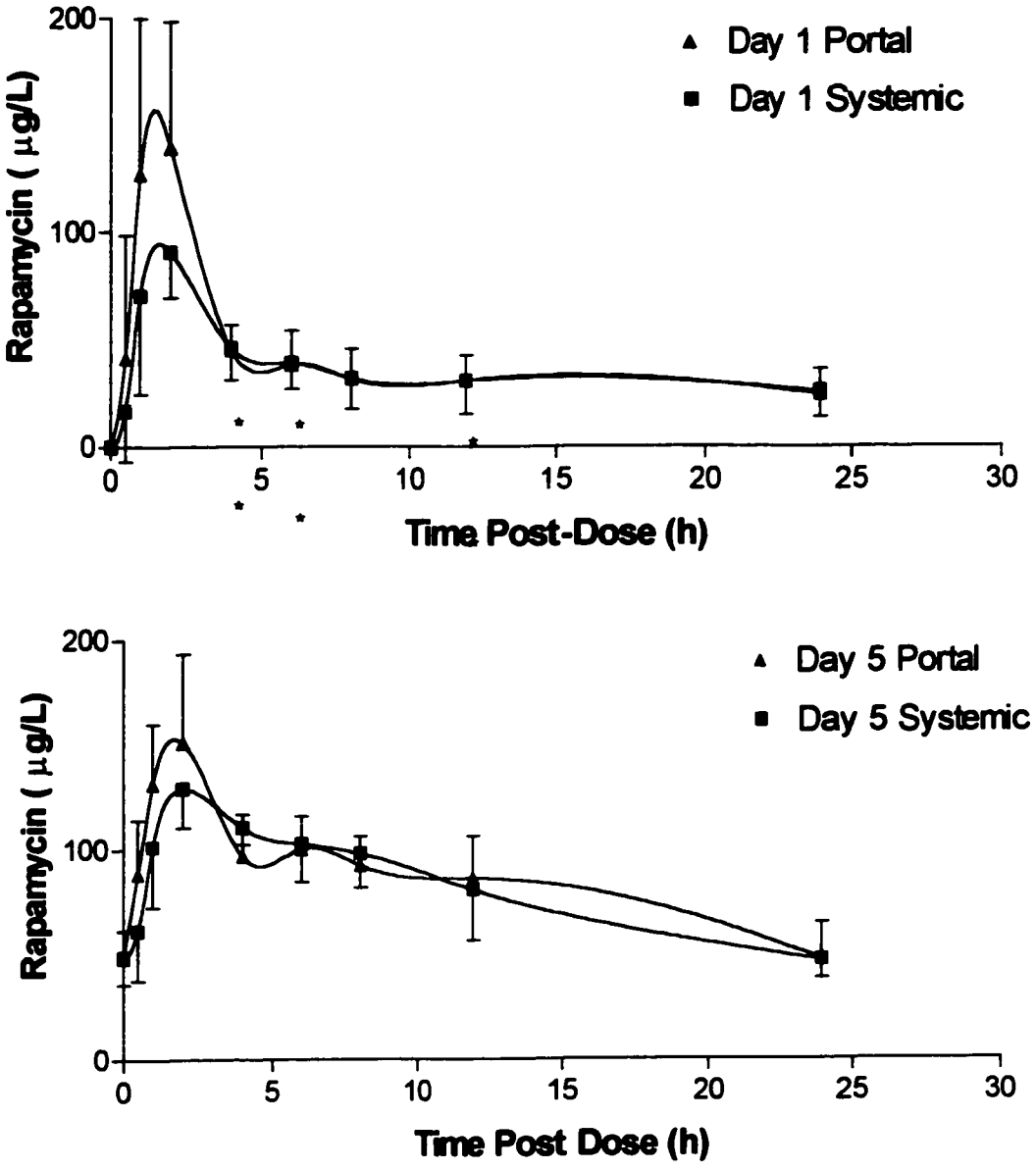

Figure VI-1. Pharmacokinetic profiles of rapamycin in the dog.

The pharmacokinetic profile of an acute oral dose (top) and chronic administration (bottom) is shown. Each point represents the mean +/- SD, n=5.

*P < 0.05 compared to the same sample site (portal or systemic) on different days. Symbols above the fitted curve refer to the portal results, while those below refer to the carotid results.

dog; this animal was excluded from the study. Pharmacokinetic parameters were calculated individually for each dog, using rapamycin blood levels drawn at the portal and carotid (systemic) sites. The details of the PK calculations are presented in Table VI-1, summarised by the duration of drug administration and site of blood sampling.

When comparing rapamycin levels over the acute and chronic dosing intervals, there were significant differences for both sampling sites at 4, 6, and 12h. For the PK parameters, there was only a significant difference in acute vs. chronic dosing for the portal site for the apparent volume of distribution (Vz). There are similarities in the PK parameters between the acute and chronic treatments and portal and systemic sampling sites, with only a few pairs of results showing statistically significant differences. There were no statistical differences in the PK parameters when comparing systemic to portal sampling sites after either acute or chronic dosing.

b. Normalised rapamycin pharmacokinetics

Because the primary interest of this study was to examine differences in drug levels, it was desirable to find a different way to compare these results. In an effort to present the results in a manner that is more easily compared, data from the PK profile for each dog was normalised in two ways: by dividing the blood concentration at each time point by the maximal concentration attained either the portal or systemic samples in that experiment. This was done to compare the relative drug exposure as opposed to the absolute exposure over the dosing interval. The impetus was to decrease the inter-subject variability seen in this diverse group of dogs.

The canine PK profiles that are normalised to maximal systemic level (SYSmax) are depicted in Figure VI-2, with the PK parameters summarised in Table VI-2. Similarly, the PK profiles that are normalised to the maximal portal level (PORTmax) are in Figure VI-3 and the PK parameter summary in Table VI-3.

Table VI-1 Canine rapamycin pharmacokinetic parameters

A. Acute administration, portal levels

Dog	T1/2β (h)	AUC24 (μg*h/L)	Cl/F (L/h*kg)	Vz/F (L/kg)	MRT 24 (h)	MRT inf (h)
1	9.8	1304	1.65	23.3	6.8	11.2
2	25.7	550	2.42	89.8	8.8	98.2
3	48.7	1148	0.71	50.1	9.7	66.3
4	28.9	n/a[1]	2.25	93.7	n/a[1]	37.8
5	57.4	1219	0.61	50.3	9.2	77.9
mean	34.1	1055†	1.53	61.4¥	8.6	58.3
SD	19.0	343	0.84	29.8	1.3	34.2

B. Acute administration, systemic levels

Dog	T1/2β (h)	AUC24 (μg*h/L)	Cl/F (L/h*kg)	Vz/F (L/kg)	MRT 24 (h)	MRT inf (h)
1	10.3	996	2.05	30.6	8.0	13.7
2	n/a[2]	410	n/a[2]	n/a[2]	9.9	n/a[2]
3	36.3	1077	0.86	45.0	10.6	52.1
4	12.2	n/a[1]	3.82	66.4	n/a[1]	17.3
5	95.4	1088	0.41	56.9	10.6	134.5
mean	44.5	893‡	1.69	65.9	9.8	50.2
SD	36.9	324	1.34	38.5	1.2	49.5

C. Chronic administration, portal levels

Dog	T1/2β (h)	AUC24 (μg*h/L)	Cl/F (L/h*kg)	Vz/F (L/kg)	MRT 24 (h)	MRT inf (h)
1	6.9	1707	1.28	12.8	9.2	12.2
2	16.6	2177	0.69	16.6	10.4	25.4
3	15.2	2588	0.62	13.6	10.2	23.0
4	22.6	1972	0.65	22.6	9.5	30.8
5	14.0	1689	1.02	20.5	9.5	20.3
mean	15.1	2027†	0.85	17.2¥	9.7	22.3
SD	5.6	373	0.29	4.3	0.5	6.8

D. Chronic administration, systemic levels

Dog	T1/2β (h)	AUC24 (μg*h/L)	Cl/F (L/h*kg)	Vz/F (L/kg)	MRT 24 (h)	MRT inf (h)
1	10.7	1960	0.98	15.2	9.8	16.6
2	21.5	2039	0.67	20.9	10.2	30.4
3	13.5	2372	0.73	14.1	10.2	20.5
4	19.7	1988	0.69	20.8	9.8	27.6
5	174.6	1453	0.21	53.5	9.7	243.1
mean	48.0	1962‡	0.66	24.9	9.9	67.6
SD	70.9	329	0.28	16.3	0.2	98.2

[1] n/a = missing value, unable to calculate
[2] n/a = divergent curve, unable to calculate β
†,‡,¥ = $p < 0.05$ between matched symbols

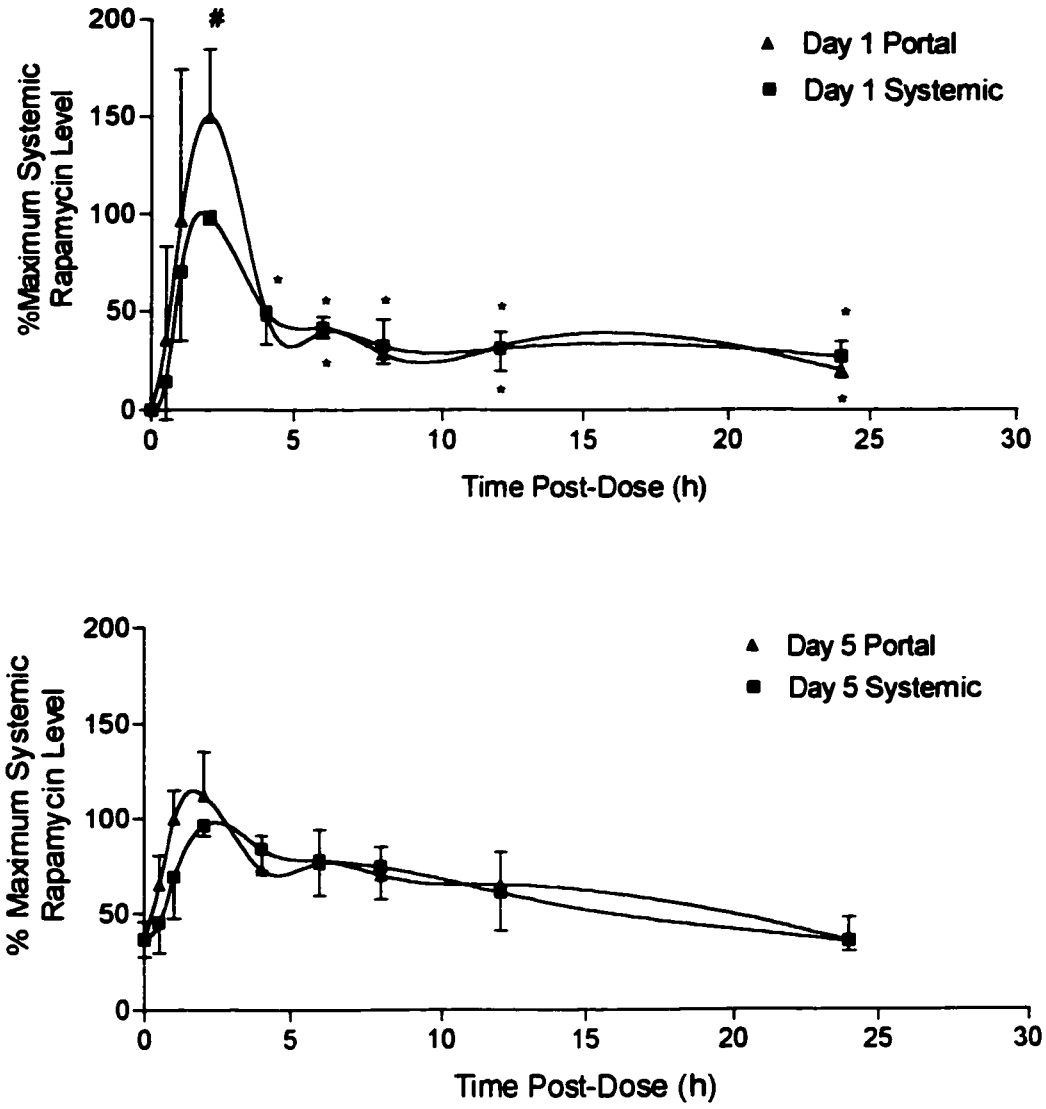

Figure VI-2. Pharmacokinetic profiles of rapamycin in the dog normalised to maximum systemic level.

Acute oral dosing (top) and chronic administration (bottom) is shown. Each point represents the mean +/- SD, n=5.

* $P < 0.05$ compared to the same sample site (portal or systemic) on different days.
# $P < 0.05$ compared to the same day (Day 1) at different sample sites .

Table VI-2 SYSmax Normalised canine rapamycin pharmacokinetic parameters

A. Acute administration, portal sampling

Dog	T1/2β (h)	AUC24 (%*h/L)	Cl/F (L/h*kg)	Vz/F (L/kg)	MRT 24 (h)	MRT inf (h)
1	9.2	1078	2.01	26.7	6.8	10.8
2	29.5	932	1.34	57.0	8.7	37.7
3	34.4	1171	0.87	43.4	9.8	47.5
4	29.3	n/a[1]	1.69	71.4	n/a[1]	38.2
5	147.3	1140	0.31	65.7	9.2	204.4
mean	49.9	1080	1.24	52.8	8.6	67.7
SD	55.3	106	0.67	18.0	1.3	77.6

B. Acute administration, systemic sampling

Dog	T1/2β (h)	AUC24 (%*h/L)	Cl/F (L/h*kg)	Vz/F (L/kg)	MRT 24 (h)	MRT inf (h)
1	10.3	823	2.48	36.8	8.0	13.6
2	n/a[2]	694	n/a[2]	n/a[2]	9.9	n/a[2]
3	36.3	1111	0.83	43.6	10.6	52.0
4	19.1	n/a[1]	2.06	56.7	n/a[1]	24.6
5	46.4	1016	0.77	51.2	10.6	65.9
mean	28.0	911	1.54	47.1	9.8	50.2
SD	16.3	188	0.87	8.7	1.2	49.5

C. Chronic administration, portal sampling

Dog	T1/2β (h)	AUC24 (%*h/L)	Cl/F (L/h*kg)	Vz/F (L/kg)	MRT 24 (h)	MRT inf (h)
1	6.9	1453	1.51	15.0	9.1	12.2
2	16.6	1577	0.95	22.9	10.4	25.4
3	15.2	2022	0.79	17.4	10.2	23.1
4	24.7	1247	1.04	36.9	9.6	33.8
5	16.5	1340	1.21	28.9	9.5	22.8
mean	16.0	1528	1.10	24.2	9.8	23.4
SD	6.3	303	0.27	8.9	0.5	7.7

D. Chronic administration, systemic sampling

Dog	T1/2β (h)	AUC24 (%*h/L)	Cl/F (L/h*kg)	Vz/F (L/kg)	MRT 24 (h)	MRT inf (h)
1	10.7	1667	1.15	17.9	9.7	16.6
2	18.8	1478	0.99	26.7	10.2	27.2
3	12.2	1831	0.97	17.0	10.3	19.4
4	20.5	1258	1.12	33.2	9.9	28.8
5	68.5	1139	0.61	59.9	9.6	91.5
mean	26.1	1475	0.97	30.9	9.9	36.7
SD	24.0	284	0.21	17.5	0.3	31.1

[1] n/a = missing value, unable to calculate
[2] n/a = divergent curve, unable to calculate β

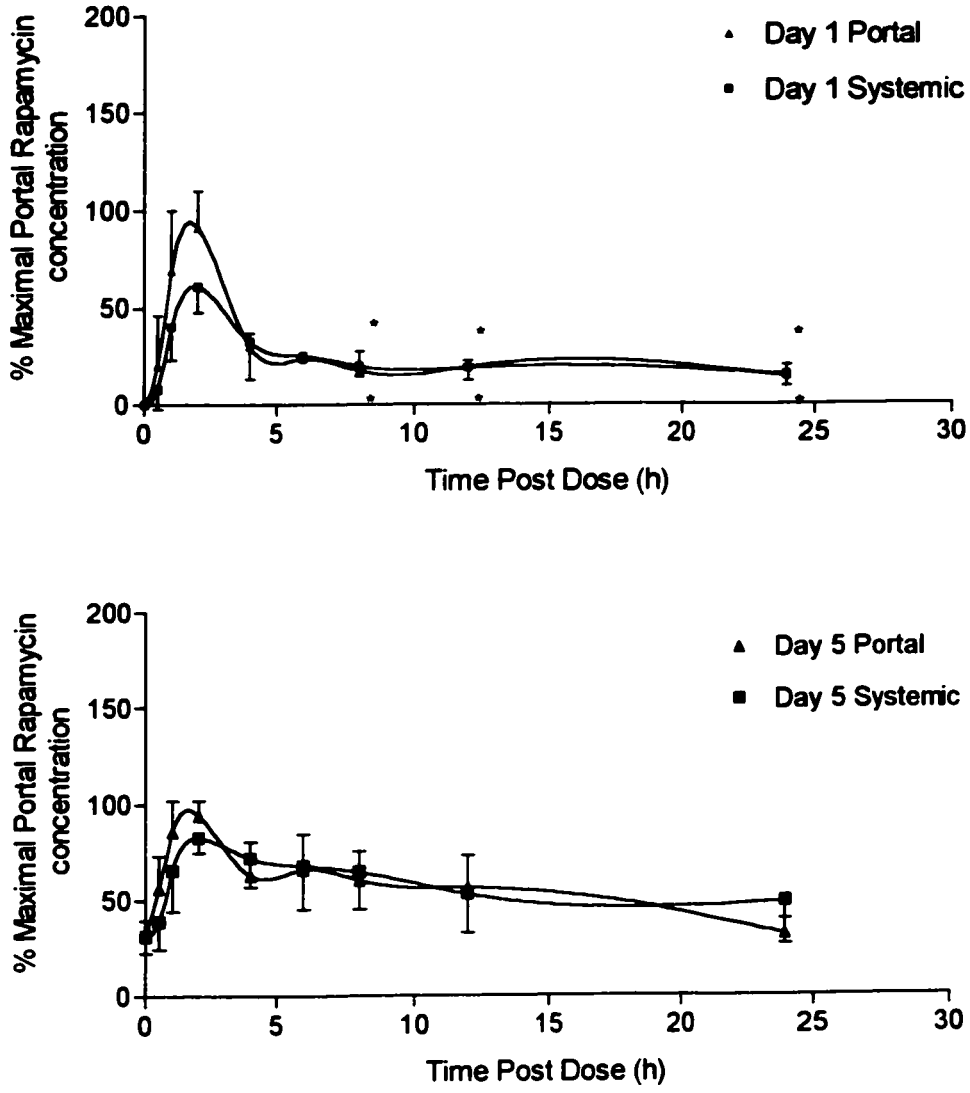

Figure VI-3. Pharmacokinetic profiles of rapamycin in the dog, normalised to maximal portal level.

The PK profiles of acute (top) and chronic (bottom) oral dosing are shown in portal and systemic blood. Each point represents the mean +/- SD, n=5.

* $P < 0.05$ between days

Table VI-3 PORTmax Normalised canine rapamycin pharmacokinetic parameters

A. Acute administration, portal levels

Dog	T1/2β (h)	AUC24 (%*h/L)	Cl/F (L/h*kg)	Vz/F (L/kg)	MRT 24 (h)	MRT inf (h)
1	9.4	588	3.68	49.7	6.8	10.9
2	29.9	544	2.27	97.9	8.8	38.3
3	42.3	368	1.41	86.4	9.8	57.9
4	29.2	n/a[1]	2.00	84.5	n/a[1]	38.1
5	57.1	673	1.10	91.0	9.2	77.5
mean	33.6	543	2.09	81.9†	8.7	44.5
SD	17.7	129	1	18.73	1.3	24.9

B. Acute administration, systemic levels

Dog	T1/2β (h)	AUC24 (%*h/L)	Cl/F (L/h*kg)	Vz/F (L/kg)	MRT 24 (h)	MRT inf (h)
1	10.4	449	4.55	67.8	8.0	13.7
2	n/a[2]	406	n/a[2]	n/a[2]	9.9	n/a[2]
3	36.8	605	1.51	80.4	10.6	52.7
4	19.1	n/a[1]	2.43	67.1	n/a[1]	24.6
5	46.5	601	1.21	86.6	10.6	66.1
mean	28.2	515	2.43	75.5‡	9.8	39.3
SD	16.4	103	1.51	9.6	1.2	24.3

C. Chronic administration, portal levels

Dog	T1/2β (h)	AUC24 (%*h/L)	Cl/F (L/h*kg)	Vz/F (L/kg)	MRT 24 (h)	MRT inf (h)
1	6.9	1532	1.43	14.3	9.1	12.1
2	16.6	1502	1.00	24.0	10.4	25.4
3	15.2	1541	1.01	22.8	10.2	23.0
4	24.7	954	1.36	48.3	9.6	33.8
5	16.5	1083	1.50	35.8	9.5	22.8
mean	16.0	1322	1.26	29.0†	9.8	23.4
SD	6.3	282	0.24	13.2	0.5	7.8

D. Chronic administration, systemic levels

Dog	T1/2β (h)	AUC24 (%*h/L)	Cl/F (L/h*kg)	Vz/F (L/kg)	MRT 24 (h)	MRT inf (h)
1	9.9	1719	1.13	16.3	9.8	15.9
2	18.8	1406	1.04	28.0	10.2	27.2
3	12.1	1411	1.26	22.1	10.2	19.2
4	21.3	977	1.43	44.1	9.7	29.6
5	67.5	921	0.76	73.8	9.6	90.1
mean	25.9	1287	1.12	36.9‡	9.9	36.4
SD	23.7	334	0.25	23.1	0.3	30.5

[1] n/a = missing value, unable to calculate
[2] n/a = divergent curve, unable to calculate β
†,‡ $p < 0.001$ between matched parameter

The SYSmax normalisation resulted in a PK profile that remained similar to the non-normalised curve. There were statistically significant differences in rapamycin blood concentration in the acute versus chronic dosing profile at both portal and systemic sites for the timepoints of 6, 12, and 24h and also between the portal levels for acute vs. chronic dosing at 4 and 8h post dose. Additionally, with the SYSmax normalised results, there was a significant difference between the portal and systemic levels at 2h post dose in the acute dosing profile. However, there were no statistical differences at all in the summarised PK parameters when the different sampling sites or acute versus chronic dosing data were compared.

For the PORTmax PK profile, there were statistical differences in both the portal and systemic levels at 8, 12 and 24h between the acute and chronic periods, but there were no statistical differences between sampling sites in either of the acute and chronic dosing intervals. For the summarised PK parameters, there was a difference in Vz for both systemic and portal sites between the acute and chronic dosing intervals in the PORTmax parameters. There were no statistically different changes when comparing the portal parameters to the systemic parameters in this normalised group.

To compare overall drug exposure and drug exposure during specific sections of the PK profile, AUCs were calculated from the neat and normalised data for various intervals and compared with each other. These results are summarised with the Tmax and Cmax data in Table VI-4. The only statistical differences in Cmax was for the PORTmax normalised data, where a significant difference was shown in Cmax between the portal and systemic sites in the acute interval, and a significant difference in the systemic Cmax between the acute and chronic dosing interval.

There are statistical differences between acute and chronic dosing for AUC24, AUC12 and AUC8 for both the portal and systemic sites for the non-normalised data and for the PORTmax normalised data. There were no statistically significant differences when comparing the

Table VI-4 Canine Rapamycin Area-Under-the-Curve and Cmax.

A. Non-normalised Data

	Tmax (min)[1]	Cmax (μg/L)	AUC 24 (μg*h/L)	AUC 12 (μg*h/L)	AUC 8 (μg*h/L)	AUC 4 (μg*h/L)
Acute Systemic	108 (27)	92 (25)	893 (324)#	516 (181) ¥	393 (127)##	241 (82)
Acute Portal	108 (27)	144 (55)	1055 (343)*	642 (274)#	513 (226)#	341 (156)
Chronic Systemic	144 (91)	134 (16)	1962 (329)#	1193 (157) ¥	836 (85)##	422 (54)
Chronic Portal	96 (33)	158 (34)	2027 (373)*	1225 (174)#	868 (120)#	478 (94)

B. SYSmax Normalised Data

	Cmax (%)	AUC 24 (%*h/L)	AUC 12 (%*h/L)	AUC 8 (%*h/L)	AUC 4 (%*h/L)
Acute Systemic	100 (--)	911 (188)	549 (69)	422 (33)	263 (22)
Acute Portal	165 (27)	1080 (106)	624 (129)	479 (131)	415 (52)
Chronic Systemic	100 (--)	1475 (284)	896 (143)	565 (72)	312 (14)
Chronic Portal	118 (16)	1528 (303)	924 (153)	654 (95)	357 (47)

C. PORTmax Normalised Data

	Cmax (%)	AUC 24 (%*h/L)	AUC 12 (%*h/L)	AUC 8 (%*h/L)	AUC 4 (%*h/L)
Acute Systemic	62 (13)# ¥	526 (89) ‡	337 (71) †	262 (53)#	241 (82)
Acute Portal	100 (--)¥	611 (57) ‡‡	407 (34) ††	315 (22)*	341 (156)
Chronic Systemic	87 (13)#	1287 (334) ‡	785 (188) †	544 (115)#	422 (54)
Chronic Portal	100 (--)	1322 (282) ‡‡	802 (159) ††	564 (92)*	306 (28)

[1] results are expressed as mean (SD), n=5

* $p < 0.05$, # $p < 0.01$, †‡¥ $p < 0.001$ within a parameter, between matched symbols

systemic site with the portal site in a single dosing period for either of the non-normalised or PORTmax normalised AUCs. There was no significant difference in the AUCs of the SYSmax normalised data.

c. Rapamycin metabolite profiles in the dog

Rapamycin metabolites were measured over the dosing interval in two dogs. These results are presented in Figure VI-4 and Figure VI-5. These data demonstrate that the metabolites are present in the following (descending) relative concentrations: over the dosing interval: (C1-C14)-hydroxy > 39-O-demethyl > 16-O-demethyl ≥ (C15-C27)-hydroxy ≥ 27-,39-O-didemethyl

These metabolites were not present before rapamycin was administered, and after the oral dose, increased in concentration in response to the rapamycin level in both portal and systemic blood. The amount of metabolite present in comparison to the amount of rapamycin present was not completely consistent or completely proportional throughout the dosing interval.

The maximal metabolite:parent drug ratio appeared in the acute phase 4 to 6h post dose in both the portal and carotid blood samples. The metabolites were also measured in selected blood samples in all five dogs. The portal 2h and systemic 2h and 8h post dose metabolite levels are presented in Figure VI-6. Significant differences were found between the acute and chronic dosing periods at the portal 2h post-dose timepoint for the levels of the two major metabolites, (C1-C14)-hydroxy and 16-O-demethyl.

There were also significant differences between the portal and carotid levels of these two metabolites at 2h in both acute and chronic dosing periods. Next, two dogs were chosen and Measured Metabolite Ratios were calculated through the entire dosing interval by adding the absolute amounts of the five measured metabolites together and dividing

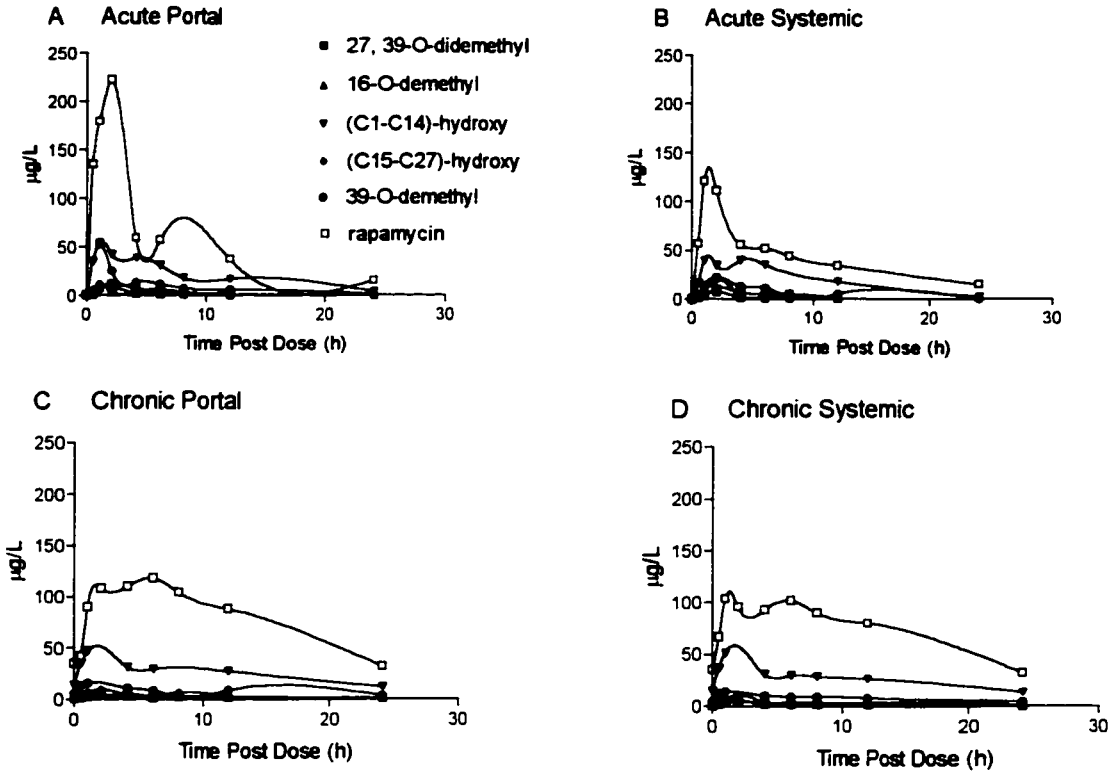

Figure VI-4 Rapamycin metabolites over the dosing interval in dog 1.

Panes A and B represent acute dosing interval profiles.
Panes C and D are from the chronic dosing interval.

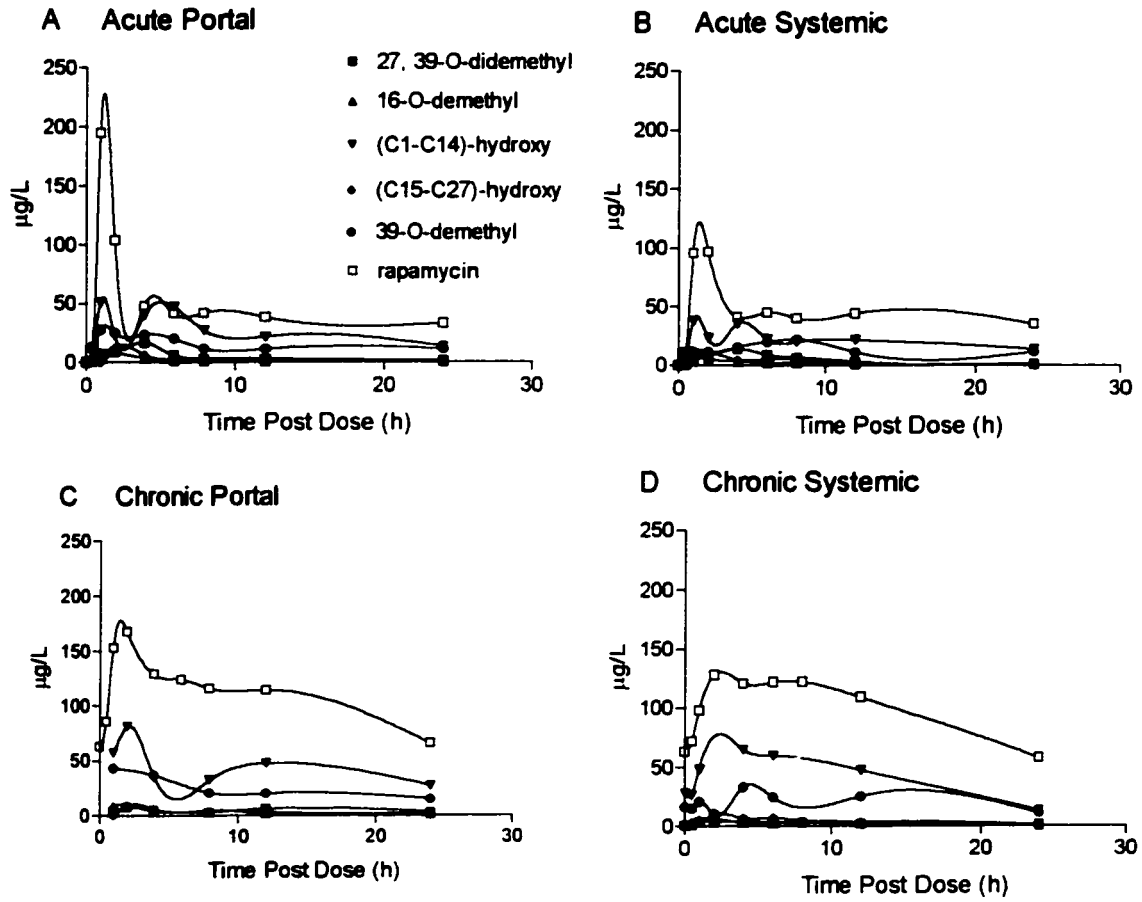

Figure VI-5 Rapamycin and metabolites over the dosing interval in dog 2.

Panes A and B represent acute dosing interval profiles.
Panes C and D are from the chronic dosing interval.

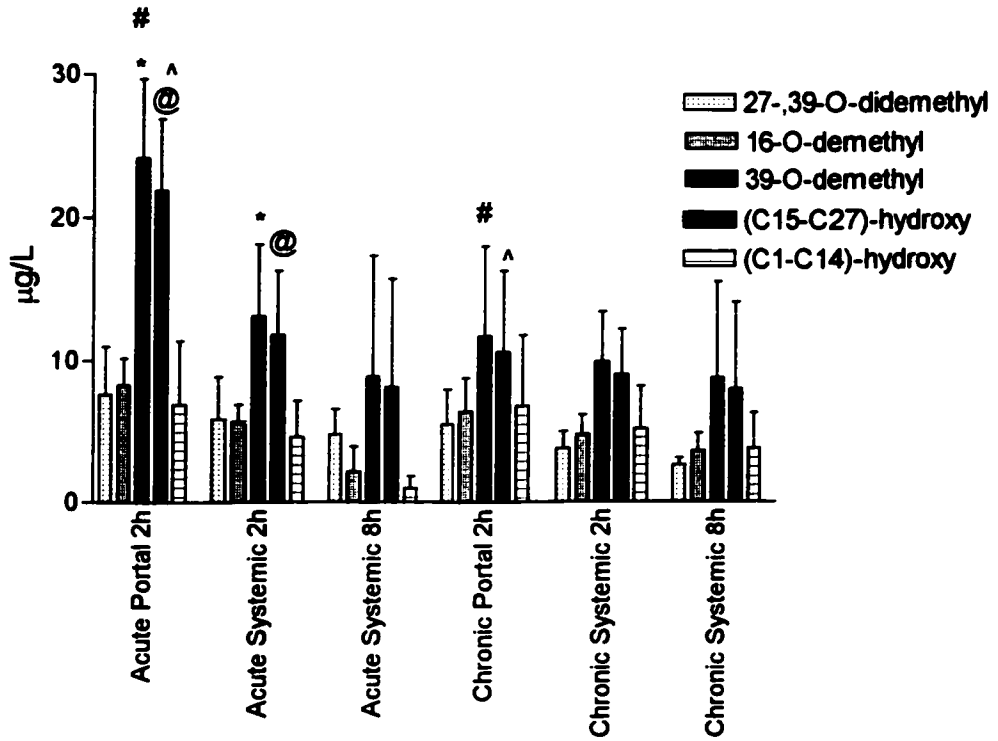

Figure VI-6 Canine rapamycin metabolite levels at 2h and 8h post dose.

Each bar repredents the mean +/- SD, n=5. $p < 0.05$ for matched symbols.

it by the concentration of rapamycin at each timepoint. Figure VI-7 presents the ratio of the measured metabolite to that of parent drug throughout the dosing interval. The ratio of measured metabolite to rapamycin varied from 0.2 to 1.1 in dog 1, and from 0.5 to 2.3 in dog 2. During the acute dosing interval, the ratio is high at 0.5 to 1.0-hours post dose, and drops sharply at 1 to 2-hours post dose at both portal and systemic sites, which subsequently rebounds to very high levels at 4-hours post dose. This is followed by a gradual decline to lower levels at the end of the dosing interval. This is due to the drastic changes in rapamycin levels over the dosing interval rather than the smaller changes in metabolite levels over time.

The ratios for the chronic dosing intervals are somewhat more consistent, varying from 0.5 to 1.3 in dog 1 and only from 0.5 to 0.9 in dog 2. At the start of the chronic dosing interval, the measured metabolite ratio is at or near its maximum, and shows fairly consistent levels through the rest of the dosing interval, without the dramatic drop in ratio at 1 to 2-hours post dose, as observed in the acute dosing interval.

4. DISCUSSION

The process by which the body protects itself from foreign (xenobiotic) substances, including poisons, toxins and drugs, is a multi-step, dynamic process[2]. After oral exposure to a foreign substance, the substance may be absorbed by the small intestine. The intestine in the first barrier to the uptake of xenobiotics. The foreign substance must first withstand digestive processes, then pass from within the lumen of the intestine into the enterocytes that line the gut. Here it is subjected to exclusion from the enterocyte by p-glycoprotein (p-gp), a 170 kDa apical surface protein that "pumps" a wide array of xenobiotics from the cell. If the concentration gradient is sufficient to exceed the luminal velocity of p-gp, the xenobiotic will remain in the enterocyte for a short period of time before exiting the cell

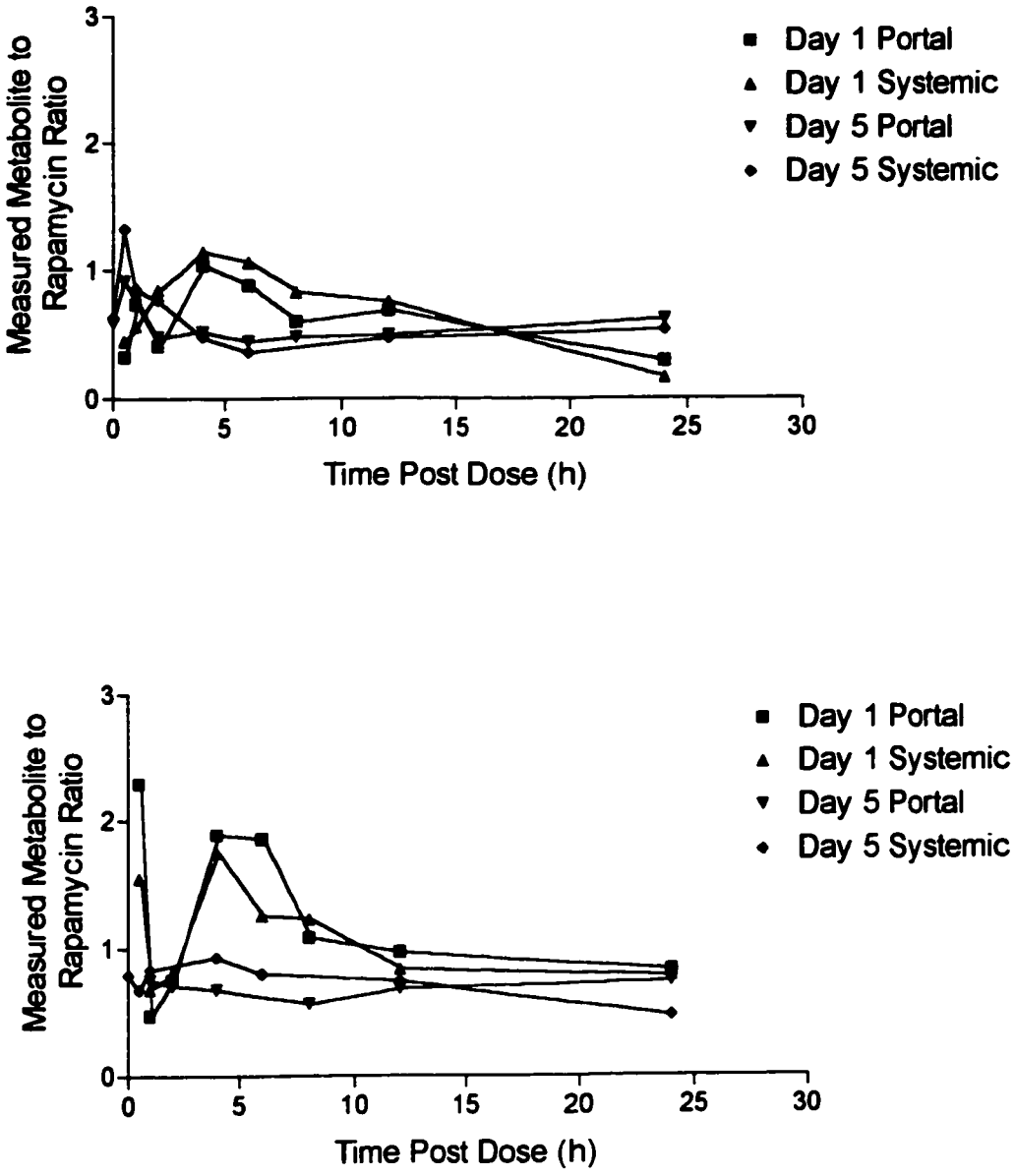

Figure VI-7 Measured rapamycin metabolite ratios in the acute and chronic dosing intervals in the dog. Panels A and B are two different dogs receiving 2.5 mg/kg/d oral rapamycin.

basolaterally, toward the muscularis mucosa, the mesentic capillaries and the lymphatic ducts. While within the enterocyte, it is a potential substrate for a series of enzymes, including CYP enzymes, that are responsible for the metabolism or biotransformation of many xenobiotics.

There is significant overlap in substrate specificity between p-gp and CYP enzymes, presumably for the purpose of maximizing the detoxification and exclusion of foreign substances that are ingested before they can reach the systemic circulation. If the foreign substance is able to make it through the intestinal barrier intact, it passes into the blood in the mesenteric capillaries and into the portal vein and will go directly to the liver. The liver is the second barrier to xenobiotics and is a major site of CYP expression and other metabolic and catabolic enzyme expression. It is responsible for a large amount of xenobiotic biotransformation and excretion of parent drug and metabolites into the bile. Thus, before the xenobiotic reaches the systemic circulation, it is subjected to two rounds of metabolism and excretion processes: first in the intestine, second liver. Together, the intestinal and hepatic processes described here are referred to the first pass extraction phenomenon, which minimises the amount of xenobiotic drug passing into the peripheral circulation.

The first pass phenomenon may be relevant to rapamycin for several reasons. Rapamycin is a p-gp substrate[3]. Rapamycin is also a CYP 3A4 substrate, and is metabolised *in vitro* by microsomes isolated from human intestine and liver[4]. The degree of metabolism and relative importance of both the liver and intestine in the *in vivo* metabolism of rapamycin are not known. It was desirable, therefore, to study the differences in portal and systemic PK in an experimental animal model.

The study of immunosuppressant delivery to and extraction by individual organs is a poorly studied process. There have been relatively few studies examining systemic and portal blood levels. One study investigated the effect of erythromycin on hepatic CsA metabolism

in the pig by sampling portal venous and jugular venous blood[5]. Another illustrated the increased pre-hepatic PK of the Sandimmune formulation of CsA in a single dose canine study[6]. Neither study provided detailed PK descriptions of drug metabolite behaviour, and to date there have been no studies investigating rapamycin in this manner.

In the current study, the differences found in the acute and chronic dosing intervals indicate that changes have occurred in the dog that affect volume of distribution. Presumably, the changes in rapamycin distribution occur significantly between the acute and chronic dosing periods because of the large number of tissue binding sites that are available at first exposure, but are unavailable at steady state. This is not surprising, as the acute dose is introduced into the body of a subject without prior drug exposure. Presumably the vascular, intrastitial and tissue binding sites for the drug would be fully available to bind rapamycin for the initial, acute dose. Later, after steady state is achieved, some (or most) of the tissue sites would be occupied, causing a new dose of rapamycin to be retained to a greater degree in the vascular compartment rather than dissipating into the tissues. The large apparent Vz indicate that rapamycin is widely distributed in this model, which agrees with data published examining the PK parameters of several other models.

Detailed pharmacokinetic investigations of rapamycin in the monkey, rabbit, and rat have been previously reviewed[7]. In general, rapamycin had a $t_{1/2}$ of > 9.5 h in all animal species tested, except for one study with monkeys which found a $t_{1/2}$ of 5.6 h after oral dosing. In the present study, $t_{1/2}\beta$ was long, varying from an average of 44.5 to 48.0 h in systemic blood, and from 15.1 to 34.1 h in portal blood. This may be a reason why the dog is a model that is very sensitive to immunosuppressive agent toxicity.

Rapamycin is rapidly absorbed in all these models. The volume of distribution found in the rat (10.8 L/kg) and rabbit (2.56 L/kg) indicated that a substantial proportion of the drug distributes into extravascular tissue. However, there was considerable variability between

the animal models used and between the routes of administration. In addition, a recent study indicated that rapamycin is unstable *in vitro* in both whole blood and plasma at 37°C and that the instability was different for the various species tested[8]. This instability could account for up to 13% of the clearance of the drug in rabbits, 90% in rats, and 36% in humans if the blood specimens are not stored at 4°C or frozen rapidly after collection[8].

One parameter that we were unable to examine in this experiment was bioavailability (F). Because we did not compare the PK profiles of an oral dose to the profile of an intraveneous (IV) dose, there is no way to estimate bioavailability, which factors into the calculations for Vz and clearance. This may have introduced another degree of variability into the experiment, as the bioavailability of rapamycin is low and variable in both the human and rabbit[7, 9].

The relatively few pairs of PK parameters in non-normalised data for the current study that show statistical difference may be partly due to the large degree of inter-subject variability exhibited in these dogs, as evident in the large standard deviations in the calculated parameters. This could be addressed by using a single breed of dogs rather than mongrels, or by increasing the sample size.

The lack of differences found between the portal and systemic blood levels of rapamycin in the absorptive phase was surprising. It was expected that there would be a statistical difference in most portal versus systemic blood levels up to the late elimination phase and steady state samples; in volume of distribution; clearance; and possibly short term AUC. Because the liver is physically situated between the gut and the rest of the body, it receives nutrients and other substances as absorbed before the rest of the body. This is accomplished by the closed flow of blood from the intestines through the mesenteric veins to the portal vein[10]. The portal vein is joined by the gastro-duodenal vein and the splenic vein, which carries blood to the liver from the spleen and accounts for approximately 25% of the

bloodflow through the portal vein. The mesenteric flow accounts for approximately 75%. In the dog, the spleen also acts as a point of sequestration of blood cells, that can be mobilised by adrenergic stimulation for rapid release into the bloodstream, through the splenic vein[11]. Unfortunately, in this experiment, the portal catheters were situated in the portal vein proximal to the point of connection of the splenic vein. This may have produced lower than expected results in some of the portal samples by way of dilution if the animal was agitated, resulting in a blunted peak in the absorptive phase. Additionally, this is also an extremely difficult model to maintain, with significant sources of variation possibly arising from difficulties in blood sampling, catheter maintenance and the agitationcaused by these procedures during the experiments.

It was predicted that normalisation of the blood levels would mitigate inter-subject variability in absolute absorbance and distribution of drug during the dosing interval, and permit observation of subtle or masked differences in rapamycin concentration and calculated PK parameters. Two normalisation procedures were done to further elucidate the source of the variation. As the SYSmax normalisation resulted in calculated PK parameters without statistical differences between acute and chronic dosing and portal and systemic blood levels, the normalisation process had the opposite of the anticipated effect. It was hoped that if variability in drug absorption and first-pass metabolism could be accounted for, the differences between portal and systemic drug levels and drug exposure over time would be accentuated. In this normalisation model, the difference in portal and systemic blood levels was significant only at 2 hours post dose ($p < 0.05$), but not at Cmax, which occurred at an average of 108 minutes after the acute dose for both the portal and systemic sites, and at 96 and 144 min after the chronic dose for the portal and systemic sites, respectively. The SYSmax normalisation also resulted in the loss of significant differences in all AUC and calculated PK parameters. The net effect of the SYSmax normalisation was to make the data more uniform, by accounting for variability that was introduced by the pre-systemic compartments, the intestine and liver.

In the PORTmax normalised data, significant differences were found in the PK parameters for Vz of both portal and systemic analyses between acute and chronic dosing. The significant differences were restored to the AUC profile at 8, 12 and 24h post-dose at both sites when comparing the acute and chronic dosing intervals. Also, there is a significant difference in Cmax that is newly identified between the systemic data for acute vs chronic dosing, and also between the portal and systemic sites in the acute dosing interval. This suggests two things. For the acute dose, the relative maximum concentration of rapamycin that reaches the liver is higher than that which reaches the periphery. Also, there is significant contribution of the liver via extraction which decrease rapamycin concentration in the blood going into the systemic circulation. Dilution into the blood and uptake into the peripheral tissues accounts for part of this decrease in rapamycin as it passes across the liver. This illustrates that the liver plays an important role in the metabolism and excretion of rapamycin as part of the first-pass effect, with particular relevance to acute, high level rapamycin exposure.

It is important that relationships between the two sampling compartments changed differentially depending on how the data was normalised. This suggests that there are multiple factors involved in the metabolic processes and dispositional activity affecting an oral dose of rapamycin. There are pre-hepatic, hepatic and post-hepatic activities all impacting the shape of the time-concentration curve as well as the magnitude of the maximal concentration.

By normalising blood levels to SYSmax, this accounts for variability in the magnitude of pre-hepatic as well as hepatic processes. This permits differences to be seen in the 2h post dose levels, but loss of statistical difference in the AUC and Vz. By normalising blood levels to PORTmax, this accounts for variability in the magnitude of pre-hepatic processes only. This permits differences to be seen in Cmax , shorter AUCs and Vz. The effect of the

normalisation was generally to decrease the size of the standard deviation, to facilitate achievement of statistical difference in this small group of subjects. This indicates that the normalisation procedure was at least partially effective.

The rapamycin metabolite levels in the dog show a similar profile to that demonstrated in humans[12]. Here, (C15-C27)-hydroxy and 16-O-demethyl comprise ~50% of the trough rapamycin level and a larger proportion of the carotid 8 hour sample post dose, but a smaller proportion of carotid 2 hour sample. It appears that there is less metabolite present in the chronically dosed portal blood samples perhaps indicating a more efficient excretion process for these metabolites from the enterocyte back into the intestinal lumen, for example, by p-gp. Rapamycin metabolites have not been tested directly as p-gp substrates. There are other possibilities, including an inhibition of pre-hepatic metabolic process in the intestinal wall. For example, CYP inhibition by auto- or competitive substrate binding, negative feedback, or down regulation of CYP expression by rapamycin or rapamycin metabolites could be occurring in this model.

Overall, there are lower levels of rapamycin metabolites present in the systemic circulation versus the portal circulation in the acute dosing interval, which is evident by the significant difference in the two major metabolites at 2 hours. This is likely due to hepatic factors, such as an efficient process of biliary excretion of rapamycin metabolites, perhaps coupled with the effect of enterohepatic circulation in the intestinal uptake and re-circulation of excreted rapamycin metabolites from the gut lumen into the portal circulation. This may portray a minimal role for the liver metabolic enzymes in formation of rapamycin metabolites that circulate in body.

Clinical liver transplantation demonstrates a one-year patient survival of 93% and graft survival of 90% in a non-emergency setting[13]. The recent improvement in liver transplant success is obviously multi-factoral. Surgical advances; the use of more complex

combinations, though lower amounts of individual immunosuppressants; the relatively high regenerative capacity of the liver and its relative resistance to antibody-mediated rejection; and the exposure of the liver to high post-dose drug levels may all contribute to excellent graft survival. The low incidence of chronic rejection may be due to increased dug exposure, or due to the elasticity of the liver to recover from injury. As chronic rejection is not well understood, and in the kidney the phenomenon of chronic rejection is thought to be linked not only with early rejection episodes but also with CsA nephrotoxicity, this is an extremely hard issue to address. Unlike the kidney[14], long-term outcome in liver transplantation is not correlated with early graft injury[15, 16]. The lack of appropriate animal models for development and study of chronic rejection contributes to the lack of knowledge in this area.

Because of the success of liver transplantation and the relatively low target or achieved levels of immunosuppressants required to maintain a liver graft rejection-free, compared to other solid organ transplant types[17], the hypothesis was that a higher Cmax and increased AUC in the time zero to 4-hour period would contribute to the relative immunopriviledge enjoyed by this site. The practices of abbreviated-AUC monitoring and peak or 2-hour post dose monitoring may speak to this issue. Where traditional trough level monitoring of immunosuppressives has been done to ensure adequate levels, some investigators choose to use multiple timepoint monitoring to evaluate drug exposure[18]. The sampling of trough, 2h and 4 or 6h post dose drug levels in CsA Neoral dosed liver transplant patients permits the construction of a peak exposure profile that correlates more strongly with overall drug exposure[18, 19]. The mini-AUC may have a more direct relationship with improved graft survival, avoidance of rejection and positive patient outcome than trough level monitoring, which does not always closely correlate with AUC. This has also been investigated in liver transplantation with tacrolimus treatment[18, 20]. With CsA and tacrolimus, this monitoring technique may therefore insure adequate peak level exposure to immunosuppressive agent, and therefore promote graft survival. The relevance of mini-AUC modelling may be less

important in rapamycin therapy, as in the current study, the shorter AUCs were not augmented at the portal site.

Another reason to consider peak portal levels is related to pancreatic islet transplantation. This technique involves embolisation of isolated islets into the preferred site: the liver via the portal vein[18]. The islets are therefore exposed to the very high levels of immunosuppression that are discussed here. Islets, however, are much more sensitive than hepatocytes, and do not posses the same regenerative capacity or resistance. In the past, immunosuppression with CsA for islet transplants was not associated with prolonged functioning islet grafting, whereas graft survival for pancreas transplants is much higher with similar immunosuppressive regimens[21].

Not only are CsA and tacrolimus very toxic to islets *in vivo* and *in vitro*[22, 23], but oral dosing of CsA produces surprisingly high portal levels that are within the range of concentrations that produce destruction of these islet cells[24]. In a previous study, portal/carotid PK were investigated using CsA in these dogs, and showed portal Cmax was significantly higher than systemic Cmax, as was portal AUC4. However, there was not a significant difference in the portal and systemic AUC12. This illustrates that while CsA exposure over the entire dosing interval is similar, higher peak levels and mini-AUC augmentation in the portal blood is relevant and important to immunosuppressive and toxic processes within the liver. Perhaps the liver plays a larger role in the absorptive phase of the CsA dosing interval, but a greater role in the distribution phase of rapamycin dosing.

The current study indicates that rapamycin provides for adequate drug exposure over the dosing interval without dramatic differences in the short-term AUC of the portal and systemic circulation. It may be more suitable for use with islet transplantation than other more potentially toxic immunosuppressives that have different portal-systemic PK relationships.

5. REFERENCES

1. O'Brien D, Semple H, Molnar G. A chronic conscious dog model for direct transhepatic studies in normal and pancreatic islet cell transplanted dogs. J Pharm Methods 1991; 25:157-70.

2. Hall SD, Thummel KE, Watkins PB *et al.* Molecular and physical mechanisms of first-pass extraction. Drug Metab Dispos 1999; 27:161-6.

3. Yacyshyn BR, Bowen-Yacyshyn MB, Pilarski LM. Inhibition by rapamycin of P-glycoprotein 170-mediated export from normal lymphocytes. Scan J Immunol 1996; 43:449-55.

4. Sattler M, Guengerich FP, Yun C-H, Christians U, Sewing K-F. Cytochrome P-450 enzymes are responsible for biotransformation of FK506 and rapamycin in man and rat. Drug Met Dispos 1992; 20:753-61.

5. Freeman DJ, Grant DR, Carruthers SG. The cyclosporin-erythromycin interaction: impaired first pass metabolism in the pig. Br J Pharmacol 1991; 103:1709-12.

6. Gridelli B, Scanlon L, Pellicci R *et al.* Cyclosporine metabolism and pharmacokinetics following intraveneous and oral administration in the dog. Transplantation 1986; 52:388-91.

7. Yatscoff RW, Wang P, Chan K, Hicks D, Zimmerman J. Rapamycin: distribution, pharmacokinetics and therapeutic range investigations. Ther Drug Monit 1995; 17:666-71.

8. Ferron GM, Jusko WJ. Species differences in sirolimus stability in humans, rabbits and rats. Drug Met Dispos 1998; 26:83-4.

9. Ferron GM, Mishina EV, Zimmerman JJ, Jusko WP. Population pharmacokinetics of sirolimus in kidney transplant patients. Clin Pharmacol Ther 1997; 61:416-28.

10. Kalt DJ, Stump JE. Gross anatomy of the canine portal vein. Anat Histol Embryol 1993; 22:191-7.

11. Hoit BD, Gabel M, Fowler NO. Influence of splenectomy on hemodynamics during cardiac tamponade. Am J Physiol 1991; 261:R907-R911.

12. Streit F, Christians U, Schiebel H-M *et al.* Sensitive and specific quantification of sirolimus (rapamycin) and its metabolites in blood of kidney graft recipients by HPLC/electrospray-mass spectrometry. Clin Chem 1996; 42:1417-25.

13. Terasaki P. Clinical Transplants. UNOS 1993.

14. Theodorakis J, Schneeberger H, Illner WD, Stangl M, Zanker B, Land W. Aggressive treatment of the first rejection episode using first-line anti-lymphocyte preparation reduces further acuter rejection episodes after human kidney transplantation. Transpl Int 1998; 11:S86-S89.

15. Knechtle SJ. Rejectin of the liver transplant. Semin Gastrointest Dis 1998; (9):126-35.

16. Klopmaker LI, Gouw AS, Haagsma EB *et al.* Selective treatment of early acute rejection after lever transplantation: effects on liver, infection rate and outcome. Transpl Int 1997; 10:40.

17. Oellerich M, Armstrong VW, Schutz E, Shaw LM. Therapeutic drug monitoring of cyclosporine and tacrolimus. Clin Biochem 1998; 31:309-16.

18. Dumont RJ, Ensom MH. Methods for clinical monitoring of cyclosporin in transplant patients. Clin Pharmacokinet 2000; 38:427-47.

19. Levy GA. Neoral use in the liver transplant recipient. Transplant Proc 2000; 32:2S-9S.

20. Ku YM, Min DI. An abbreviated area-under the curve monitoring for tacrolimus with liver transplant patients. Ther Drug Monit 1998; 20:216-23.

21. Robertson RP, Davis C, Larsen J, Stratta R, Sutherland DE. Pancreas and islet transplantation for patients with diabetes. Diabetes Care 2000; 23:112-6.

22. Helmchen U, Schmidt W, Siegel E, Creutzfeldt W. Morphological and functional changes of pancreatic B cells in cyclosporine A-treated rats. Diabetologia 1984; 27:416-8.

23. Nielsen J, Mandrup-Poulsen T, Nerup J. Direct effects of cyclosporine A on human pancreatic beta-cells. Diabetes 1986; 35:1049-52.

24. Shapiro AMJ, Gallant HL, Hao EG, Wong J, *et al.* Portal vein immunosuppressant levels and islet graft toxicity. Transplant Proc 1998; 30:641.

VII. RAPAMYCIN PKS AND STEADY STATE METABOLITE LEVELS IN LIVER TRANSPLANT PATIENTS

1. RATIONALE

The importance of rapamycin metabolites in the transplant patient is dependent on their relative activities in context with their concentrations at steady state and throughout the dosing interval. To date, PK studies have only been conducted in healthy volunteers and in renal transplant patients. The PK behaviour of rapamycin and its metabolites metabolites in liver transplant recipients is not known and was investigated in five compassionate release patients. Steady state levels of rapamycin and its metabolites were investigated in 14 liver transplant recipients.

2. MATERIALS AND METHODS

a. Source of drugs and metabolites

Rapamycin oral formulation (non-aqueous liquid) was provided by Wyeth-Ayerst Inc. (Montréal, Canada) under a compassionate release protocol. Rapamycin powder and DMR , for use in the analytical laboratory, were also provided by Wyeth-Ayerst (Princeton, NJ). Rapamycin metabolites were generated and isolated in our laboratory as described in Chapter 2.

b. Patient samples

Six patients were part of a preclinical compassionate release program for CsA or tacrolimus treatment failure. They were converted to rapamycin oral therapy for prophylaxis of liver transplant rejection. On the date of conversion, patients received a loading dose of 15 mg, which was reduced to 8 mg per day thereafter.

On the day of conversion, the patient was fasted overnight and a pre-dose specimen taken. The patient was given the rapamycin oral liquid diluted in orange juice or milk. Blood samples were drawn at 0.5, 1.0, 2.0, 4.0, 8.0, 12 and 24 hours post-dose to construct the PK profile. A

repeat profile was done on day 5 post-conversion to investigate changes in the PK parameters. Periodic trough level monitoring of these patients was also conducted.

Blood was drawn into EDTA-containing tubes, stored at 4°C and analysed for rapamycin parent within three days of collection. Blood was then frozen at –70°C until analysed for rapamycin metabolites within 2 years.

c. Rapamycin and metabolite concentration determination

Rapamycin was determined using the HPLC-UV method described in Chapter 2. Rapamycin metabolites were measured using the HPLC-MS method described in Chapter 2.

d. PK and statistical calculations

PK parameters were calculated using Win-Nonlin v.1.0, Standard edition. A non-compartmental model was used, with the linear trapezoidal rule for AUC calculation and uniform weighting throughout. The analysis and PK parameters are described in more detail in Chapter IV. Statistical analysis was conducted to demonstrate differences between acute and chronic dosing, for the PK parameters and drug and metabolite blood levels. This was done using Wilcoxon signed rank test. Prism Graph Pad software was used for graphing and statistical calculation. A p statistic of less than 0.05 was considered statistically significant.

3. RESULTS

a. Rapamycin PKs in liver transplant patients

Five of the six patients completed the PK study without adverse event. In the sixth patient, a dose of 50 mg was inadvertently given on the day of conversion. For that reason, this patient was excluded from this analysis.

The PK profiles of rapamycin in liver transplant patients on day 1 (acute) and day 5 (chronic) post conversion are presented in Figure VII-1. The acute profile shows a sharp rise in

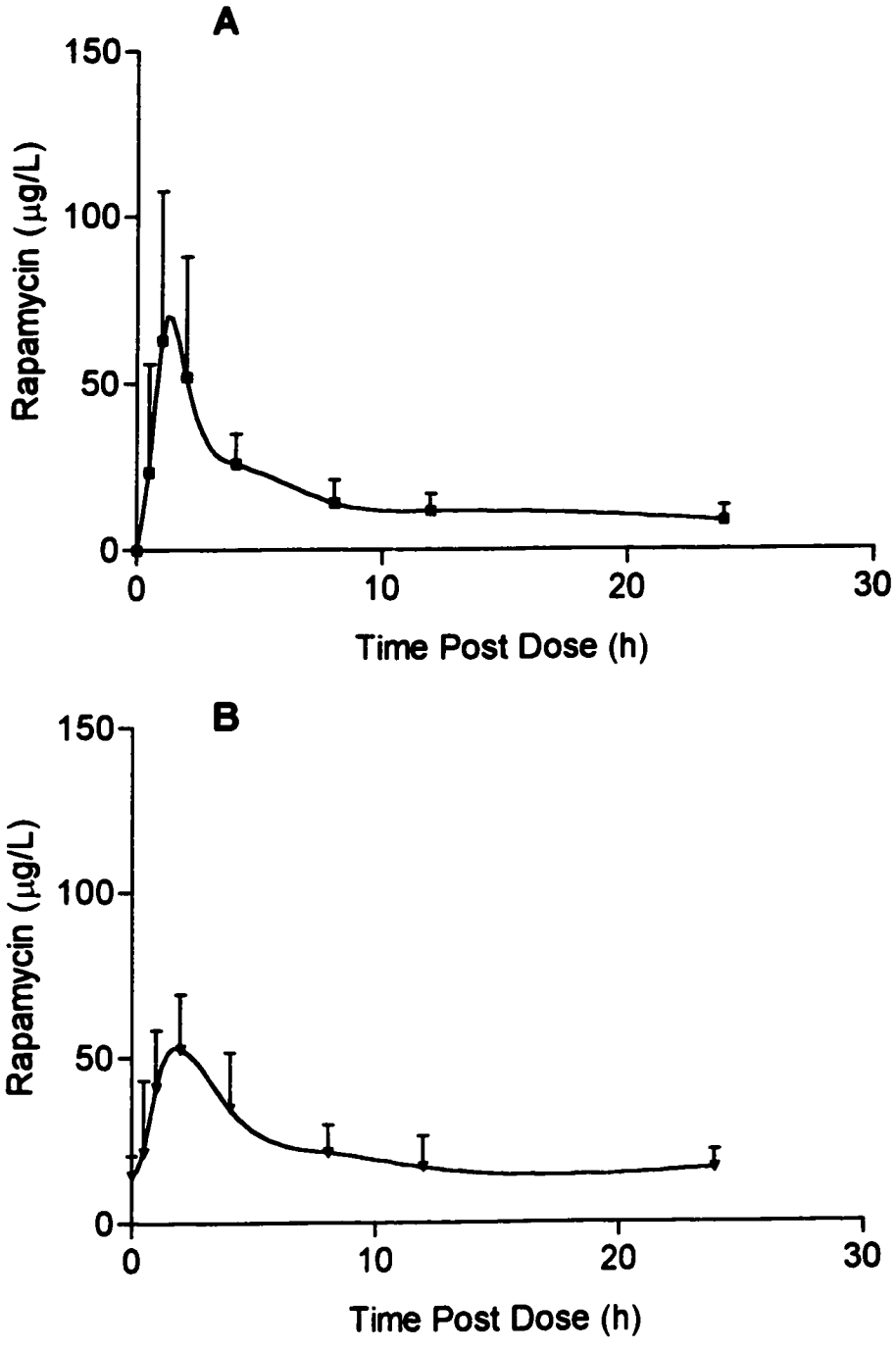

Figure VII-1 Rapamycin pharmacokinetics in liver transplant patients.

Panel A depicts the acute (Day 1) dosing period. Panel B depicts the chronic (Day 5) dosing period. Each point represents mean +/- SD, n=5.

concentration to Cmax, and a bi-modal elimination phase that extends to the end of the dosing interval. The chronic profile is similar, but with a blunted rise to Cmax. There were no significant differences at any of the timepoints post-dose between the acute and chronic dosing periods.

The summary of the PK parameters is presented in Table VII-1. There were no significant differences when comparing the acute and chronic PK parameters.

Each concentration-versus-time profile was also dose corrected and replotted. The averaged dose-corrected PK profile is presented in Figure VII-2. The corrected plots for the acute and chronic dosing intervals are very similar. There are no significant differences at any timepoints between the acute and chronic dosing periods.

b. Rapamycin metabolite levels in liver transplant patients

The mean concentrations of rapamycin and five metabolites were determined over the acute and chronic dosing intervals, and are presented in Figure VII-3. In the acute dosing interval, the peak level of metabolites was reached between 30 minutes and 2h after the oral dose. The relative abundance of the metabolites throughout the profile was generally: (C1-C14)-hydroxy > (C15-C27)-hydroxy ≥ 16-O-demethyl ≥ 39-O-demethyl > 27-,39-O didemethyl. In the chronic dosing interval, peak levels of metabolite were reached at approximately 4h after the oral dose. The abundance of the metabolites throughout the chronic profile was similar to the acute profile: (C1-C14)-hydroxy > (C15-C27)-hydroxy ≥ 39-O-demethyl ≥ 16-O-demethyl > 27-,39-O didemethyl.

The proportions of individual metabolite to parent drug over the acute and chronic dosing interval were calculated and are presented in Figure VII-4. In the acute profile, the ratio of individual metabolite to rapamycin tended to rise over the dosing interval. In the chronic profile,

Table VII-1 Human PK parameter summary, rapamycin oral dose in liver transplant patients

A. Acute interval, 15 mg loading dose

subject	T1/2β (h)	AUC24 (μg*h/L)	Cl/F (L/hr*kg)	Vz/F (L/kg)	MRT (h)	Cmax (μg/L)	Tmax (min)
1	50.1	634	5.2	379	8.0	110	60
2	13.0	535	8.5	160	7.0	88	60
3	47.5	246	12.2	834	10.4	22	232
4	56.6	632	3.5	285	9.5	66	60
5	8.9	--	55.6	714	4.2	45	90
mean	35.2	512	17	474	7.8	66	100
SD	22.4	183	22	287	2.4	35	75
population	24.2	419	20.7	721	8.1	96	60

B. Chronic interval, 8 mg dose

subject	T1/2β (h)	AUC24 (μg*h/L)	Cl/F (L/hr*kg)	Vz/F (L/kg)	MRT (h)	Cmax (μg/L)	Tmax (min)
1	15.3	434	12.5	301	9.8	40	120
2	30.6	817	3.4	149	9.6	77	120
3	42.7	357	7.7	495	9.6	46	120
4	56.6	632	3.5	285	9.5	66	60
5	15.4	653	8.5	189	8.9	66	240
mean	32.1	579	7	284	9.5	59	132
SD	17.9	184	4	134	0.3	15	66
population	52.8	552	2.8	210	9.7	53	120

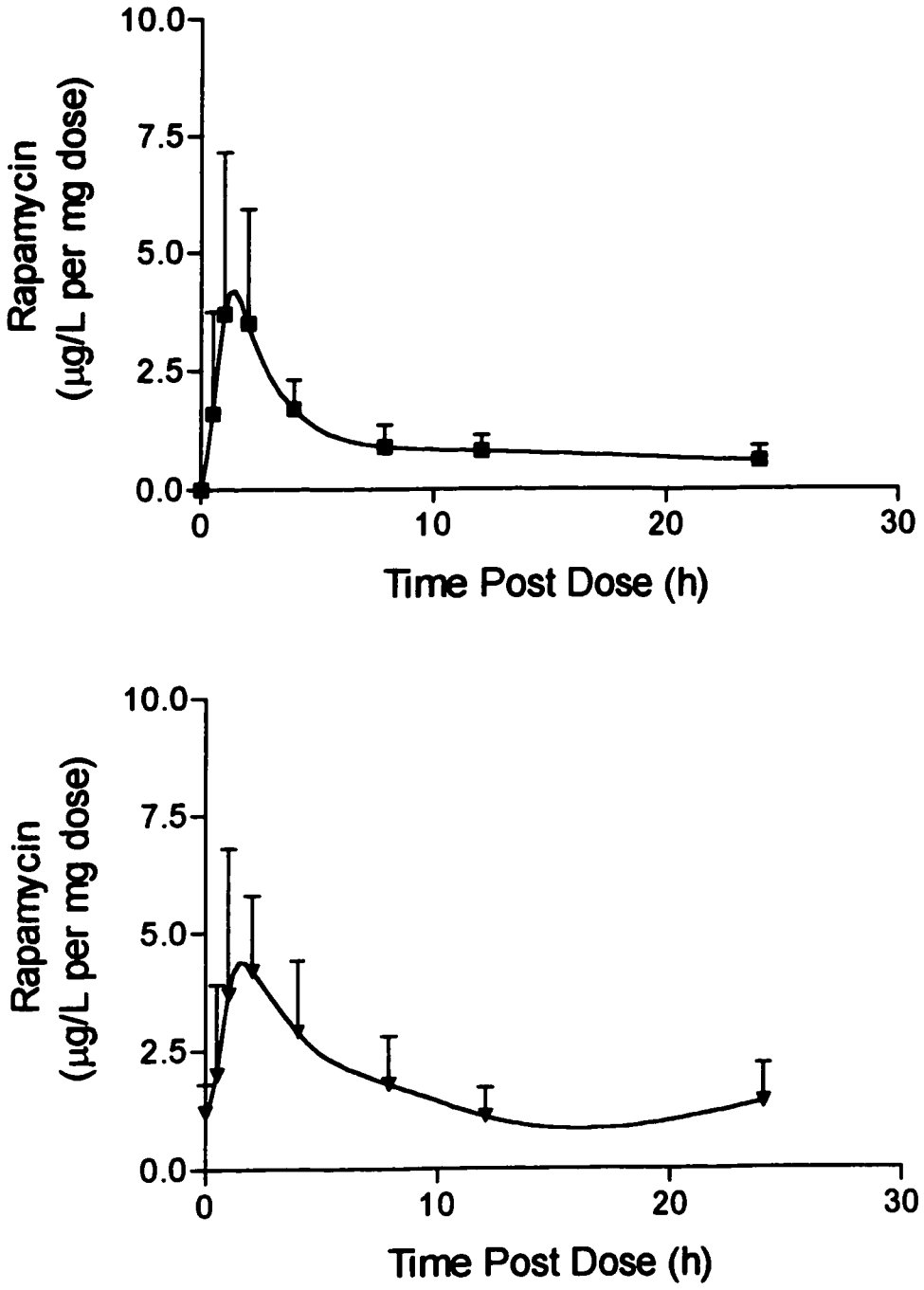

Figure VII-2 Dose corrected rapamycin pharmacokinetic profile in liver transplant patients.

The top panel depicts the acute (Day 1) dosing period, the bottom panel the chronic (Day 5) dosing period. Each point represents mean +/- SD, n=5.

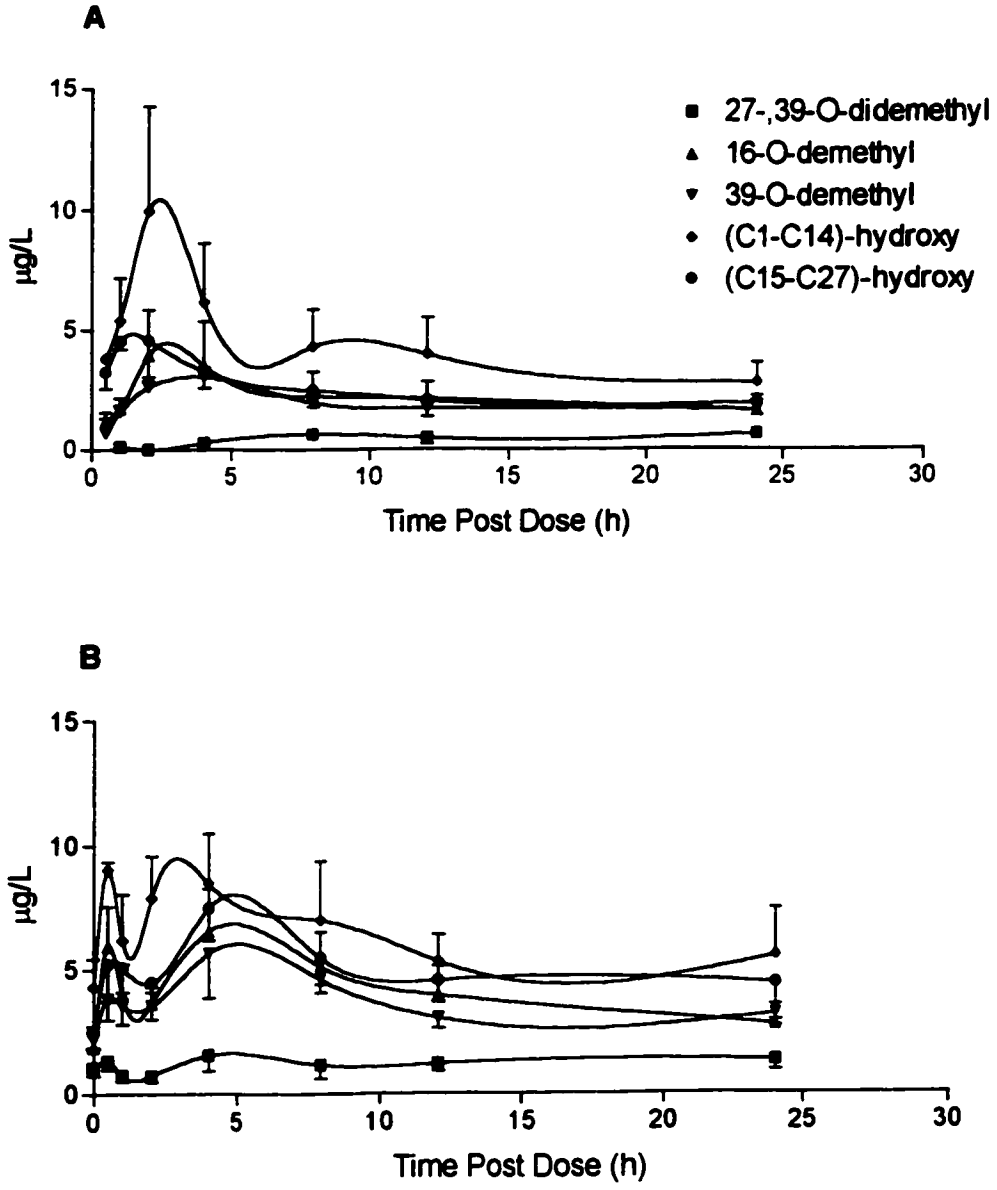

Figure VII-3 Rapamycin metabolite levels in liver transplant patients.

Panel A is the acute dosing interval, panel B is the Chronic dosing interval. Each point represents mean +/- SEM, n=5.

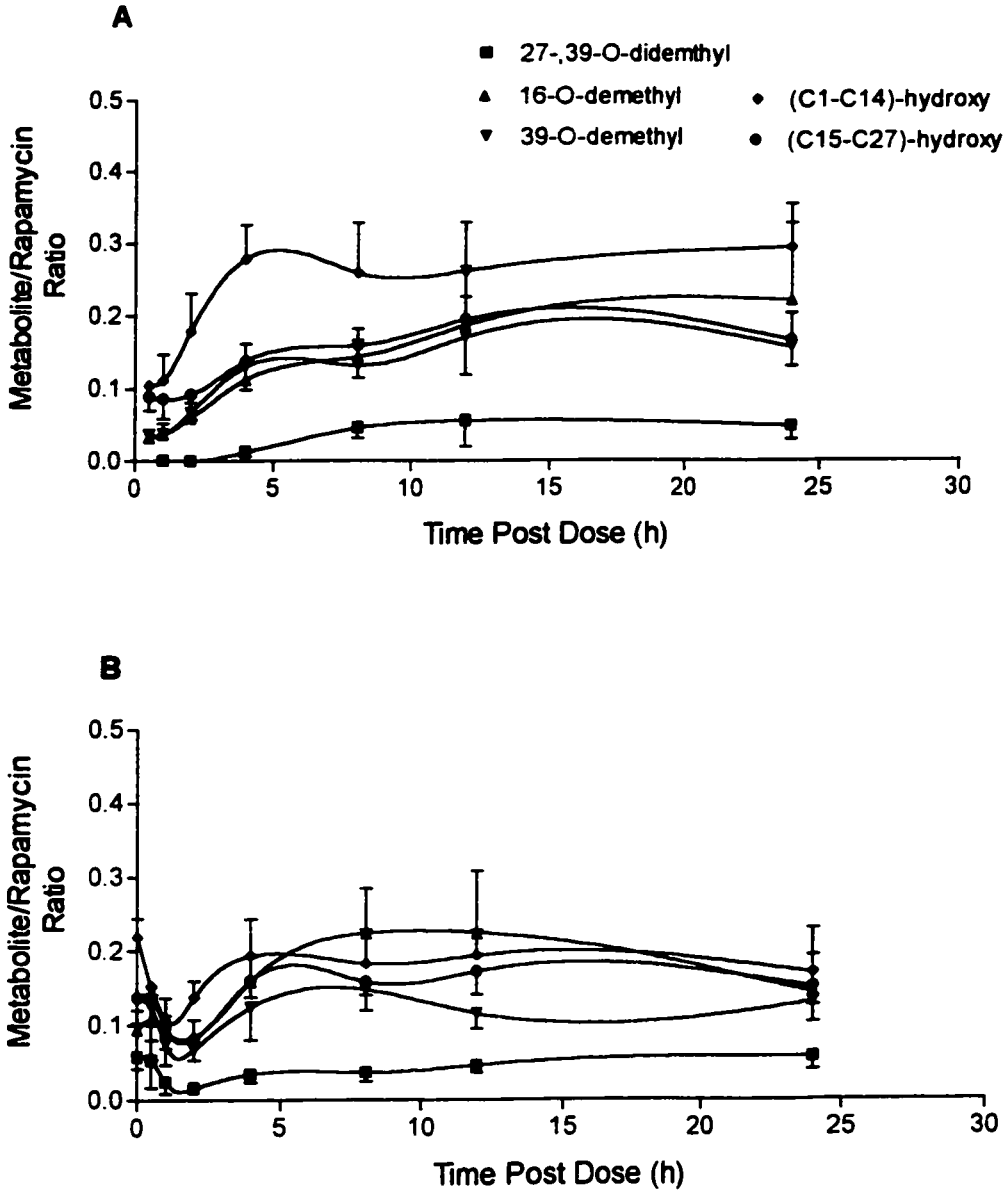

Figure VII-4 Rapamycin metabolite ratio in liver transplant patients.

Panel A is the acute dosing interval, panel B is the Chronic dosing interval. Each point represents mean +/- SEM, n=5.

the individual ratios fell from their initial levels to a minimum level at 1-2 hours post-dose, then recovered to pre-dose levels.

The proportion of total measured metabolite was compared to parent drug concentration, and the results are presented in Figure VII-5. In the acute profile, the proportion of metabolite to rapamycin started at 0.5 and rose through the dosing interval to a maximum of 1.0 at 12h post-dose, and remained high through the 24h post-dose timepoint. In the chronic profile, the relative amount of total metabolites fell from pre-dose levels, reaching a minimum of 0.28 at 30 minutes to one hour post-dose. The relative metabolite proportion then rose to pre-dose levels at 4h post-dose, and was consistent through the rest of the chronic dosing interval. There were no statistically significant differences between the acute and chronic dosing intervals when comparing total metabolite proportions at any of the timepoints.

The average of steady state 24h trough rapamycin levels with the levels of the five rapamycin metabolites are shown in Figure VII-6, with the relative proportion of each metabolite, as compared to rapamycin. The relative abundance of metabolites in steady state specimens was (C1-C14)-hydroxy > 39-O-demethyl > (C15-C27)-hydroxy ≥ 16-O-demethyl > 27-,39-O didemethyl, although this did vary somewhat from patient to patient.

The proportion of total measured metabolite to parent drug was calculated for rapamycin trough levels in individual patients, and the results are presented in Figure VII-7. The ratio of total measured metabolite to parent drug varied from 0.553 to 1.123, with an average of 0.712 for the entire population tested.

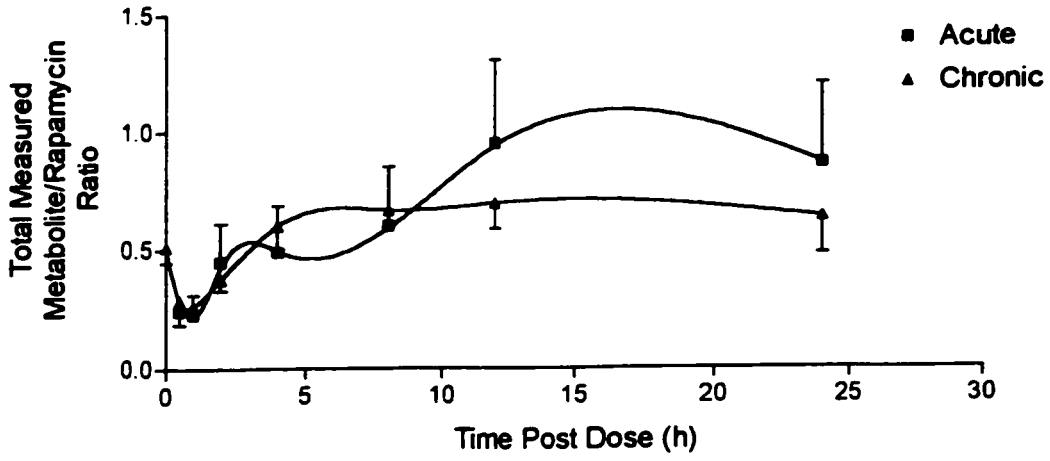

Figure VII-5 Total measured metabolite ratios in liver transplant patients over the dosing interval.

Each point represents mean +/-SEM, n = 5.

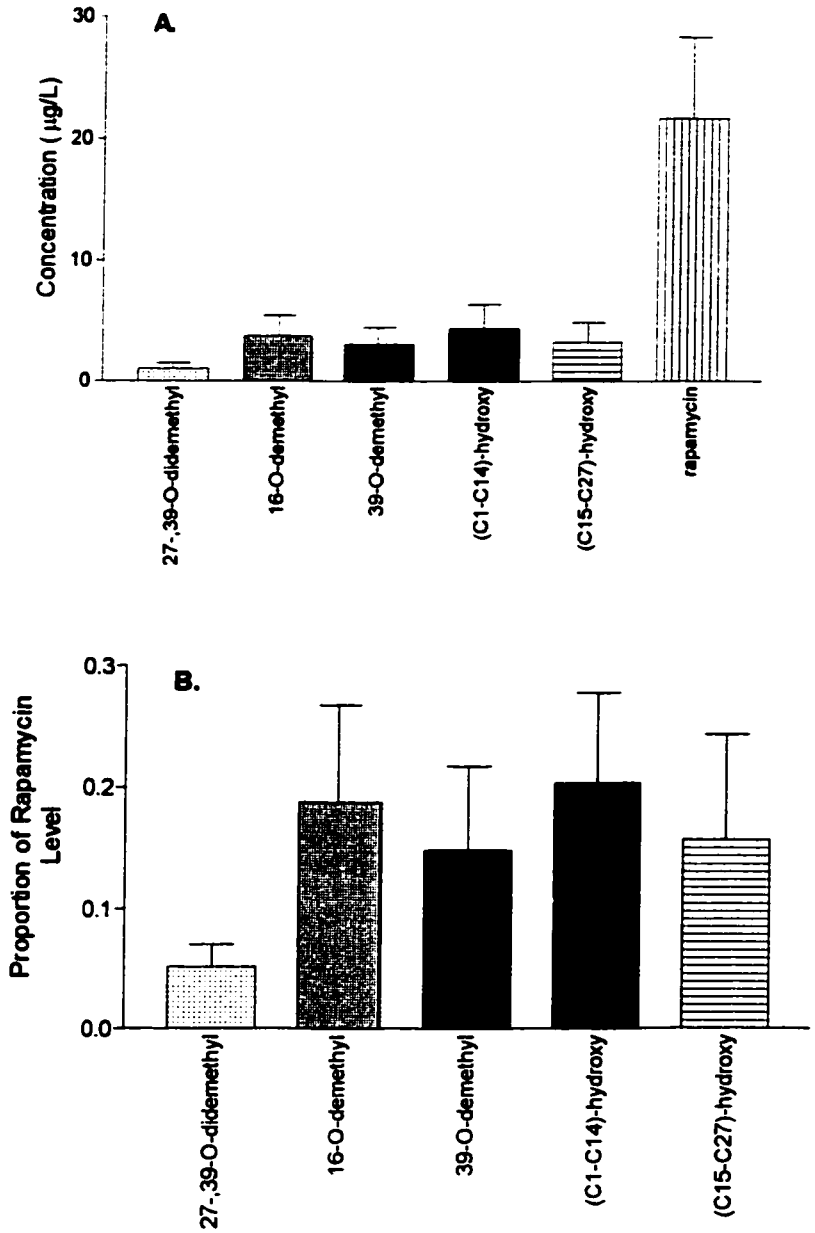

Figure VII-6 Steady state rapamycin metabolites in liver transplant patients.

Panel A is the average absolute concentration of rapamycin metabolites in 14 patients over a period of 15 months. Panel B is a graph comparing the proprtion of each metabolite to the rapamycin trough concentration for the same 14 patients.

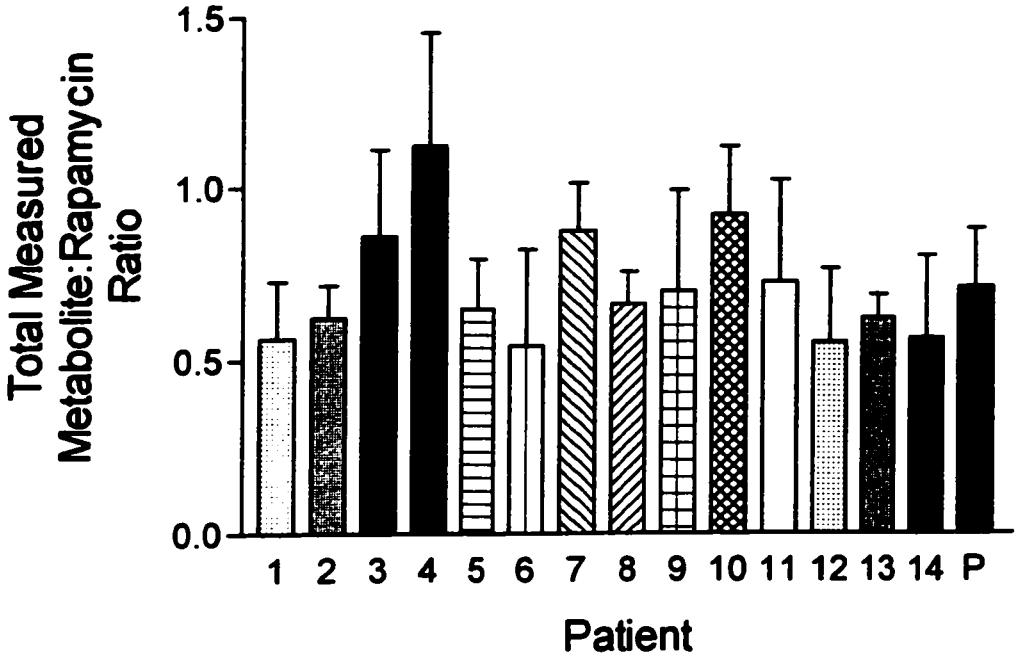

Figure VII-7 Total measured rapamycin metabolite ratios at steady state.

Each bar represents the mean +/- SD for a single liver transplant patient. The number of samples per patient varied from 3 (Patient 2) to 37 (Patient 9) over a 15 month period. The last bar, P, represents the average of all patient ratios.

4. DISCUSSION

Rapamycin, when given to liver transplant patients, produces a PK profile with several distinguishing features. The Cmax is fairly rapidly reached, in approximately 2 hours post-dose. The apparent Vz is very high, as is the apparent clearance, perhaps indicating low bioavailability in this patient population as well.

The PK parameters compare favourably with those reported for clinical renal transplant patients. Some comparisons are difficult to make, as one study was calculated using a more sophisticated multicompartmental model[1], as opposed to the non-compartmental model used in the current study. The similarities between the PK parameters of stable renal transplant patients and these newly converted liver transplant patients include: similar shaped concentration-time profiles; short Tmax; large Vz/F; and similar Cl/F.

It is notable that PK parameters of stable renal transplant patients have been shown to be altered if rapamycin is given together with Neoral CsA, resulting in a shorter Tmax, higher Cmax, AUC and trough level as compared to separate dosing[2]. The nature of this interaction is not known, and may be related to the Neoral vehicle formulation, competition between CsA and rapamycin for p-gp in the gut, or competition for CYP in the intestine and liver. Although not dosed concomitantly, the liver transplant patients in the current study were in various stages of withdrawal from CsA- and tacrolimus-based immunosuppression regimens, so the PK parameters of rapamycin may change slightly after CsA washout.

The results of this study indicate that conversion to oral rapamycin therapy in liver transplant patients produces a relatively stable PK profile for at least five days, if given a loading dose of 15 mg and a maintenance dose of 6 to 8 mg per day. The PK on day 5 may represent a near-steady state condition. There were no significant differences in PK profiles or in the absolute concentrations throughout the dosing interval for either the acute or chronic dosing periods for

neat or dose-corrected data. This was despite an approximately two-fold difference in dose given between the acute and chronic periods.

Although the dose-corrected data for acute and chronic periods are virtually overlapping, there is more variability in the uncorrected data. This affects the power of the analysis to detect statistical significance, and may high be due to inter-patient variability in absorption and bioavailability, the broad array of concomitant medications and treatments the individual patients were undertaking, and variable liver function status, as liver transplants tend to accumulate more metabolites and have a lower clearance than other organ transplants due in part to impaired hepatic functions and hepato-renal effects.

The relative abundance of metabolites was (C1-C14)-hydroxy > 39-O-demethyl > (C15-C27)-hydroxy ≥ 16-O-demethyl > 27-,39-O didemethyl, but it did vary somewhat from patient to patient. This is very similar to the results found in the canine model described in section VI. It is also consistent with literature reports of relative abundance of metabolites from renal transplant patients[3], although this is the first study where five structurally identified metabolites were measured. There are only minor discrepancies with reports found in the literature, mostly with regard to absolute levels present, and these may be due to methodological differences. For example, differential identification procedures could result in inaccuracy in peak assignment and different quantification methods used could result in different levels measured. Some investigators use peak summing for multiple metabolite conformers[3]. It is possible that the practice of adding multiple isomers of partially characterised metabolites together for a single value could over estimate the amount of metabolite present. Although there were more than five metabolites present in the blood specimens analysed here, only the five that were properly standardised were measured in the current study.

Overall, the concentrations of "primary" or metabolites with a single structural change, were higher than for the only "secondary"or multiply changed metabolites measured in this study: the di-demethylated species. This may be due to the time-kinetics required for repeated enzymatic demethylation. This is likely coupled with the increase in hydrophilicity afforded by demethylation, and the likelihood that more polar metabolites would be preferentially excreted from the body, decreasing amounts of metabolite available for the second round of metabolism. Also, the didemethylated metabolite is more hydrophilic and water-soluble and would therefore be excreted more rapidly that rapamycin or its other, less polar metabolites.

Although the metabolites studied here each account for less than 30% of the rapamycin trough level, if added together, they approach the concentration of rapamycin in the liver transplant patient. This is a significant finding when developing a therapeutic drug monitoring strategy for rapamycin.

5. REFERENCES

1. Ferron GM, Mishina EV, Zimmerman JJ, Jusko WP. Population PKs of sirolimus in kidney transplant patients. Clin Pharmacol Ther 1997; 61:416-28.

2. Kaplan B, Meier-Kriesche H, Napoli KL, Kahan BD. The effects of relative timing of sirolimus and CsA microemulsion formulation coadministration on the PKs of each agent. Clin. Pharmacol. Ther. 1998; 63:48-53.

3. Streit F, Christians U, Schiebel H-M *et al.* Sensitive and specific quantification of sirolimus (rapamycin) and its metabolites in blood of kidney graft recipients by HPLC/electrospray-mass spectrometry. Clin Chem 1996; 42:1417-25.

VIII. CONCLUSIONS

In the development and investigation of rapamycin as an immunosuppressive agent, the importance of rapamycin metabolites has been insufficiently investigated. The relevance of identification and structural elucidation as the first stage of this investigation is paramount. This has also been a limiting step in the process of evaluating the immunosuppressive and toxic effects *in vitro* and *in vivo* of these metabolites and measuring their concentrations in clinically relevant samples.

Five metabolites of rapamycin were generated using a microbial system. Their presence was confirmed in clinical blood samples and microsomal *in vitro* incubates. No intact rapamycin metabolites nor rapamycin was found in the urine of rapamycin-treated renal transplant patients; this is not a viable source of rapamycin drug metabolites, in contrast to CsA. The five rapamycin metabolites were structurally identified and their purity confirmed using ESI-MS techniques. The use of well-characterised, pure metabolites in this study has permitted the *in vitro* investigation of their immunosuppressive activities. These results have been summarised as a potency ratio, comparing each metabolite individually to the activity of rapamycin. The five metabolites tested all display considerably less immunosuppressive activity than rapamycin, with all displaying < 20% of rapamycin's activity and some displaying activity that was negligible. It is unlikely these metabolites play a large influential role in overall immunosuppression, but a role cannot yet be entirely discounted. The metabolites should be tested *in vitro* in combination with rapamycin to evaluate competition and other possible interactions. Also, experimental animal allograft studies where purified metabolites are administered and graft survival monitored would more definitively describe the relevant immunosuppressive effects of rapamycin metabolites. These studies are not possible at this time because of the extremely limited quantities of metabolite available.

Unfortunately, little useful information was gathered regarding the toxicity of rapamycin or its metabolites in an *in vitro* vascular endothelial experimental model. This confirms that the mechanism of vascular effects of rapamycin are not endothelin or prostacyclin related, in contrast to CsA and its metabolites. The issues of the effects of rapamycin and rapamycin metabolites in regard to hyperlipidemia and toxicity to platelets have yet to be addressed, as appropriate *in vitro* models to investigate the mechanisms of these relevant toxic effects did not exist when the current study were conducted.

Metabolite reactivity in an immunophilin-mediated binding assay was evaluated. It produced differential results depending on which immunophilin was used. As the cross reactivity varied from undetectable (<10%) to almost 50%, this is an important factor in interpreting the results of an immunophilin binding assay. The degree of cross reactivity does not correspond to the *in vitro* immunosuppressive activity, as one of the metabolites with the lowest immunosuppressive potency ratios demonstrates the highest cross reactivity in immunophilin binding in 4 of the 5 scenarios tested. There is also some evidence that the metabolites could produce a bias in commericial antibody-based methods for determination of rapamycin concentrations in clinical samples. This underscores the importance of testing new analytical methodology carefully for bias and unexpected reactivity before implementation.

A method for the measurement of the five rapamycin metabolites and parent drug was developed and validated using HPLC-MS technology. This permitted the measurement of levels of five rapamycin metabolites and rapamycin in liver transplant patients over the dosing interval and at steady state. The measurement of five structurally identified metabolites with an appropriately standardised method was not possible previously, because of limited information on metabolite structure and limited amounts of purified, defined metabolite available for standardisaton of such an assay. The five rapamycin metabolites measured were found to each be present at less than 30% of parent levels throughout the dosing interval and in steady

state trough specimens. The five metabolites together make up an average of 71% of the rapamycin level at trough in this patient population.

The levels of metabolites were found to be similar in canine portal and systemic samples in a PK study. The PK profile and parameters were investigated to confirm rapamycin's suitability as an appropriate immunosuppressant for use in liver and pancreatic islet transplantation. The differences in portal and systemic effects were less dramatic than for other immunosuppressants tested, and provide for accentuated long-term AUC exposure at the site of the liver. There is some indication that this may be beneficial to pancreatic islet transplants at the site of the liver, where the lower islet cellular toxicity and lack of augmented AUC4h exposure could predict improved graft survival with rapamycin therapy.

Using this information, an Immunosuppressive Index was compiled for the five rapamycin metabolites investigated. It is presented in Table VIII-1. In comparison with rapamycin, each metabolite has a low or very low Immunosuppressive Index, which accounts for expected concentration and immunosuppressive activity. Even if the Immunosuppressive Indices of all five metabolites are added together, it still represents only a small proportion of the activity of rapamycin. Thus, the therapeutic drug monitoring of rapamycin metabolites is not warranted at this time. The therapeutic drug monitoring of rapamycin should be made with a method that is specific for parent drug alone. If in the future, studies implicate rapamycin metabolites in the undesirable effects of rapamycin therapy, including hyperlipidemia and thrombocytopenia, revision of this recommendation will be necessary.

Clinical staff and transplant physicians now have a broader array of drugs than ever before for use in human organ transplantation. These drugs are used in combination to prevent rejection and avoid toxicity where possible. A thorough understanding of these drugs, their metabolism, drug-drug interactions and PK characteristics of each is an asset in designing treatment guidelines. This should also be a part of the drug development process. As more new drugs

Table VI-1 Immunosuppressive Index of five rapamycin metabolites

	Immunosuppressive Activity (MLR)	Steady State Trough Level	Immunosuppressive Index
rapamycin	1.000	1.000	1.000
27-,39-O-didemethyl	0.080	0.052	0.004
16-O-demethyl	0.173	0.148	0.026
39-O-demethyl	0.105	0.188	0.020
(C1-C14) hydroxy	0.001	0.203	<0.001
(C15-C27)-hydroxy	0.002	0.157	<0.001
Total for 5 Metabolites	0.361	0.748	~0.050

are introduced and approved for usage, it becomes apparent that these investigations are not always done completely in the pre-clinical stages. As one of the goals of new drug development is improvement of patient outcome, more extensive knowledge of drug fate, disposition and metabolite activity is an obvious asset. Improvements in drug monitoring procedures and improved patient care will follow such investigation.